Maize Ribosome-inactivating Protein as an HIV-specific Cytotoxin

LAW, Ka Yee

A Thesis Submitted in Partial Fulfillment

of the Requirements for the Degree of

Doctor of Philosophy

in

Biochemistry

The Chinese University of Hong Kong

July 2010

UMI Number: 3445952

All rights reserved

INFORMATION TO ALL USERS
The quality of this reproduction is dependent upon the quality of the copy submitted.

In the unlikely event that the author did not send a complete manuscript
and there are missing pages, these will be noted. Also, if material had to be removed,
a note will indicate the deletion.

UMI 3445952
Copyright 2011 by ProQuest LLC.
All rights reserved. This edition of the work is protected against
unauthorized copying under Title 17, United States Code.

ProQuest LLC
789 East Eisenhower Parkway
P.O. Box 1346
Ann Arbor, MI 48106-1346

Thesis / Assessment Committee

Professor Fong, Wing-Ping (Chair)

Professor Shaw, Pang-Chui (Thesis Supervisor)

Professor Wong, Kam-Bo (Thesis Supervisor)

Professor Waye, Miu Yee Mary (Committee Member)

Professor Zheng, Yong-Tang (External Examiner)

Acknowledgements

I am deeply indebted to my supervisor, Professor Shaw, Pang-Chui for his inspiration, encouragement and supervision from the preliminary to the concluding level enabled me to complete my research and the dissertation. His truly scientist intuition and passions enrich my growth as a student, a researcher and a scientist want to be.

I gratefully acknowledge Professor Wong, Kam-Bo for his valuable advice in scientific discussion which has triggered my intellectual maturity. I convey my gratitude to Professor Zheng, Yong-Tang for his valuable advice and crucial contribution to the backbone of this research and so to this thesis.

My special thanks go to Dr. Mak, Nga-Sze Amanda, Miss Wong, Yuen-Ting and Mr. Sze, Kin-Ho for their assistance and contribution, to Dr. Wang, Ruirui for her technical assistance and discussion, also her kind hospitality during my stay in Kunming.

It is my pleasure to thank Department of Biochemistry, The Chinese University of Hong Kong, Hong Kong and Key Laboratory of Animal Models and Human Disease Mechanisms, Kunming Institute of Zoology, Chinese Academy of Sciences,

Kunming, for providing a formative and important research experience for me.

Collective acknowledgments are owed to my colleagues and friends at CUHK and Kunming Institute of Zoology for creating a pleasant, helpful and memorable research atmosphere.

I express my speechless gratitude to my parents for their gentle love, inseparable support and showing me the joy of intellectual pursuit. Gary, thanks for being a supportive sibling. My husband, Hong with his love and thoughtful support, thank you.

Abstract

Ribosome-inactivating proteins (RIPs) are RNA N-glycosidases which cleave the N-glycosidic bond of adenine-4324 at the α-sarcin/ricin (SR) loop of 28S rRNA. The depurination of the SR loop results in the inhibition of protein synthesis by impairing the binding of EF-1 or EF-2 to ribosomes. RIPs are therefore highly cytotoxic and have been used as abortificiant, anti-cancer and anti-HIV agents, either alone or as a component of immunotoxins. Many type I and II RIPs, such as MAP30, GAP30, DAP30, pokeweed antiviral protein (PAP) and ricin, have been reported to possess anti-HIV activity by inhibiting viral replication *in vitro* and *in vivo* though the anti-HIV mechanism is still unclear.

Maize RIP is classified as a type III RIP. It is synthesized in the endosperm of maize as an inactive precursor (Pro-RIP), which contains a 25-amino acid internal inactivation region. During germination, a two-chain activated form (MOD) is generated by endogenous proteolysis of the internal inactivation region, whereas the two chains (16.5 and 8.5 kDa) are tightly associated without disulfide linkage. Our group has solved the crystal structures of both the Pro-RIP and MOD and found that this internal inactivation region is on the surface of the N-terminal domain in Pro-RIP . The removal of this internal inactivation region increases the inhibition of

protein synthesis of rabbit reticulocyte lysate by over 600 folds. The presence of the internal inactivation region has led us to derive a novel strategy to enhance the specificity of maize RIP towards HIV-infected cells while minimizing its cytotoxic effect on normal cells.

In this study, we provide an account on the generation of HIV-1 protease-sensitive maize RIP variants by first incorporating the HIV-1 protease recognition sequences to the internal inactivation region of the Pro-RIP. Among the five variants, three variants were cleaved and activated by HIV-1 protease *in vitro* and *in vivo*, resulting in an active two-chain form with N-glycosidase activity comparable to the fully active maize RIP. In addition, the variants inhibited viral replication in human T lymphocytes (C8166) infected by two T-tropic HIV-1 strains, HIV-1_{IIIB} and HIV-1 RF/V82F/I84V, and their cytotoxicity towards uninfected cells was similar to the non-activated precursor (TAT-Pro). In comparison to TAT-Pro, variants TAT-Pro-HIV-MA/CA and Pro-TAT-Pro-HIV-p2/NC had 2- to 70-fold increase in the inhibition of p24 antigen production in the HIV-infected cells with low cytotoxicity towards uninfected C8166 cells.

In the future, the 25 aa internal loop region of Pro-RIP can be modified for the

optimized recognition of proteases of other HIV strains. This approach opens a new opportunity for the anti-HIV application of maize RIP and other related type III RIPs. A modified maize RIP may also be applied to target other viruses and pathogens, for examples, hepatitis C and malaria, which are dependent on pathogen-encoded proteases for replication.

摘要

核糖體失活蛋白（Ribosome-inactivating proteins, RIPs）是一種 RNA 胺糖苷酶，能水解真核細胞核醣體 28S rRNA 上的 A-4324，從而阻遏了延長因數 EF-1 或 EF-2 與核糖體的結合，抑制蛋白質的生物合成。RIPs 具有很高的細胞毒性，常被開發成爲免疫毒素、抗病毒或抗癌製劑。根據亞基 (Subunit) 的數目，RIPs 可分爲三種類型。研究發現，多種I 型和II 型RIPs，如天花粉蛋白 (Trichosanthin, TCS)、美洲商陸抗病毒蛋白 (Pokeweed antiviral protein, PAP)、MAP30 和 GAP31 均在體外和體內具有抗愛滋病毒 (Human immunodeficiency virus, HIV) 的活性，但其抗愛滋病毒的機制仍未查明。

玉米 RIP 是 Ⅲ 型 RIP，它先合成爲一個 34 kDa含有25個胺基酸的結構域的失活前體（Pro-RIP），並儲存於玉米粒內。發芽時，內部失活結構域會被酶解加工後移除，成爲一個含有兩條多肽的活性 RIP（MOD）。研究證明，切除 Pro-RIP位於 N 端區包含 25 個胺基酸的酸性內部抑活區大大增加玉米RIP的核醣體抑制活性。我們分析了玉米 RIP 的失活前體 (Pro-RIP) 和其活性 RIP 的晶體結構，發現內部失活結構域位於Pro-RIP的表面。通過在這失活結構域加入HIV-1 蛋白酶（HIV-1 Protease）的目標序列，可使這結構域被HIV-1蛋白酶識別，從而殺死受HIV-1感染的細胞。

我們製備了五個可被 HIV-1 蛋白酶激活的玉米 RIP 突變體。其中三個突變體可被純化的 HIV-1 蛋白酶於細胞外和 HIV-1 感染的細胞中激活，變成含兩條多肽的活性組合，它們有和 MOD 相似的胺糖苷酶活性。此外，這些玉米 RIP 突變體可抑制 $HIV\text{-}1_{IIIB}$ 和 HIV-1 RF/V82F/I84V 在人類 T 細胞 (C8166) 的複製，但對非感染的 C8166 的毒性則和 TAT-失活前體 (TAT-Pro) 相似。與 TAT-Pro 相比，TAT-Pro-HIV-MA/CA and TAT-Pro-HIV-p2/NC 抑制 HIV 感染細胞生產 p24 抗原的能力提升了 2 至 70 倍。

除抑制本研究的 HIV-1 病毒株外，理論上也可以使玉米 RIP 識別其它 HIV 病毒株。這項研究，增加了玉米 RIP 和其它 III 型 RIP 抗 HIV 的價值。我們可於將來將玉米失活前體的內部失活結構域「開關制」的原理應用到其他 RIP 和其他病原體的蛋白酶上，例如病毒性 C 型肝炎 (Hepatitis C) 和瘧疾 (Malaria)，以增加玉米 RIP 對這些病原體的特異性。

Contents

Chapter Two Materials and methods

Abbreviations

AIDS	Acquired immunodeficiency syndrome
APS	Ammonia persulfate
BSA	Bovine serum albumin
CM	Carboxymethyl
DC	Dendritic cells
DEAE	Diethylaminoethyl
DMEM	Dulbecco's modified Eagle's medium
DMF	N,N-dimethylformamide
DMSO	Dimethyl sulfoxide
DNA	Deoxyribonucleic acid
dNTP	Deoxynucleosine 5' triphosphate
EDTA	Ethylenediaminetetraacetic acid
ELISA	Enzyme-linked immunosorbent assay
FBS	Fetal bovine serum
GAP31	Gelonium anti-HIV protein of 31kDa
HAART	Highly active antiretroviral therapy
HIV	Human immunodeficiency virus
HCl	Hydrochloric acid
IN	Integrase
IPTG	Isopropyl β-D-thiogalactopyranoside
JNK	c-Jun N-terminal kinase
LB	Luria-bertani
LDL	Low density lipoprotein

LRP	low-density lipoprotein *receptor* (LDLR)-related protein
LTR	Long terminal repeats
MA	Matrix
MTT	3-(4, 5-dimethylthiazolyl-2)-2, 5-diphenyltetrazolium bromide
NaCl	Sodium chloride
NC	nucleocapsid
NMR	Nuclear magnetic resonance
NP-40	Nonidet P-40
NRTIs	Nucleoside reverse transcriptase inhibitors
OPD	O-phenylenediamine dihydrochloride
PAP	Pokeweed antiviral protein
PBS	Phosphate-buffered saline
PIC	Pre-integrated complex
PIs	Protease inhibitors
PMSF	Phenylmethysulfonyl fluoride
RIP	Ribosome-inactivating protein
RT	Reverse transciptase
SDS-PAGE	Sodium dodecyl sulphate-polyacrylamide gel electrophoresis
TAE	Tris-acetate-EDTA
TCS	Trichosanthin
β-ME	β-mercaptoethanol

Abbreviations of amino acids

A	Ala	Alanine
B	Asx	Asparagine or aspartate
C	Cys	Cysteine
D	Asp	Aspartate
E	Glu	Glutamate
F	Phe	Phenylalanine
G	Gly	Glycine
H	His	Histidine
I	Ile	Isoleucine
K	Lys	Lysine
L	Leu	Leucine
M	Met	Methionine
N	Asn	Asparagine
P	Pro	Proline
Q	Gln	Glutamine
R	Arg	Arginine
S	Ser	Serine
T	Thr	Threonine
V	Val	Valine
W	Trp	Tryptophan
Y	Tyr	Tyrosine
Z	Glx	Glutamine or glutamate

Chapter One

Introduction

1.1 Ribosome-inactivating proteins

1.1.1 Definition and classification

Ribosome-inactivating proteins (RIPs), mostly from plants, are N-glycosidases which cleave the N-glycosidic bond of adenine-4324 located within the GAGA hairpin of the α-sarcin/ricin loop (SRL) of 28S rRNA, thus blocking the elongation factor (EF)-1- and EF-2-dependent GTPase activities. This irreversible modification makes ribosome unable to bind EF-2, thereby blocking translation and resulting in inhibition of protein synthesis and finally cell death (Hartley *et al.*, 1996, Nielsen & Boston, 2001, O'Keefe, 2001, Peumans *et al.*, 2001). RIPs have been related to plant defense. Among all the RIPs, ricin (*Ricinus communis*) and trichosanthin (*Trichosanthes kirilowii*) are well known since the end of 19th century as possessing high toxicity and abortifacient activity, respectively (Chan *et al.*, 1984, Lord *et al.*, 1994, Peumans *et al.*, 2001). RIPs are produced also by bacteria, such as *Shigella dysenteriae* producing Shiga toxin and *Escherichia coli* producing Shiga-like toxin. (Hartley & Lord, 2004, Nakao & Takeda, 2000, Sandvig, 2001). RIPs are also found in alga, for example, lamjapin is a type I RIP isolated from a marine alga (Girbes *et*

al., 2004, Liu *et al.*, 2002), as well as mushrooms (Yao *et al.*, 1998, Ye & Ng, 2002).

RIPs are classified into three types based on their physical properties. Type I RIPs, trichosanthin (TCS), pokeweed antiviral protein (PAP) (*Phytolacca Americana*), Gelonin (*Gelonium multiflorum*) and saporin (*Saponaria officinalis*), for examples, are monomeric proteins with molecular weight of about 30 kDa (Barthelemy *et al.*, 1993, Irvin & Uckun, 1992, Stirpe *et al.*, 1980). They are basic proteins with pI larger than 8 (Girbes *et al.*, 2004). Most characterized RIPs fall into this class (Barbieri *et al.*, 1993).

Type II RIPs, such as ricin and abrin (*Abrus precatorius*) (Olsnes & Pihl, 1973; 1981), are heterodimeric proteins where chain A is the catalytic subunit sharing high structural homology to Type I RIPs and chain B is a galactose-binding lectin that facilitates the intracellular delivery of chain A. The two subunits are linked by a disulphide bridge. The lectin chain binds to galactosyl moieties of glycoproteins and/or glycolipid on eukaryotic cell surface and mediates the transport of chain A to the cytosol (Beaumelle *et al.*, 1993, Olsnes, 2004, Olsnes & Kozlvo, 2001). Some type II RIPs such as nigrin b (*Sambucus nigra*) are non-toxic. The lowered toxicity may be due to the reduced capability to translocate into the cells and more rapid degradation and excretion by the cells (Battelli *et al.*, 1997, Stirpe & Battelli, 2006, Svinth *et al.*, 1998).

Type III RIPs are synthesized as inactive precursors which are activated by proteolytic cleavage of an internal loop (Mundy *et al.*, 1994). So far, only type III RIPs from maize and barley have been characterized (Bass *et al.*, 2004, Dunaeva *et al.*, 1999, Dunaeva & Goerschen, 1999). Taking maize RIP (b-32) as an example, the precursor (Pro-RIP) is produced in the endosperm as an acidic proteins (34 kDa) with pI around 6 (Hey *et al.*, 1995, Mak *et al.*, 2007). It is expressed under the control of a transcriptional activator, *Opaque-2* regulatory locus (Bass *et al.*, 2004). During germination, a series of proteolysis converts the inactive precursor into a two-chain active form, which includes the elimination of 16 aa at the N-terminal region (residues 1-16), 25 aa at the acidic internal loop region (residues 163-189) and 14 aa at the C-terminal region (residues 287-300). The two subunits (16.5 and 8.5 kDa) are tightly associated, but not covalently linked (Bass *et al.*, 2004, Mak *et al.*, 2007, Nielsen & Boston, 2001, Stirpe & Battelli, 2006). Jasmonate-induced protein of barley leaves (JIP60) is another type III RIP characterized. It is induced by jasmonic acid and activated by removal of a C-terminal region (>20 kDa) and an internal insertion which shows similar position within the primary amino acid sequence as in maize RIP (Chaudhry *et al.*, 1994).

1.1.2 Structure

Comparison of amino acid sequences of type I and II RIPs from different plants reveals high similarities between type I RIPs and chain A of type II RIPs. The structures of the catalytic subunits of type I and II RIPs are also highly conserved (Collins *et al.*, 1990, Motto & Lupotto, 2004). According to the crystal structures, RIPs are two-domain proteins with a large N-terminal domain consisting of six α-helices and a six-stranded mixed β-sheet, and a small C-terminal domain consisting of an anti-parallel β-sheet and two α-helices (Mak *et al.*, 2007, Mlsna *et al.*, 1993, Monzingo *et al.*, 1993, Xiong *et al.*, 1994). Recently, Mak and colleagues have reported the crystal structures of both the inactive precursor (Pro-RIP) and the single chain active form (MOD) of maize RIP (Mak *et al.*, 2007), while the secondary elements of MOD is comparable to the solution structure of MOD determined by NMR spectrometry (Yang *et al.*, 2007; 2010). The single-chain active form of MOD was created by fusing the two mature chains by a bipeptide sequence. It has a protein inhibitory activity similar to that of the native two-chain form (Hey *et al.*, 1995, Walsh *et al.*, 1991). Structures of Pro-RIP and MOD are highly similar. There are two domains: an N-terminal domain consisting of five α-helices and a five-stranded mixed β-sheet and a small C-terminal domain made up of four α-helices. Pro-RIP has a 25-amino acid flexible loop region (Ala163-Asp189) on the

surface of the N-terminal domain. The catalytic domain of maize RIP is resemble to other type I and II RIPs with conserved active site residues Tyr94, Tyr130, Glu207, Arg210 and Trp241 at the cleft between the N- and C- terminal domains (Mak *et al.*, 2007, Yang *et al.*, 2010).

1.1.3 Cellular entry of RIPs

Effectiveness of cellular uptake is one of the major factors affecting the cytotoxicity of RIPs. Among the three types, type II RIPs possess the highest cytotoxicity towards a wide variety of cell types. It may be due to its high cellular uptake efficiency (Falnes & Sandvig, 2000). Type II RIPs, such as ricin and abrin, consist of a lectin B-chain which facilitates the cellular uptake through binding to cell surface glycoproteins and glycolipids with terminal galactose, which are widely present on different cell types, such as HeLa cells (Hartley & Lord, 2004, Sandvig *et al.*, 1976). The A chains are endocytosed and enter cytosol from different intracellular compartments, such as endosomes, or from endoplasmic reticulum to the Golgi apparatus and finally translocated to the cytosol where the toxins execute the enzymatic function (Roberts & Lord, 2004, Sandvig & Grimmer, 2002, Sandvig & van Deurs, 1999). It is suggested that ricin is internalized through the clathrin-independent endocytosis pathway, although it is still endocytosed even the

pathway is blocked (Falnes & Sandvig, 2000). On the other hand, chain B of Shiga toxin or Shiga-like toxin targets glycolipid Gb3 receptors on cell surface, although the mechanism of cellular entry is still unclear (Sandvig, 2001, Sandvig & van Deurs, 2000).

Type I RIPs lack a cell-binding domain to facilitate cell entry, thus exhibiting much lower cytotoxicity (Stirpe & Battelli, 2006). However, they show selective toxicity towards different cell types exhibiting strong cytotoxic effects on monocytes/ macrophages (Jurkat cells and U937 cells) and choriocarcinoma cells (JAR cells), but only limited cytotoxic effects on hepatoma cells (H35 cells) (Chan *et al.*, 2000, Tsao *et al.*, 1990, Tsao *et al.*, 1986, Zheng *et al.*,1994). This suggested a specific mechanism for the entry of type I RIP into target cells. Previous studies have found that saporin and TCS are actively uptaken by α_2-macroglobulin receptor/ LDL receptor-related protein (LRP) (Cavallaro *et al.*, 1995, Chan *et al.*, 2000), which commonly distribute in macrophages, smooth muscle cells and follicular cells of ovary. In addition, some type I RIPs, like gelonin and dianthin bind to carbohydrate receptors on the cell membrane for cellular transduction (Barbieri *et al.*, 1993, Jimenez & Vazquez, 1985).

1.1.4 Enzymatic activities

1.1.4.1 N-glycosidase activity towards ribosomes

Althought all RIPs hydrolyse the same adenine residue (A_{4324} in rat liver rRNA) from a GAGA sequence in conserved SRL located in 28S rRNA (Endo & Taurugi, 1988, Guo *et al.*, 2003, Hartley *et al.*, 1996, Stirpe *et al.*, 1988, Stirpe & Battelli, 2006), some of them are more active against eukaryotic ribosomes than on *E. coli* ones. It is due to RIPs utilizing different docking sites on the ribosome to access the SRL (Peumans *et al.*, 2001). Ricin A chain has been shown to cross-linked to ribosomal proteins L9 and L10e in human lung carcinoma cells and binds to the ribosomal stalk proteins P1 and P2 in *Saccharomyces cerevisiae* (Chiou *et al.*, 2008, Vater *et al.*, 1995). Moreover, ricin does not act on *E. coli* ribosomes, but deadenylates naked *E. coli* 23S rRNA (Endo *et al.*, 1991, Marchant & Hartley, 1995). These findings explain why ricin possesses high toxicity towards eukaryotic ribosomes but low toxic effect on prokaryotic ribosomes (Barbieri *et al.*, 1993). PAP binds to yeast ribosomal protein L3 (Hudak *et al.*, 1999, Hudak *et al.*, 2000) and interacts with initiation factors 4G and iso4G in wheat germ (Wang & Hudak, 2006). TCS was found to binds to L10a, ribosomal stalk proteins P0, P1 and P2, as well as mitotic checkpoint protein MAD2B protein *in vitro* (Chan *et al.*, 2007, Chan *et al.*, 2001, Xia *et al.*, 2005). The charge-to alanine mutations in the C-terminal domain of

TCS which abolishes the interaction with ribosomal stalk protein P2, exhibits an 18-fold decrease in inhibition translation in rabbit reticulocyte lysate (Chan *et al.*, 2007). A recent crystallographic study of TCS complexed to a P protein peptide showed that TCS interacts with an 11 aa motif (SDDDMGFGLFD) at the C-terminal of the P proteins which is the conserved elongation factor binding domain. It has been suggested that similar interaction with P proteins may present in other RIPs (Too *et al.*, 2009).

1.1.4.2 Polynucleotide:adenosine glycosidase activity

Several type I and II RIPs, including ricin, PAP, TCS and saporin-L1, were found to be capable of removing multiple adenine residues from a wide variety of nucleic acids, such as RNA, poly(A), tRNA and viral RNA of tobacco mosaic virus (TMV) to different extents (Barbieri *et al.*, 1992, Barbieri *et al.*, 1997, Barbieri *et al.*, 1996). By detecting the amount of adenine released using quantitative high-performance liquid chromatography (HPLC), the three isoforms of PAP (PAP-I, PAP-II and PAP-III) were found to possess a concentration-dependent deadenylation activity on HIV-1 RNA, TMV RNA and bacteriophage RNA (Rajamohan *et al.*, 1999a, Rajamohan *et al.*, 1999b). Further investigation found that PAP with intact catalytic site and C-terminal deletion showed a drastic decrease in antiviral activity,

which suggested that the depurination ability of ribosomes by PAP may not related to its antiviral activity (Tumer *et al.*, 1997). This indicates that RIPs are capable to deadenylate different polynucleotides and implicates their broad biological roles.

1.1.4.3 Depurination of capped mRNA

PAP can distinguish between capped and uncapped mRNA and depurinate the capped ones. Wild-type PAP and mutants that do not depurinate tobacco and rabbit ribosomes, inhibit the *in vitro* translation by depurinating capped mRNA (Hudak *et al.*, 2000). The cap structure of mRNA interacts with cap-binding protein eIF4E which mediates the translation initiation by enhancing the binding of the 40S ribosomal subunit to the mRNA. PAP recognizes and binds to the cap and depurinates the mRNA downstream of the cap *in vitro* (Hudak *et al.*, 2002).

1.1.5 Biological activities

RIPs are found in many plant species and presumbly play a role in plant defense. It is believed that the highly toxic type II RIPs, like ricin and abrin, protect the seeds against plant-eating predators (Van Damme *et al.*, 1998). Type I RIPs was found to have a direct but weak antifungal activity (Peumans *et al.*, 2001) and they protect transgenic plants against viral infection (Wang & Tumer, 2000).

1.1.5.1 Antiviral activity

A number of type I and type II RIPs have been found to possess antiviral effect towards a wide variety of virus, like plant, fungal and animal viruses. Numerous studies have been conducted to investigate the anti-human immunodeficiency virus type 1 (HIV-1) activity of TCS, PAP and other RIPs (Peumans *et al.*, 2001, Stirpe *et al.*, 1992, Stirpe & Battelli, 2006). TCS is found to preferentially inhibit the replication of HIV-1 in acutely infected T-lymphoblastoid cells and chronically infected macrophages (Shaw *et al.*, 2005, Wang *et al.*, 2003, Wang *et al.*, 2002, Zheng *et al.*, 2000). TAP 29, a *Trichosanthes* anti-HIV protein has been shown to inhibit viral infection and replication with low toxicity (Lee-Huang *et al.*, 1991). Phase I/II clinical trials of TCS or combination of TCS with zidovoudine and dideoxinosine showed that it can lower the serum HIV-1 p24 antigen level and enhance the level of $CD4^+$ cells in patients with acquired immunodeficiency syndrome (AIDS) and AIDS-related complex (Kahn, 1992). However, high immunogenicity, short plasma half-life and neurotoxicity of TCS have hindered the further development of TCS as an anti-HIV-1 therapeutic agent (Chan *et al.*, 2000, He *et al.*, 1999, Wang *et al.*, 2004). PAP has been developed into different immunoconjugates by linking to monoclonal antibodies to recognize CD4, CD5 and CD8 antigen, which inhibited HIV-1 replication in normal cells infected by experimental virus strains, as well as clinical isolated strains (Erice *et al.*, 1993, Zarling

et al., 1990). The anti-HIV activity of TXU-PAP, a PAP molecule conjugated to anti-CD7 antibody, has been evaluated in mouse model of human AIDS, as well as its toxicity and pharmacokinetics in HIV-infected chimpanzees and adult patients (Uckun *et al.*, 1999, Uckun *et al.*, 1998). It has been reported that no HIV-1 viral genome is detected in the mouse model treated with TXU-PAP (Uckun *et al.*, 1998). TXU-PAP inhibited HIV-1 replication to below-detection levels in three of the four HIV-1 infected chimpanzees, but it showed a medium plasma elimination half-time of 5.1 to 12.0 h. For HIV-1 infected adult patients, TXU-PAP showed more favorable pharmacokinetics with relatively long plasma elimination half-life of 12.4 ± 1.4 h and was capable of reducing the viral burden in six of six patients evaluated (Uckun *et al.*, 1999). GAP31 (Gelonium anti-HIV protein of 31kDa) is capable of inhibiting HIV-1 infection and replication and a 33-amino-acid segment of the N-terminus of GAP31 (K10-K42) is the shortest peptide sufficient for HIV-1 inhibition, DNA and RNA binding, and ribosome inactivation (Lee-Huang *et al.*, 1991; 1994). The anti-HIV mechanism of RIP has been investigated but the data are not conclusive. It is known that selected RIPs can inhibit the activity of the reverse transcriptase and integrase (Au *et al.*, 2000, Jiratchariyakui *et al.*, 2001). It has been found that MAP30 and GAP31 fragments without ribosome-inactivating activity still retain anti-HIV activities (Lee-Huang *et al.*, 1991; 1994). On the other hand, TCS variants with reduced

ribosome-inactivating activity loss almost all anti-HIV activity (Wang *et al.*, 2002), but later it is found that the anti-HIV effect of TCS is independent of ribosome inactivation (Wang *et al.*, 2003). By investigating the effect of a JNK inhibitor (CPE-11004) on the anti-HIV-1 activity of TCS, it is believed that ribotoxic stress may be an important factor and the action is via the MAPK signal pathway (Ouyang *et al.*, 2006). Low dosage of TCS (less than 1μg/ml) is capable of inducing immune suppression via the activation of IL-4/IL-10 secreting CD8 T cells and it has been suggested that TCS regulates the T cell-mediated immune response, instead of direct killing of HIV-infected CD4 T cells (Zhou *et al.*, 2007). For pokeweed antiviral protein (PAP), several studies have suggested that its antiviral activity may not be due to the depurination of host ribosomes. Instead PAP inhibits translation by depurinating HIV-1 RNAs (Hudak *et al.*, 2000, Rajamohan *et al.*, 1999b). Moreover, PAP activates a stress-induced kinase JNK without causing cleavage of caspase-3 or PARP, and it has been suggested that translational arrest and JNK activation are independently triggered and together may cooperate in the induction of apoptosis (Chan Tung *et al.*, 2008). A recent study showed that TCS inhibits HIV replication by preventing HIV-1 DNA integration. TCS binds to the HIV-1 long terminal repeats (LTR) in a transient manner and depurinate the HIV-1 LTR (Zhao *et al.*, 2009).

1.1.5.2 Abortifacient activity

The extract of the roots of *Trichosanthes kirilowii* have long been used in Chinese traditional medicine to induce abortion (Leung *et al.*, 1986, Maraganore *et al.*, 1986). The effect is attributed by TCS which causes death of the fetus by inhibiting protein synthesis in syncytiotriphoblasts. These cells bear LRP, like macrophage, are highly sensitive to TCS (Battelli *et al.*, 1992, Yeung *et al.*, 1988).

1.2 Human immunodeficiency virus

1.2.1 History, distribution and subtype diversity

Human immunodeficiency virus (HIV) is a lentivirus, a sub-class of retrovirus. HIV targets the activated $CD4^+$ lymphocytes and several other cell types including macrophages and dendritic cells. The substantial loss of $CD4^+$ lymphocytes leads to immunodeficiency resulting in consequent fatal infections.

In late 1970s and 1980s, patients with marked depletion of the $CD4^+$ T-lymphocyte subset in the peripheral blood were reported. The disease was first brought attention in 1981 when the Center for Disease Control reported five individuals with severe immunodeficiency in the Morbidity and Mortality Weekly Report. It is suggested that such similar immunodeficiency disease is transmitted by

sexual route, intravenous drug administration and blood. In 1981, a new retrovirus associated with AIDS in the United States, Europe, and central Africa and exhibits morphologic an genetic characteristics typical of the lentivirus genus, was named human immunodeficiency virus type 1 (HIV-1). A related human retrovirus, HIV-2 was then recovered in West Africa in 1986. It has been reported that the lower prevalence of HIV-2 is related to its low transmission efficiency; such as vertical transmission from HIV-2-infected breast-feeding mothers in the absence of antiretroviral treatment (de Silva *et al.*, 2008).

HIV-1, which causes the worldwide epidemic of acquired immunodeficiency syndrome (AIDS), is divided into three groups, named O, N and M. Group M is predominant and has spread throughout the world causing 95% global HIV infection (Figure 1.1). Group M can be divided into many subtypes (A-K), where subtype B, originally described in north America and Europe, is now dominant in China since 1996 (Lu *et al.*, 2008, McCutchan, 2006, Sharp & Hahn, 2008, Weiss, 2000). By the end of 2008, it was estimated that there were 33.4 million infections in the world (Figure 1.1). National HIV infection levels are highest in Africa, estimated 22.4 million people living with HIV as of December 2008, two thirds of global total. Second high infection levels are in south and south-east Asia where estimated 4.7 million people were living with HIV in 2008 (World Health Organization, 2009).

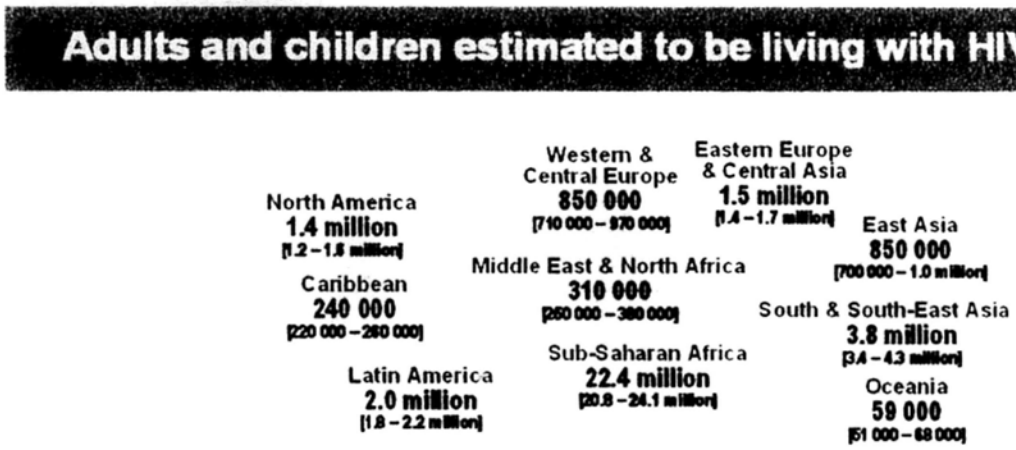

Figure 1.1 Global HIV prevalence and distribution (World Health Organization, 2009)

According to the new data in the AIDS epidemic update 2009 by WHO, in the end of 2008, there are estimated 850,000 people living with HIV in China, where Yunnan is a major site of the AIDS epidemic. Yunnan has long been a major trafficking location from the "Golden triangle' of opium/heroin production which includes Myanmar, Thailand, Laos and Vietnam. From the HIV-1 cases detected in intravenous drug users in 1989 till 2006, around 49,000 HIV-1 cases were identified in Yunnan, representing about 25% of the national totals (Lu *et al.*, 2008) (Figure 1.2).

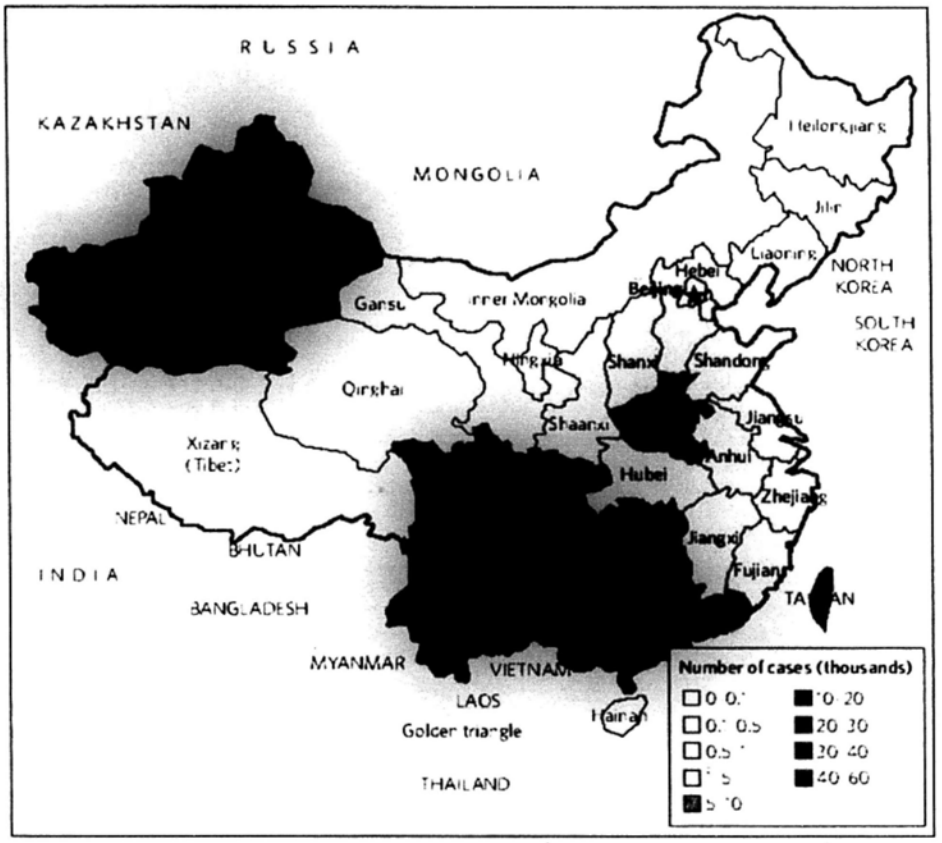

Figure 1.2 Geographic distribution of cumulative reported HIV-1 cases in China (Lu *et al.*, 2008).

1.2.2 Tropism of HIV-1

HIV-1, likes many other primate lentiviruses, uses CD4 and other co-receptors (CCR5 or CXCR4) to enter susceptible cells. The main target for HIV-1 is CD4 positive ($CD4^+$) cells, such as T-lymphocytes, macrophage, and dendritic cells (DC). In the early study of HIV-1 infection, mitogen-activated human peripheral blood mononuclear cells (PBMC), $CD4^+$ T leukemia cell lines including Jurkat, H9, MT-2 and MT-4, are used for virus isolation and propagation. Most of the human T-cell lines undergo cell death after cytopathic infection and release large quantities of

virion, while H9 cells become persistently infected with low cytopathic effects (Freed & Martin, 2007). Based on viral transmission and replication kinetics, HIV-1 is classified into two types, including macrophage (M)-tropic virus and T-cell (T)-tropic virus (Cheng-Mayer *et al.*, 1988). M-tropic HIV-1 viruses, also called R5 strain, replicate in PBMC and macrophage in low replication kinetics during early, asymptomatic phase of HIV-1 infection. M-tropic viruses use β-chemokine receptor, CCR5 for viral fusion and do not induce syncytium formation (Choe *et al.*, 1996, Freed & Martin, 2007, Kozak *et al.*, 1997). T-tropic viruses, called as X4 strain, using α-chemokin CXCR4 coreceptors exhibit a rapid and high cytopathicity and replication properties, and form syncytia in T-cell lines (Fenyo *et al.*, 1989, Sullivan *et al.*, 1995). Fouchier and co-workers used PCR analysis to study V3 DNA sequence of HIV-1 envelope (*env*) gene of 402 primary HIV-1 isolates and revealed a limited codons for amino acid residues that are responsible for phenotype of syncytium-inducing HIV-1 isolates (Fouchier *et al.*, 1995). In addition, several reports have claimed that the phenotypic difference can be attributed to mutation in V2 and V3 regions of the HIV-1 *env* gene (Fouchier *et al.*, 1995, Schuitemaker *et al.*, 1995, Watkins *et al.*, 1997).

1.2.3 Viral structure

Both HIV-1 and HIV-2 are members of primate lentiviruses. Like other retroviruses, mature HIV virions have spherical morphology of 100-120nm diameter and contain a virus capsid, which consists of capsid proteins (p24), nucleocapsid proteins (p7/p9), the single-stranded RNA genome,three viral enzymes (protease, reverse transcriptase and integrase), and accessory proteins Npu, Vif, Vpr and Nef (Freed & Martin, 2007).

The viral capsid is surrounded by a matrix protein which plays an important role in the early stage of viral replication to transport the viral DNA into the nucleus of host cell. The virion envelope is composed of a lipid bilayer membrane and a tetrameric envelope protein complex, with a surface subunit (gp120) and a transmembrane subunit (gp41), which facilitates the viral entry through binding to CD4 and chemokine co-receptors. Other viral structural proteins, such as capsid protein (p24), matrix protein (p17), protease, reverse transcriptase and integrase, are encoded by genes located within the open reading frames of *gag* and *pol* respectively (Figure 1.3).

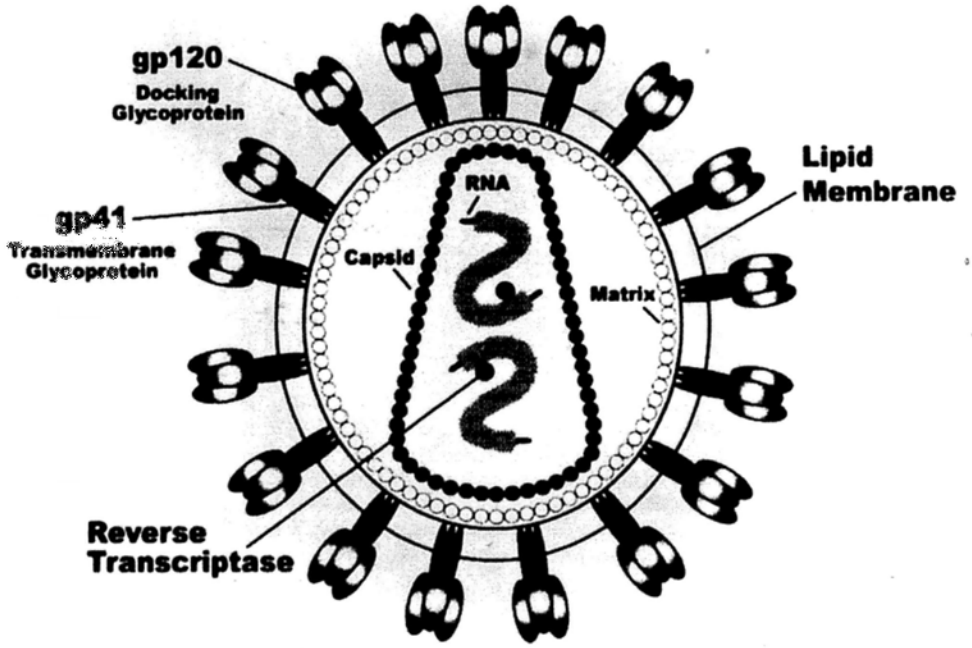

Figure 1.3 Schematic representation of a mature HIV-1 virion (http://en.wikipedia.org/wiki/HIV).

1.2.4 HIV-1 genes

Nine open reading frames are encoded by the HIV-1 genome. Gag, Pol, and Env polyproteins which are subsequently proteolyzed into different proteins are common to all retroviruses. The four Gag proteins are matrix (p17, MA), nucleocapsid (p7, NC), capsid (p24, CA) and p6. The three Pol proteins are protease (p11, PR), reverse transcriptase (p66/51, RT) and integrase (p32, IN) and two envelope proteins, gp120 and gp41. In addition, HIV-1 encodes six accessory proteins, Vif, Vpr and Nef are in viral particle; Tat and Rev are essential for gene regulation and Vpu assists viral assembly (Figure 1.4) (Frankel, 1998).

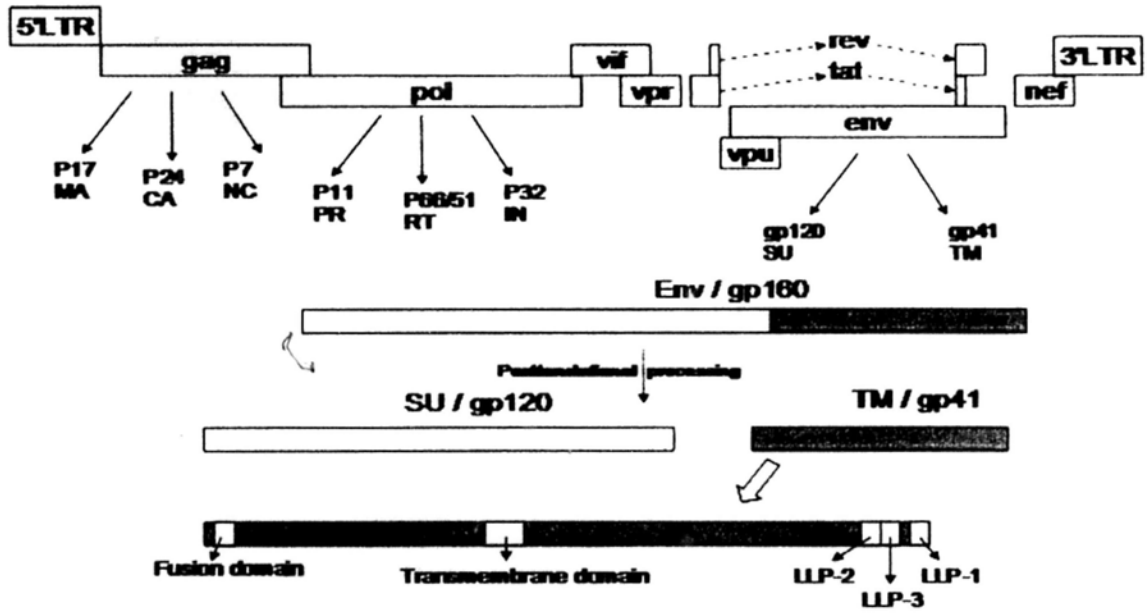

Figure 1.4 Linear organization of the HIV-1 genome (Costin, 2007).

1.2.5 HIV-1 life cycle

The life cycle of HIV can be roughly divided into two distinct phases: the early phase includes infection and integration, and the late phase includes the expression of viral genes, viral assembly and release (Nisole & Saib, 2004, Taylor *et al.*, 2008).

The envelop glycoproteins gp120 and gp41 recognize the primary receptor CD4 and recruits chemokine receptors (CCR5 and CXCR4), then triggers conformational changes of envelop glycoproteins, resulting in the fusion of viral and cellular membranes and the release of viral nucleocapsid into the cytoplasm. Immediately after cell fusion, the viral core dissembles and the two single stranded viral RNA (9.2 kb) are then reverse transcribed by HIV reverse transcriptase to generate a proviral partially double-stranded DNA product. The reverse-transcribed DNA product is then

transported through cytoplasm into the nucleus as pre-integrated complex (PIC) containing Gag and Pol proteins. After the import of the PIC into the nucleus, linear copies of the reverse transcript are integrated into the chromosomal DNA of the host cell for viral RNA synthesis and infectious particle production (Frankel, 1998, Sierra *et al.*, 2005). In activated T lymphocytes, integrated viral DNA serves as the template for RNA polymerase II, which incorporated with Tat protein and cellular nuclear factor-kappaB (NF-$_K$B) for production of high level of viral RNA. Unspliced or partially spliced transcripts are transported from the nucleus to the cytoplasm by Rev protein. Env precursor gp160 translated in endoplasmic reticulum, while the Gag and Gag-Pol polyproteins synthesized in the cytoplasm by ribosomes, are then transported to the plasma membrane via different pathways. Progeny virus particles start budding and are released as immature virus. Subsequent proteolytic processing of Gag and Pol proteins by HIV protease during or immediately after budding generates mature HIV virions.

The rapid viral replication rate together with the intrinsic mechanisms of HIV reverse transcriptase ensures the rapid viral evolution and high viral diversity. Massive amount (over ten billion) of new viruses is produced each day in an HIV-infected individual. HIV reverse transcriptase lacks a proofreading, resulting in approximately 3.4×10^{-5} mutations per base pair per replication (Taylor *et al.*, 2008).

Additionally, HIV-1 recombination can lead to further viral diversity when the same cell is co-infected by two separate strains of HIV virus (Robertson *et al.*, 1995).

1.2.6 Current HIV therapy

The current therapeutic strategy, highly active antiretroviral therapy (HAART), involves the use of at least three classes of antiretroviral agents, including entry inhibitors, fusion inhibitors, reverse transcriptase inhibitors, integrase inhibitors and protease inhibitors (Bailey & Fisher, 2008, Palella *et al.*, 1998). HAART has been improved by the development of new drugs. During 2009, World Health Organization (WHO) has worked to update the guideline to review the drug regimens, antiretroviral therapy and management of co-infections (WHO, 2009). Nevertheless, Stavudine (a nucleoside analog reverse transcriptase inhibitor) which is commoly used in the scaling-up of antiretroviral therapy in less-developed countries, cause cumulative toxicity in patients (WHO, 2009). Newer and more patient friendly antiretroviral therapy may never reach the majority of infected individuals in low-income countries due to the high cost. Adverse effects have also been associated with HAART. For examples, drug-drug interactions among protease inhibitors (PIs) and nucleoside reverse transcriptase inhibitors (NRTIs) can cause undesirable effects on absorption. Resistant virus strains with rapid mutations have been an uphill tasks

in HIV therapy (Johnson *et al.*, 2008, Sinoussi, 1996). Prolonged treatment of antiviral drugs increases the rate of heart disease, diabetes, liver disease and cancer in aging HIV-infected patients (Bedimo, 2008, Florescu & Kotler, 2007).

1.3 Aim of study

In the present study, I aim (1) to generate HIV-protease activated maize RIP variants by substituting HIV-1 protease cleavage sites in the internal inactivation region, (2) to test the effectiveness of the removal of internal region of modified variants by HIV-1 protease *in vitro* and in HIV-infected cells, (3) to examine the *in vivo* N-glycosidase activity of modified variants after the removal of the internal inactivation region and (4) to investigate the anti-HIV activity of maize RIP and the variants, as well as the correlation with the N-glycosidase activity.

Chapter Two

Materials and methods

2.1 Materials

2.1.1 Chemicals

Chemical Reagents	Formula Weight	Source
2-mercaptoethanol (2-ME) (C_2H_6OS)	78.10	Sigma-Aldrich Coperation, USA
Acrylamide: Bis-acrylamide Solution 30% Ratio 37:5:1	/	Sigma-Aldrich Coperation, USA
Agarose powder	/	Sigma-Aldrich Coperation, USA
Ammonium persulfate (APS) ($(NH_4)_2S_2O_8$)	228.20	Sigma-Aldrich Coperation, USA
Ampicillin, sodium salt ($C_{16}H_{18}N_3NaO_4S$)	371.39	USB Corperation, USA
Bromophenol blue ($C_{19}H_{10}Br_4O_5S$)	669.96	Sigma-Aldrich Coperation, USA
Chloramphenicol ($C_{11}H_{12}C_{l2}N_2O_5$)	323.13	Sigma-Aldrich Coperation, USA
Comassie® Brilliant Blue R ($C_{45}H_{44}N_5O_7S_2Na$)	825.97	USB Coperation, USA
Deoxynucleotides (dNTP)	/	Novagen, germany
Ethanol (CH_3CH_2OH)	46.07	Merck, germany
Ethidium bromide (EtBr)	394.00	Amresco, USA
Ethylenediaminetetraacetic acid (EDTA) ($C_{10}H_{16}N_2O_8$)	292.24	Sigma-Aldrich Coperation, USA
GeneRuler™ DNA ladder Mix	/	Invitrogen Coperation, USA

Glycine ($C_2H_5NO_2$)	75.07	USB, USA
Hydrochloric acid (HCl)	36.46	Merck, germany
Isopropanol (C_3H_8O)	60.1	Merck, germany
LB agar	/	USB, USA
LB broth	/	USB, USA
Methanol (CH_4O)	32.1	Merck, Germany
Tetramethyl-Ethylene-Diamine (TEMED) ($C_6H_{16}N_2$)	116.24	Bio-Rad Laboratories Inc., USA
Phenylmethyl-sulfonyl fluoride (PMSF) ($C_7H_7FO_2S$)	174.19	Sigma-Aldrich Coperation, USA
Potassium chloride (KCl)	74.55	USB, USA
Potassium phosphate monobasic (KH_2PO_4)	136.09	Sigma-Aldrich Coperation, USA
Sodium acetate anhydrous (NaAc) (CH_3COONa)	82.03	Sigma-Aldrich Coperation, USA
Sodium chloride (NaCl)	58.4	USB, USA
Sodium Dodecyl Sulfate (SDS) ($CH_3(CH_2)_{11}OSO_3Na$)	288.38	Sigma-Aldrich Coperation, USA
Sodium phosphate dibasic dihydrate ($Na_2HPO_4 \bullet 2H_2O$)	177.99	Sigma-Aldrich Coperation, USA
Sodium hydroxide (NaOH)	40.00	Sigma-Aldrich Coperation, USA
Sucrose ($C_{12}H_{22}O_{11}$)	342.3	Sigma-Aldrich Coperation, USA
Tris ($C_4H_{11}NO_3$)	121.12	USB, USA

2.1.2 Buffers

2.1.2.1 Preparation of buffers

Buffer was prepared by dissolving chemicals in distilled water (dH_2O) and adjusted to the desired pH using HCl, NaOH or acetic acid unless otherwise specified.

2.1.2.2 Commonly used buffers

RF1 (competent cell preparation)

30 mM KAc, 100 mM $RbCl_2$, 10 mM $CaCl_2$, 50 mM $MnCl_2$, 15% glycerol. pH was adjusted to 5.8 by HAc and no back titration was performed. The solution was sterilized by filtration through a 0.2 μm filter.

RF2 (competent cell preparation)

10 mM MOPS, 75 mM $CaCl_2$, 10 mM $RbCl_2$, 15% glycerol. The pH was adjusted to 6.5 with KOH and the solution was sterilized by filtration through a 0.2 μm filter.

6X DNA loading buffer

0.25% (w/v) bromophenol blue, 40% (w/v) sucrose and 0.25% (w/v) xylene cyanol FF. The buffer was stored at 4°C.

50X TAE buffer stock

2 M Tris-acetate and 50 mM EDTA.

LB broth

20 g of LB broth powder (USB) was added to 1L dH_2O. The solution was sterilized by autoclaved. Ampicillin was used at 100 μg/ml (final concentration), respectively.

LB agar plate

35 g/L LB agar powder (USB) was added to 1L dH_2O. The solution was sterilized by autoclaved. Antibiotics were added to the agar media when their temperature fell below 60°C. Ampicillin was used at 100 μg/ml and 50 μg/ml (final concentration), respectively.

SDS running buffer

25 mM Tris base, 192 mM glycine and 0.1% (w/v) SDS

6X SDS loading buffer

12% (w/v) SDS, 375 mM Tris-HCl, 60% (v/v) glycerol, 0.01% bromophenol blue, 5% (v/v) β-ME, pH 6.8 and the buffer was stored at 4°C.

Commassie brilliant blue staining solution

Acetic acid, methanol and dH_2O were mixed in a ratio of 1:3:10. 0.05% (w/v)

Commassie brilliant blue R250 was then added.

Destain solution

40% (v/v) methanol and 10% (v/v) acetic acid.

Blocking Buffer

5% non-fat dry milk, 10 mM Tris pH 7.5, 100 mM NaCl, 0.1% Tween 20.

Transfer buffer

250 mM Tris base, 1.92 M glycine, 200 ml methanol, 1% SDS, pH 8.5

10X TBS buffer

100 mM Tris-HCl, 1.5 M sodium chloride, pH 7.6

RIPA buffer (Radio Immuno Precipitation Assay buffer)

150 mM sodium chloride, 1.0% NP-40, 0.5% sodium deoxycholate, 0.1% SDS and

50 mM Tris, pH 8.0.

2.1.3 Strains and plasmids

Complementary DNA (cDNA), Maize [Δ1-16, Δ287-300]-Pro-RIP (Pro-RIP-WT) and [Δ1-16, Δ163-164, Δ167-189, Δ287-300]-Pro-RIP (MOD-WT), obtained from Prof. R.S. Boston of Department of Botany, North Carolina State University, were used as template to perform Polymerase Chain Reaction (PCR) reaction. After amplification, the gene was inserted into the bacterial expression vector pET3a (Novagen). N-terminal TAT-fusion variants were generated by polymerase chain reaction mutagenesis. *Escherichia coli* (*E. coli*) strain DH5α (Novagen) was used for plasmid DNA amplification, and *E. coli* strain C41 (DE3) and BL21 (DE3) pLysS, (Novagen) were used for protein expression.

2.1.4 Primer list

The sequences of primers used in the study are list as follows:

TAT-Δ5aa Maize RIP- F (Forward primer)

5' -GGAATTCCATATGTACGGTCGTAAAAAACGTCGTCAGCGTCGTCGTAAGTTCACT GAAATCTTCCCCGTG-3'

Maize-RIP-R (Reverse primer)

5' -CGGGATCCTCAAGCCGCCGCAGTAGTTTG-3'

Pro-RIP-HIV-25-F (Forward primer)

5' -CCTATTGTTCAAAATATGCAGATGCCGGAG GTATCCCAGAACTAC-3'

Pro-RIP-HIV-25-R (Reverse primer)

5' -ATTTTGAACAATAGGATAATTTTGACTAAC-3'

253-3aa-F (Forward primer)

5'-CCTCAGATGCAGATGCCGGAGCCTGTATCCCAGAACTACCCCATCGTAGCCGACAC

GAAGAGC -3'

253-3aa-R (Reverse primer)

5'-CATCTGCATCTGAGGCTGATTTTGTACAATAGGATAATTTTGTTTCTTTTTCTTCGCC

AG -3'

253-2aa-F (Forward primer)

5'-CCTCAGATGCAGATGCCGGAGCCTGAGGTATCCCAGAACTACCCCATCGCC

GACACGAAGAGC -3'

253-2aa-R (Reverse primer)

5'-CATCTGCATCTGAGGCATCTGATTTTGTACAATAGGATAATTTTTCTTTTTCTTCGCC

AG -3'

HIV-1RT/IN-F (Forward primer)

5'-TTTTTAGATGGACGAAAGATTCTTTTCCTTGACGGGGCGGCTGACCCACAG-3'

HIV-1RT/IN-R (Reverse primer)

5'-TAGTATTTTCCGTATGCCGTCGAGGAAGAGGATCTTGCGCTTCTTCTTCTTCGC-3'

HIV-1p2/NC-F (Forward primer)

5'-ATGCAACGTGGTAATGCAACAATAATGATGCAGCGAGGAGCGGCTGACCCACAG-3

'

HIV-1p2/NC-R (Reverse primer)

5'-CATAATAGTAGCGCCGCGCTGCATCATGATGGTGGCCTTCTTCTTCTTCGC-3'

RIP-upstream-F (Forward primer)

5' -GATGTCGGCTCTTCCTATCATTGT-3'

RIP-upstream-R (Reverse primer)

5' -CCAGCTCACGTTCCCTATTAGTG -3'

RIP-downstream-F (Forward primer)

5' -TGCCATGGTAATCCTGCTCAGTA-3'

RIP-downstream-R (Reverse primer)

5' -TCTGAACCTGCGGTTCCACA-3'

2.2 Methods

2.2.1 Preparation of competent cells

E.coli DH5α and C41 competent cells from -80°C glycerol stock were streaked on an LB agar plate (DH5α and C41) and incubated at 37°C overnight. Starter culture was prepared by picking a single colony and inoculated into 5 ml LB medium. The culture was shaken at 37°C with 250 rpm until OD600 reached 0.3. Then, the culture was transferred into 100 ml of medium and continued shaking at 37°C until OD600 reached 0.45. The cells were placed on ice for 5 min. The bacteria were then collected by centrifugation at 8000 rpm (7000 g) for 10 min at 4°C (Beckman JA-14 rotor). The cell pellet was resuspended in 40 ml of RF1 and kept on ice for 5 min. Then, cells were re-centrifuged and the pellet was resuspended in 4ml of RF2. The suspension was kept on ice for 15 min and then divided into 100 µl

aliquots and snap-frozen in liquid nitrogen. The cells were stored at -80°C until used.

2.2.2 Molecular cloning

2.2.2.1 Amplification of target genes by PCR

PCRs were used to amplify and add restriction sites to the target genes. A pair of primers was designed to anneal to the DNA template. The primers acted in forward (5' to 3' with respect to the reading frame) and reverse (3' to 5' with respect to the reading frame) pair. The primers were designed so there was no self-complementation between the primer pairs. PCRs were performed to amplify the target genes (Appendix table 1). Composition of reaction mixture and the general reaction scheme are listed in Tables 2.1 and 2.2 respectively. The reactions were carried out by Phusion High-Fidelity DNA Polymerase (Finnzymes) in 500 µl eppendorf tubes in a MJ PTC-100, where lid heating was available. The resulting DNA products were analyzed by agarose gel electrophoresis or stored at -20°C.

Table 2.1 PCR amplication mixture	
Distilled water	35.5 µl
5X HF buffer	10 µl
10mM dNTPs (2.5 mM each of dATP, dCTP, dGTP and dTTP)	1 µl
Forward primer (25 µl)	1 µl
Reverse primer (25 µl)	1 µl
DNA Template	1 µl
Phusion Taq (5 U/µl)	0.5 µl
Total	50 µl

Table 2.2 PCR cycle				
		Temperature	Time	Number of cycles
Initial denatureation		95°C	5min	
	Denaturation	95°C	30 sec	
	Annealing	55°C	30 sec	35
	Elongation	72°C	90 sec	
Final extension		72°C	10 min	
	End	4°C	∞	

2.2.2.2 Agarose gel electrophoresis

Agarose gel 1.0 % (w/v) was prepared with 1 µl of ethidium bromide (10 mg/ml) added. PCR products were mixed with 6X loading buffer to give a final concentration of 1X. The gel was submerged into a gel tank containing 1X TAE buffer. After loading the samples and GeneRuler^{TM} DNA Ladder Mix (Invitrogen) into the wells, electrophoresis was performed with a constant voltage of 120 V. The agarose gel was then placed onto a Spectroline TC-302 transilluminator (302 nm) for the visualization of DNA.

2.2.2.3 Extraction and purification of DNA

Protocol was modified from the instructions provided by the manufacturer (Gel *Advanced*™ Gel Extraction Miniprep System, Viogene). Target DNA fragment was excised from the agarose gel with the illumination of a Spectroline UV transilluminator. 500 µl of GEX buffer was added to the Eppendorf tube containing the gel slice. The mixture was incubated at 60°C until the gel completely dissolved. A column was placed onto a collection tube and the gel mixture was loaded onto the column. The column was then centrifuged at 13,000 rpm (12,110 g) for 30 s using a desktop centrifuge (Minispin, Eppendorf) and the flow-through was discarded. The column was then washed with 500 µl of WF buffer and then centrifuged at 13,000 rpm (12,110 g) for 30 s. The flow-through was discarded. After that, the column was washed with 700 µl of WS buffer containing ethanol and then centrifuged at 13,000 rpm (12,110 g) for 30 s. The column was further centrifuged for 3 min to remove all residual buffer. After that, the column was placed onto a new Eppendoff tube and 30 µl of warm water (65°C) was added onto the column membrane. It was allowed to stand at room temperature for 2 min. DNA was then eluted through centrifugation at 13,000 rpm (12,110 g) for 2 min.

2.2.2.4 Restriction digestion of DNA

Gel-purified DNA fragments and pET3a vector were digested by BamHI and NdeI (New England Biolabs Inc.) in the buffer recommended by the manufacturer at 37°C for 2 h. Detailed conditions for restriction digestion are listed in Table 2.3. After digestion, 6X DNA loading dye was added to stop the reaction and the reaction mixture was analyzed by agarose gel electrophoresis as described in Section 2.2.2.2. Target DNA fragment was extracted and purified from the gels by Gel *Advanced*™ Gel Extraction Miniprep System as described in Section 2.2.2.3 for subsequent ligation.

Table 2.3 Restriction enzyme digestion mixture

	pET3a Vector	Insert
Undigested vector / insert	10 µl	27 µl
10X BamHI buffer	2 µl	4 µl
BamHI	1 µl	1 µl
NdeI	1 µl	1 µl
Distilled water	6 µl	7 µl
Total	20 µl	40 µl

2.2.2.5 Ligation of digested DNA fragment and expression vector

Ligation reaction of digested PCR products and vectors were set up as shown in Table 2.4. Ligation mixtures were incubated at 16°C for 16 h using T4 DNA ligase (New England BioLabs Inc.), followed by transformation to competent cells for plasmid amplification.

Table 2.4 Ligation mixture	
10X T4 ligase buffer	2 μl
Linealized plasmid	5 μl
Digested DNA insert	12 μl
T4 DNA ligase (400 U/μl)	1 μl
Total	20 μl

2.2.2.6 Transformation and selection of transformants

Ligation products were incubated with 100 μl of *E. coli* strain DH5α competent cells on ice for 30 min, then heat-shocked at 42°C for 2 min and cold-shocked for 10 min on ice. LB medium (900 μl) was added to the cells for recovery for 1 h at 37°C with constant shaking at 250 rpm. Then, cells were centrifuged at 13,000 rpm (12,110 g) for 1 min and cell pellet was resuspended by the residual supernatant (~100 μl) and spread on LB agar plates with ampicillin. The plates were incubated at 37°C for 16 h.

2.2.2.7 Verification of insert by PCR

To confirm colonies carry the plasmid with the desired inserts, well-separated colonies of the transformed DH5α cells on LB agar plates were picked by toothpicks and subjected to PCR using primer pairs in the original amplification reactions (Section 2.2.2.1). The composition of PCR reaction mixture and the reaction scheme are listed in Table 2.5 and 2.6 respectively. The PCR products were then analyzed by

agarose gel electrophoresis.

Table 2.5 PCR reaction for verification of plasmid	
5X HF buffer	10 µl
Plamsid DNA	1µl
10mM dNTPs (2.5 mM each of dATP, dCTP, dGTP and dTTP)	1 µl
TAT-Δ5aa Maize RIP- F (forward primer) (25 µM)	1µl
Maize-RIP-R (reverse primer) (25 µM)	1µl
Taq DNA polymerase (5 U/µl)	1µl
Distilled water	35µl
Total	50 µl

Table 2.6 PCR condition for verification of plasmid

		Temperature	Time	Number of cycles
Initial denatureation		95°C	5min	
	Denaturation	95°C	30 sec	
	Annealing	55°C	30 sec	35
	Elongation	72°C	90 sec	
Final extension		72°C	10 min	
	End	4°C	∞	

2.2.2.8 Extraction and purification of plasmid DNA

Positive clones checked as described in Section 2.2.2.7 were picked and inoculated into 5 ml of LB medium with 100 µg/L of ampicillin and incubated at 37°C for 16 h with constant shaking at 250 rpm. The procedures of plasmid extraction were modified from the instructions provided by the manufacturer (Mini *Plus*™ Plasmid DNA Extraction system, Viogene). Overnight bacterial culture was

centrifuged at 13,000 rpm (12,110 g) by desktop centrifuge (Minispin, Eppendorf) for 30 s. Supernatant was discarded and 250 µl of MX1 buffer was added to resuspend the cell pellet. 250 µl of MX2 buffer was then added and the tubes were inverted gently for several times to lyse the cells until the lysate was clear. The mixture was then incubated at room temperature for 5 min. Then, 350 µl of MX3 was added and mixed immediately by inversion for several times until white precipitate was formed, followed by centrifugation at 13,000 rpm (12,110 g) for 10 min. After centrifugation, supernatant was transferred to a DNA-binding column sitting on a collection tube, and centrifuged at 13,000 rpm (12,110 g) for 30 s. Flow-through was discarded. Then, 500 µl of WF buffer was added and centrifuged at 13,000 rpm (12,110 g) for 30 s to wash the membrane. Flow-through was discarded. 700 µl of WS buffer was then added and centrifuged at 13,000 rpm (12,110 g) for 30 s to wash the column. Flow-through was discarded. As any residual ethanol could affect the quality of DNA and inhibit subsequent enzymatic reactions, the column was further centrifuged for 3 min to remove all residual ethanol. Finally, the column was transferred to a clean eppendorf tube and 50 µl of warm water (65°C) was added onto the column membrane. After incubation at room temperature for 2 min, the column was centrifuged at 13,000 rpm (12,110 g) for 2 min to elute purified DNA. Purified plasmid DNA was stored at -20°C.

2.2.2.9 Confirmation of insertion in plasmid DNA

2.2.2.9.1 Restriction enzyme digestion

Restriction digestion was performed at 37°C for 2 h. Details of the reaction mixture are listed in Table 2.7. After digestion, 6X DNA loading dye was added to stop the reaction and the DNA insert was analyzed by agarose gel electrophoresis.

Table 2.7 Restriction enzyme digestion for verification of plasimd

Purified plasmid	4 µl
10X BamHI buffer	2 µl
BamHI	0.5 µl
NdeI	0.5 µl
Distilled water	13 µl
Total	20 µl

2.2.2.9.2 DNA sequencing

Sequence of verified plasmid DNA was carried out by Tech Dragon Limited. The sequencing results were aligned with the original target sequence using the program ClustalW (Pearson, 1990) to check if the sequence contained any undesired mutations.

2.2.3 Expression of recombinant maize RIP

2.2.3.1 Transformation

Plasmid DNA were used to transform freshly thawed *E. coli* strain C41

competent cells by incubating 1 μl of the plasmids with 100 μl competent cells on ice for 30 min. A heat shock at 42°C for 2 min and cold shock for 10 min on ice were then applied. The mixtures were then plated out onto LBA plate and incubated at 37°C for 16 h.

2.2.3.2 Preparation of starter culture

A well-separated bacterial colony was picked and inoculated into 20 ml LB medium with 100 μg/L ampicillin. The culture was incubated at 37°C for 16 h with shaking at 250 rpm.

2.2.3.3 Expression of recombinant proteins

The starter culture was centrifuged and inoculated to 1 L of LB culture medium. The culture medium was then incubated at 37°C at 250 rpm. When OD600 reached 0.4-0.6, IPTG was added to a final concentration of 0.4 mM for induction. The broth was allowed to grow for 16 h at 25°C with shaking at 250 rpm.

2.2.3.4 Cell harvesting

Cells were harvested by centrifugation at 4°C, 8,000 rpm (7000 g) for 10 min (Beckman JA-14 rotor). The supernatant was discarded, and the cell pellet was either

resuspended in sonication buffer or stored at -20°C.

2.2.3.5 Releasing the cell content

Cell pellets derived from 1 L of culture was resuspended in 40 ml sonication buffer A (50mM sodium acetate buffer, 100mM NaCl and 8M urea, pH 5.5) with 1 mM PMSF. The cells were then lysed by sonication on ice, with a medium probe for 10 cycles of 30 s bursts, each with 30 s intervals (Branson sonifier 250). Cell lysate was then centrifuged at 4°C, 20,000 rpm (31,360 g) for 45 min (Beckman JA-20 rotor) to remove cell debris. Whole lysate, supernatant and pellet were analyzed by Sodium Dodecyl Sulfate Polyacrylamide Gel Electrophoresis (SDS-PAGE).

2.2.3.6 SDS-PAGE analysis of protein expression

SDS-PAGE was performed using a Mini-PROTEAN 3 Electrophoresis Cell (Bio-Rad). The apparatus was set up according to the manufacturer's instructions. Resolving gel (Separating gel) solution was transferred into the space between the inner and outer glass plates. 200 µl of isopropanol was added on top of the gel to ensure a horizontal gel surface and to keep the gel solution away from atmospheric oxygen which inhibits polymerization of acrylamide. After the resolving gel has polymerized, isopropanol was removed, and stacking gel solution was added on top

of the resolving gel. A comb with a 10- or 15-well former was inserted into the stacking gel before polymerization. Details of gel composition are listed in Table 2.8. After the stacking gel was solidified, the comb was removed and the gel cassette was then assembled into an electrophoresis cell. The inner and the outer chambers were filled with fresh SDS running buffer. 6X SDS gel loading buffer was added to the protein samples, followed by denaturation at 95°C for 5 min. Protein samples were then loaded into the wells and Precision Plus Protein Unstained Standards (Bio-Rad) was used as a marker. A constant current of 35 mA per gel was applied until the dye front reached the bottom of the gel. After that, the gel was disassembled from the glasses and stained with Commassie brilliant blue staining solution for 1 h and subsequently destained by destain solution. Finally, the gel was equilibrated in distilled water.

Table 2.8 Composition of resolving and stacking SDS-PAGE gel	
Resolving gel (15%)	
Distilled water	1.7 ml
30% acrylamide solution (Acrylamide: Bis-acrylamide = 40:1)	3.75 ml
1.5 M Tris (pH 8.8)	1.9 ml
10% SDS	75 µl
APS	75 µl
TEMED	3 µl
Total	7.5 ml
Stacking gel (5%)	
Distilled water	2.7 ml
30% acrylamide solution (Acrylamide: Bis-acrylamide = 40:1)	0.65 ml
1.0 M Tris (pH 6.8)	0.5 ml
10% SDS	40 µl
APS	40 µl
TEMED	4 µl
Total	4 ml

2.2.4 Purification of TAT-fused maize RIP and variants

2.2.4.1 Cation-exchange chromatography

Cell lysate was collected by centrifugation at 4°C and loaded onto a HiTrap™ SP FF column (GE Healthcare) pre-equilibrated with 5 bed-volume of buffer A (50 mM sodium acetate, 100 mM NaCl and 8 M urea, pH 5.5), at 1 ml/min. Then, buffer A was used to wash the column at 2 ml/min to remove unbound proteins. Protein was eluted using a gradient of 0–1 M NaCl in buffer B (50 mM sodium acetate, 1 M NaCl, pH 5.5) at 2 ml/min. Fractioned proteins were analyzed by 15% SDS-PAGE electrophoresis. Fractions with target protein were pooled for the next

cation-exchange chromatography.

HiTrap™ SP XL column (GE Healthcare) was pre-equilibrated with 5 bed-volume of buffer C (50 mM sodium acetate, 100 mM NaCl and 4 M urea, pH 5.5) at 1 ml/min. Fractions of target protein collected after SP-FF chromatography were pooled and diluted to 5-fold using buffer C (50 mM sodium acetate, 100 mM NaCl and 4 M urea, pH5.5), and then loaded onto the pre-equilibrated column. The protein was eluted using a gradient of 0–1 M NaCl in buffer D (50 mM sodium acetate, 1M NaCl, pH5.5). Fractioned proteins were analyzed by 15% SDS-PAGE electrophoresis. Target proteins were pooled for further purification.

The pI values of TAT-fused proteins were about 9.8. At pH 5.5, the target proteins are positive charged and bind to cation exchange resins. The aim of two rounds cation exchange chromatography is for step-wise removal of urea, as well as the other cytoplasmic proteins in the target fractions.

2.2.4.2 Desalting chromatography

Concentrated target proteins were further purified by desalting column in order to remove urea. HiPrep™ 26/10 Desalting Column was pre-equilibrated with Buffer D (10 mM Tris–HCl, 1 mM EDTA, 10% glycerol, pH 7.0) at 5 ml/min. Protein (5 ml) was loaded onto pre-equilibrated column at 4 ml/min. Fractioned proteins were

analyzed by 15% SDS-PAGE electrophoresis. Fractions containing target protein were concentrated by Amicon Centricon Centrifugal Filtration Device with membrane cut-off values of 10 kDa (Millipore). Protein concentration was determined by measuring OD280 and applying the Beer-Lambert law (Section 2.2.8). Cocktail of protease inhibitors (Roche) was added to the protein solution which was stored at -80°C.

The purpose of using desalting chromatography is for buffer exchange. The target protein was finally stored in neutral buffer system without urea (pH 7.0) for further enzymatic and anti-HIV assays performed in cell system.

2.2.4.3 Determination of protein concentration

Absorbance of protein solution at 280 nm was determined for quantitation of protein. Extinction coefficient for the protein was estimated by ProtParam (http://au.expasy.org/tools/protparam.html). Concentration of the protein was estimated by applying the Beer-Lambert Law:

$$\mathbf{A} = \varepsilon \mathbf{l} \mathbf{c}, \text{ where,}$$

A = Absorbance ε = Molar extinction coefficient ($M^{-1}cm^{-1}$) l = Path length of sample (cm)

c = Concentration of compound in solution (M^{-1})

2.2.5 Cell culture

2.2.5.1 Cell lines

Cell lines, C8166 and J774A.1, were purchased from American Type Culture Collection (ATCC). RPMI 1640 supplement with 10% fetal bovine serum (FBS) was used to culture human lymphocyte cells C8166. Dulbecco's modified Eagle's medium (DMEM) supplemented with 10% FBS was used for mouse macrophage cells J774A.1. Unless mentioned otherwise, the cells were grown in a 95% O_2, 5% CO_2 water saturated incubator at 37°C. Culture media were changed two times per week and sub-cultured whenever confluence was reached.

2.2.5.2 Viruses

HIV-1_{IIIB} (subtype B) and HIV-1 RF/V82F/I84V were obtained from the culture supernatant of H9/HIV-1_{IIIB} and MT-2/HIV-1 RF/V82F/I84V cells respectively. HIV-1 RF/V82F/I84V virus includes single and double protease gene mutant strains which were selected *in vitro* in the presence of the protease inhibitors DMP323 (a cyclic urea protease inhibitor) or P9941 (a C-2 symmetrical diol protease inhibitor). The 50% HIV-1 tissue culture infection dose ($TCID_{50}$) in C8166 cells was determined and calculated by the Reed and Muench method (Dulbecco, 1988). Virus stocks were stored in aliquots at -70°C. The titer of virus stock was 3.4×10^6 $TCID_{50}$

per ml (Wang *et al.*, 2008).

2.2.6 N-glycosidase activity assay by quantitative polymerase chain reaction

2.2.6.1 Cell treatment

J774A.1 (1×10^6 per dish) in 2 ml DMEM with 10% FBS were plated in tissue culture dish (60 × 15mm) for attachment overnight. Human T lymphocytes (C8166) (1×10^6 per dish) in 2 ml RPMI with 10% FBS were plated in tissue culture dish (60 × 15 mm). Protein samples (5 μM) were added and incubated for 6 hr. After incubation, medium was removed and cells were washed once by ice-cold PBS.

2.2.6.2 RNA isolation

RNA was isolated from treated cells using modified TRIZOL RNA isolation protocol (Chomczynski & Mackey, 1995). Cells were lysed directly by adding 1 ml TRIZOL reagent into tissue culture dish and incubated at room temperature for 5 min. Lysed samples were transferred to Diethylpyrocarbonate (DEPC)-treated Eppendorf tubes and frozen at -20°C overnight. 200 μl chloroform was added, mixed vigorously by inverting the tubes and incubated at room temperature for 10 min. Samples were then centrifuged at 13,000 rpm (12,110 g) for 20 min at 4°C. The top clear layers were collected and transferred to new Eppendorf tubes and equal volume of

isopropanol was added for RNA precipitation. Then, samples were centrifuged at 13,000 rpm (12,110 g) for 20 min at 4°C. Colorless pellets were then formed at the bottom of tubes and supernatants were discarded. Ethanol was then added to wash the pellets. After centrifugation of samples at 13,000 rpm (12,110 g) for 15 min at 4°C, ethanol was removed. The last drop of ethanol was discarded by additional centrifugation at 13,000 rpm (12,110 g) briefly at 4°C. RNA was finally dissolved in 30 ml of DEPC distilled water and stored at -80°C.

2.2.6.3 cDNA synthesis

RNA was reverse-transcribed with SuperScript™ II Reverse Transcriptase kit (Invitrogen). RNA samples (5 μg) were prepared by adding DEPC distilled water to final volume 11 μl. Then, dNTP mix (1 μl) were added and mixed well with RNA samples. The reaction samples were incubated at 65°C for 5 min. The reaction tubes were then placed on ice before addition of 4 μl 5X First Strand Buffer and 2 μl 0.1 M DTT. The reaction tubes were then incubated at 42°C for 60 min followed by additional incubation at 70°C for 15 min. cDNA samples were stored at -20°C before use.

2.2.6.4 Quantitative real-time PCR

Quantitative real-time PCR (qRT-PCR) was performed in Applied Biosystems® 7500 Fast Real-Time PCR System (Applied Biosystems) using Power SYBR® Green PCR Master Mix kit (Applied Biosystems). cDNA samples were diluted 10 to 10000-fold from the reverse transcription reaction. The real-time PCR reaction solutions were set up according to the kit manual (Table 2.9) and the PCR conditions are listed as below (Table 2.10). Two primer sets were used in the present study. The upstream primer set was designed to detect total 28S rRNA , whereas the downstream primers detect the altered sequences by the N-glycosidase activity of RIP (Melchior & Tolleson, 2009).

Table 2.9 Real-time PCR reaction for N-glycosidase activity

Control gene	
cDNA template	1 μl
Upstream forward primer (5 μM)	1 μl
Upstream reverse primer (5 μM)	1 μl
SYBR® Green PCR Master Mix	10 μl
Distilled water	7 μl
Total	20 μl

Target gene	
cDNA template	1 μl
Downstream forward primer (5 μM)	1 μl
Downstream reverse primer (5 μM)	2 μl
SYBR® Green PCR Master Mix	10 μl
Distilled water	6 μl
Total	20 μl

Table 2.10 Real-time PCR condition for N-glycosidase activity		
Temperature	Time	No. of cycle
95°C	10 min	
95°C	10 sec	35
60°C	30 sec	

2.2.7 Cytotoxicity assay

MTT (3-(4, 5-dimethylthiazolyl-2)-2, 5-diphenyltetrazolium bromide) cell viability assay was performed on HIV-1_{IIIB} acutely infected or non-infected human T-cells. Cell medium (100 µl) containing C8166 cells were seeded on 96-well plate (3×10^4 cell/ well) while the outmost rows filled with 200 µl actoclaved distilled water. 100µl of six different concentrations of proteins were added and incubated at 37°C in 5% CO_2 for 72h followed by incubation with MTT (5mg/ml) for 4h, then 100µl 50% DMF-10% SDS was then added. After the formazum was dissolved completely, 595nm/630nm values were measured using a colorimetric microplate reader (Model 3550, Bio-Rad). The result was presented in terms of percentage to control as mean ± SEM. Two-way ANOVA with Bonferroni test as the post hoc test for multiple comparisons was used to compare cell viability after treatment with different proteins.

2.2.8 Syncytium formation assay

Six different concentration of proteins (100 μl) were added in a 96-well plate. C8166 cells (3×10^4 cells/well) were seeded and inoculated with 100 $TCID_{50}$ HIV-1 or HIV-1 RF/V82F/I84V and then incubated at 37°C in a humidified incubator with 5% CO_2 for 72h. Control assays were performed without the testing proteins in HIV-1-infected and uninfected cultures. The number of syncytium in each well was counted under light microscope. Percentage inhibition of syncytial cell formation was calculated from the percentage of syncytial cell number in treated culture compared with that of the infected control culture (Wang *et al.*, 2008).

2.2.9 p24 ELISA assay

HIV-1 p24 antigen in cell-free medium was measured using capture ELISA as described previously (Zheng *et al.*, 2000). Briefly, 96-well plates were coated with McAb p5F1 followed by blocking with 5% skim milk, then triton X-100-treated cell-free culture medium was added, and incubated for 2h at 37°C. The plates were then incubated with diluted human polyclonal anti-HIV-1 sera, followed by incubation with HRP-labeled goat anti-human IgG and OPD (O-phenylenediamine dihydrochloride) substrate. The plates were read by Bio-Tek ELx 800 ELISA reader at 490/630 nm within 30min of stopping the reaction. The inhibition percentage of

p24 antigen expression was calculated. The concentration of proteins reducing p24 antigen expression by 50% (EC_{50}) was determined from the dose-response curve.

2.2.10 Expression and purification of HIV-1 protease

Plasmid containing the cDNA of HIV-1 protease was kindly provided by Dr. C.C. Wan, School of Biomedical Sciences, The Chinese University of Hong Kong. HIV-1 protease was cloned into expression vector pET3b and transformed into *E. coli* BL21 (DE3) pLysS, and glycerol stocks of transformed *E. coli* were prepared for storage at -80°C. Single colony was inoculated to 1L of LB broth with 100 μg/ml ampicillin and chloramphenicol. The bacterial culture was incubated at 37°C with shaking at 250 rpm, until OD600 reached 0.3-0.5, then 0.4 mM IPTG was added for protein induction at 37°C for 3 h and harvested as described in Section 2.2.2.4.

HIV-1 protease was expressed as inclusion bodies and purified as described (Lin *et al.*, 1994). The cell pellet was resuspended in ice-cold buffer X (10 mM Tris, centrifuged at 10,000 g for 10 min (Beckman JA-25.5 rotor) and the pellet was washed by ice-cold buffer X containing 1% (v/v) Triton X-100. The suspension was re-centrifuged and the pellet was dissolved in buffer B (10 mM Tris (pH 7.5), 8 M urea and 10 mM dithiothreitol). The soluble protease was collected by centrifugation at 20,000 rpm (31,360 g) (Beckman JA-20 rotor) and loaded onto 5 ml HiTrap™

DEAE-FF column (GE Healthcare). The protease containing breakthrough was collected and refolded by dialysis at 4°C for 4-10 h against 4 L 1mM DTT, 1% (v/v) glycerol, and 10 mM sodium acetate, pH 3.5. Precipitant was removed by centrifugation at 10,000g for 20 min (Beckman JA-25.5 rotor). The supernatant was further dialyzed against 10 mM sodium acetate, pH 3.5, for 2 h at 4°C and concentrated by Amicon Centricon Centrifugal Filtration Device with membrane cut-off values 5 kDa (Millipore). The protease was stored at -80°C.

2.2.11 Cleavage of TAT-fused maize RIP variants

2.2.11.1 *In vitro* cleavage of TAT-fused maize RIP variants

HIV-1 protease cleavage reactions are listed in Table 2.11. Small-scaled and large-scaled digestions were performed separately by incubating protein samples with purified recombinant HIV-1 protease at 37°C for 16 h. Negative control was set up by using distilled water instead of HIV-1 protease. After incubation, 6X SDS loading buffer was added to 20 µl reaction solution and incubated at 95°C for 3 min. The proteins were then resolved in 15% SDS PAGE and analyzed by Western Blot analysis listed in 2.2.4.12.2.

Table 2.11 *In vitro* digestion of TAT-fused maize RIP and variants by HIV-1 protease

Small – scale digestion	
50 mM sodium acetate buffer (pH 5.5)	2 µl
TAT-fused maize RIP (100 µM)	10 µl
Purified HIV-1 protease (5 mg/ml)	3 µl
Distilled water	5 µl
Total	20 µl

Large – scale digestion	
50 mM sodium acetate buffer (pH 5.5)	45 µl
TAT-fused maize RIP (100 µM)	280 µl
Purified HIV-1 protease (5 mg/ml)	80 µl
Distilled water	45 µl
Total	450 µl

2.2.11.2 Cleavage of TAT-fused maize RIP variants in HIV-infected cells

HIV-1_{IIIB} acutely infected human T-cell C8166 cell line (1×10^6/ml) was incubated with maize RIP variants (0.2mg/ml) at 37°C for 72 h before isolation of cytoplasmic proteins. The cells were washed thoroughly with 5ml ice-cold PBS twice before trypsinization at 37°C for 10 min. Cell pellets were then washed with 5 ml ice-cold PBS, then were resuspended and lyzed in 200µl modified RIPA buffer with 1mM PMSF. Cytoplasmic proteins were isolated from cell debris by centrifugation at 13000 rpm (12,110 g), 4°C for 15 min. Isolated protein solution was then mixed with 6X SDS loading buffer and incubated at 95°C for 3 min. The proteins were then resolved in 15% SDS PAGE. The cellular uptake of proteins and

the removal of internal inactivation region *in vivo* were detected by Western blot analysis list in 2.2.4.12.2.

2.2.11.3 Western Blot analysis

PVDF (polyvinylidene difluoride) membrane were first immersed in methanol for 30 sec and transferred to transfer buffer for 3-5 min. The resolved proteins were transferred from gel to PVDF (polyvinylidene difluoride) membrane by semi-dry transfer at 10 mA for 30 min in transfer buffer. The membranes were then removed from the transfer apparatus and immediately placed into blocking buffer for 30 min at 37°C. For the incubation with primary antibody, anti-MOD polyclonal antibody was diluted (1:10000) in 5 ml blocking buffer. The blot was then removed from the blocking buffer and incubated with the primary antibody solution overnight at 4°C. After primary antibody blotting, the primary antibody solution was decanted and 5 ml wash buffer (1X TBS buffer with 0.1% Tween 20) was added and washed for 30 min with agitation, with the wash buffer changed every 5 min. The secondary antibody (anti-rabbit IgG) (Santa Cruz Biotechnology, Inc.) was diluted (1:5000) in 5 ml blocking buffer and added to the blot. The blot was then incubated with agitation for 1 hr at room temperature. Afterwards, the secondary antibody solution was decanted and 5 ml wash buffer was added and rinsed for 30 min with agitation, with

the wash buffer changed every 5 min. The blot was placed in a clean tray containing chemiluminescent working solution (Amersham ECL Western bloitting detection reagents and ananlysis system, GE Healthcare). The final volume required was 0.125 ml/cm^2 membrane. The tray was shaken on an orbital shaker for 1-2 min. The membrane was then placed on a clean wrap and excessive detection reagent and air bubbles were drained off and smoothed out gently. The wrapped blot was then placed in an X-ray film cassette and exposed to a sheet of X-ray film (Super HR-T 30, Fujifilm). After exposure of 15-60 sec, the film was developed immediately.

Chapter Three

Design of HIV-1 protease-activated maize RIP

3.1 Introduction

3.1.1 Structure of maize RIP

Walsh and colleagues have first purified and characterized a unique class of RIP which is generated as an inactive precursor (34-kDa) in the endosperm of maize (*Zea mays* L.). During germination, the precursor is activated by proteolytic processing and converted into a two-chain form by eliminating 16 aa at the N-terminus (residues 1-16), a 25 aa central region (residues 163-187) and a 14 aa C-terminus region (residues 287-300) (Figure 3.1) (Walsh *et al.*, 1991). The active form consists of two subunits which are tightly associated without covalent linkage. By constructing different recombinant maize RIP variants with deletion of different inactivation regions, Walsh's group has found that the 25 aa central region governs the major inactivation. The removal of this internal region increases the inhibition of protein synthesis in rabbit reticulocyte lysate by over 600 folds, whereas removal of the N or C-terminal region merely increase the activity by six and five folds respectively (Hey *et al.*, 1995).

The crystal structure of two synthetic forms of maize RIP has been solved by Mak and colleagues in 2007, which is the first type III RIP structures reported (Figure 3.2). Pro-RIP is an inactive precursor with the 16-aa N-terminal and 14-aa C-terminal sequences deleted. MOD is an one-chain active form where two amino acid residues Leu-Glu tether the two chain of the naturally mature maize RIP. The crystal structure of the two forms are highly similar, except the presence of the internal inactivation loop (Ala163-Asp189) on the protein surface of Pro-RIP (Mak *et al.*, 2007). The secondary structure of the crystal structure of MOD and its solution structure by NMR sepectrometry were comparable (Yang *et al.*, 2010): most α-helices and β-strands are similar in length. Although it only has 15-21% sequence homology, maize RIP's N-glycosidase domain is structurally similar to other representatives of type I and II RIPs. The active site residues including Tyr94, Tyr130, Glu207, Arg210 and Trp241 at the cleft between N- and C- terminal are also conserved (Mak *et al.*, 2007, Yang *et al.*, 2007; 2010). Based on *in silico* docking, the internal loop region is found to sterically hinder the interaction of maize RIP with the ribosome by preventing the proper placing of the adenine ring of A-2697 of yeast ribosomes (analogous to A-4324 in rat 28S rRNA) to the active site pocket. Pull-down assay illustrated that Pro-RIP cannot interact with rat ribosomes and surface plasmon resonance analysis showed that the dissociation constant (K_D) of

Pro-RIP on purified rat ribosomes is about 80-fold higher than that of MOD (Mak *et al.*, 2007).

The presence of the internal inactivation region has led us to derive a novel strategy to enhance the specificity of maize RIP towards HIV-infected cells while minimizing its cytotoxic effect on normal cells. In this study, I provide an account on the generation of HIV-1 protease-activated maize RIP variants by incorporating HIV-1 protease recognition sequences to the internal inactivation region of the inactive precursor (Pro-RIP) (Figure 3.3).

```
Maize_RIP_inactive_precursor    MAEITLEPSDLMAQTNKRIVPKFTEIFPVEDANYPYSAFIASVRKDVIKH 50
One-chain_active_form (MOD)     M---------------KRIVPKFTEIFPVEDANYPYSAFIASVRKDVIKH 35
                                ********************************

Maize_RIP_inactive_precursor    CTDHKGIFQPVLPPEKKVPELWFYTELKTRTSSITLAIRMDNLYLVGFRT 100
One-chain_active_form (MOD)     CTDHKGIFQPVLPPEKKVPELWFYTELKTRTSSITLAIRMDNLYLVGFRT 85
                                **************************************************

Maize_RIP_inactive_precursor    PGGVWWEFGKDGDTHLLGDNPRWLGFGGRYQDLIGNKGLETVTMGRAEMT 150
One-chain_active_form (MOD)     PGGVWWEFGKDGDTHLLGDNPRWLGFGGRYQDLIGNKGLETVTMGRAEMT 135
                                **************************************************

Maize_RIP_inactive_precursor    RAVNDLAKKKKMATLEEEEVKMQMQMPEAADLAAAAAADPQADTKSKLVK 200
One-chain_active_form (MOD)     RAVNDLAKKKKM------------------------ADPQADTKSKLVK 160
                                ************                        ************

Maize_RIP_inactive_precursor    LVVMVCEGLRFNTVSRTVDAGFNSQHGVTLTVTQGKQVQKWDRISKAAFE 250
One-chain_active_form (MOD)     LVVMVCEGLRFNTVSRTVDAGFNSQHGVTLTVTQGKQVQKWDRISKAAFE 210
                                **************************************************

Maize_RIP_inactive_precursor    WADHPTAVIPDMQKLGIKDKNEAARIVALVKNQTTAAAATAASADNDDDE 300
One-chain_active_form (MOD)     WADHPTAVIPDMQKLGIKDKNEAARIVALVKNQTTAAA------------ 248
                                ************************************

Maize_RIP_inactive_precursor    A 301
One-chain_active_form (MOD)     -
```

Figure 3.1 Amino acid sequence alignment of the inactive precursor and the active form of maize RIP (MOD) (Hey *et al.*, 1995). Maize RIP inactive precursor is from NCBI accession no. P28522.

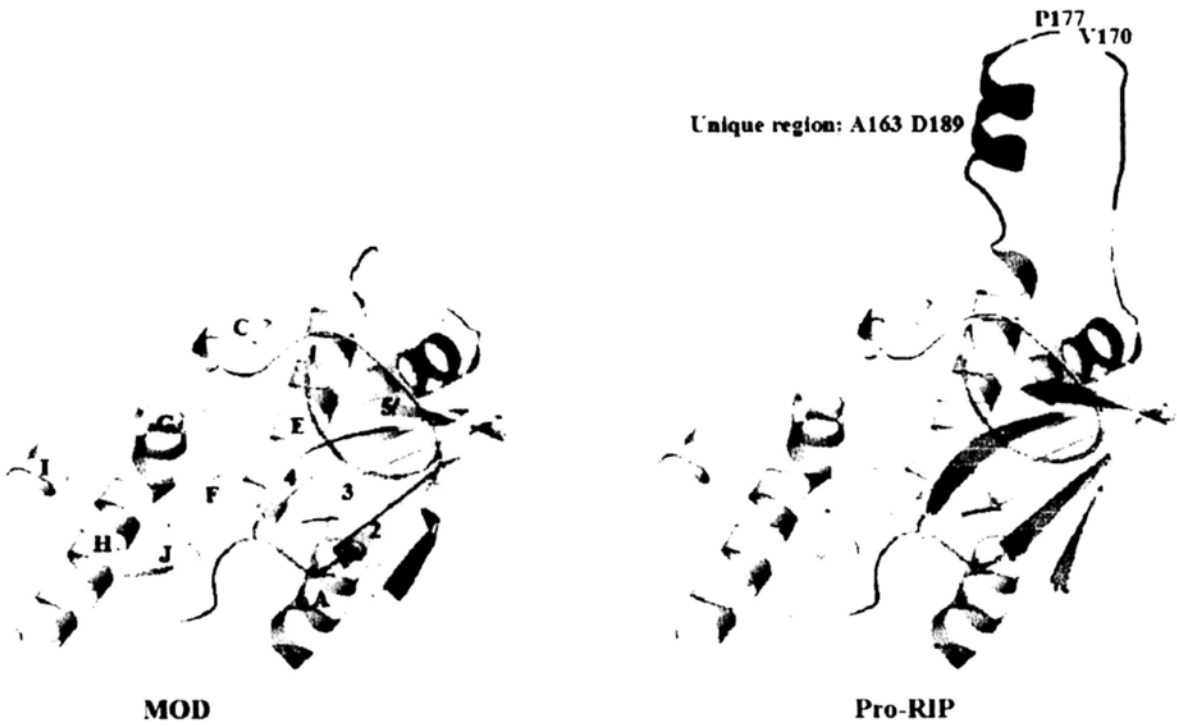

Figure 3.2 Structures of Pro-RIP and MOD. The structures of Pro-RIP and MOD are similar with a large N-terminal consisting of five-stranded mixed β–sheet, five α–helices (A-J) and a small C-terminal domain composed of α-helices (1-4), except a unique inactivation region A163-D189 in Pro-RIP (region indicated in red) (Mak *et al.*, 2007). The diagram is prepared by Dr. A.N.S. Mak.

3.1.2 HIV-1 protease – structure and substrate specificity

HIV-1 protease (HIV-1 PR), a unique subclass of the family of aspartic protease, is a homodimeric enzyme. The 99-aa HIV-1 PR is encoded within the Pol open reading frame of the large Gag-Pol precursor and is flanked by the $p6^{pol}$ and reverse transcriptase (RT) domains at its N and C termini. The symmetric subunits require

dimerization to form a conserved single active site which is formed at the dimer interface. The active site includes six amino acids with a pair of catalytic aspartic acid, Asp25 and Asp25. It is hypothesized that strong hydrogen-bonding forces between the Thr26 and Thr26 residues are essential for the conformational stability, therefore the dissociation of the dimeric active form results in depletion of enzymatic activity (Darke *et al.*, 1988, Dunn *et al.*, 2002, Freed & Martin, 2007, Louis *et al.*, 1999, Mager, 2001, Wlodawer & Gustchina, 2000). Studies of the proteolytic processing of synthetic substrate analogs by HIV-1 protease illustrated that the active binding cleft can accommodate six to eight residues (P4-P4') and give specific and efficient cleavage (Darke *et al.*, 1988, Tözsér *et al.*, 1992). Hazebrouck and colleagues tested the minimal length of HIV-1 PR cleavage sequences by insertional mutagenesis of the *E. coli* thymidylate synthase. They found that five amino acids are sufficient for HIV-1 PR cleavage (Hazebrouck *et al.*, 2001).

Ten HIV-1 PR cleavage sites of Gag and Gag-Pol polyproteins, as well as their kinetics characteristics have been identified (Table 3.1) (Louis *et al.*, 1999, Tözsér *et al.*, 1991a). The variation of the cleavage efficiency is affected mainly by two factors, amino acid sequence of the cleavage site and accessibility of the cleavage site by HIV-1 PR (Freed & Martin, 2007, Hazebrouck *et al.*, 2001). *In vitro* synthetic peptide cleavage study and random phage display library have been used to delineate

similarities and differences between the substrate specificities of HIV-1 protease (Beck *et al.*, 2000, Beck *et al.*, 2002). The minimum recognition sequences for specific and efficient cleavage is from position P4 through P3' flanking the scissile bond (Bagossi *et al.*, 2005, Krausslich *et al.*, 1989), where P1, P1', P2 and P2' positions are more restrictive. It is suggested that hydrophobic and unbranched at the β-carbon residues at the P1 position is optimal for retroviral proteases, whereas polar and beta-branched side chains prevent hydrolysis. Studies of the 46 cleavage sequences of retroviral proteases showed that almost 90% of the P1 sites are Phe, Tyr, Leu and Met (Pettit *et al.*, 1991, Tözsér *et al.*, 1992). Retroviral protease cleavage sites are classified into two types. Type 1 cleavage sites include a proline residue (Pro) at the P1' position, whereas type 2 have leucine (Leu), Alanine (Ala) or Valine (Val) hydrophobic residue in the P1' position (Pettit *et al.*, 1991). For both type 1 and 2 cleavage sites, P2' are commonly occupied by aliphatic residues (Leu, Ala, Ile and Val) while Ile is excluded in P2' position in type 2 cleavage sites. However sequence homology is low among naturally occurred substrate sequences in HIV-1 PR and no consensus sequence for HIV-1 PR has been defined (Rognvaldsson *et al.*, 2007, You *et al.*, 2005).

The cleavage of HIV-1 Gag precursor by HIV-1 protease is an ordered and accurate process required for appropriate assembly of infectious viral particles.

Several studies have suggested that the first cleavage occurs at the N-terminus of the p2/NC protein, whereas the intermediate cleavage occurs at the MA/CA and p1/p6 sites. The order of cleavage has been shown to be p2/NC > p1/p6 ≥ MA/CA >CA/p2 *in vitro* (Krausslich *et al.*, 1989, Pettit *et al.*, 2005a, Wiegers *et al.*, 1998). The relative cleavage rate at different sites within the precursors have been evaluated and rates vary as much as 400 folds between sites (Pettit *et al.*, 1994; 2002,).

Table 3.1 Kinetic parameters of HIV-1 protease using oligopeptides representing the cleavage sites in HIV-1 Gag and Gag-Pol polyproteins (Tözsér *et al.*, 1991a).

HIV-1 virus site	Substrate sequence	*kcat/Km*
MA/CA	VSQNY↓PIVQ	45.3
CA/p2	KARVL↓AEAMS	90.0
p2/NC	TATIM↓MQRGN	74.0
NC/p1	ERQAN↓FLGKI	1.0
P1/p6	RPGNF↓LQSRP	0.6
In p6	DKELY↓PLTSL	0.02
TF/PR	VSFNF↓PQITL	6.9
PR/RT	AETF↓YVDGAA	10.0
RT/RH	CTLNF↓PISP	24.1
RT/IN	IRKIL↓FLDG	202.0

3.1.3 TAT-mediated delivery of protein

HIV-1-encoded *trans*—activator TAT protein (HIV-1 Tat) (86 aa) was first found to have the ability of crossing cell membrane and transactivating viral genome in the late 80's (Frankel & Pabo, 1988, Green & Loewenstein, 1988). Fawell and colleagues demonstrated that β-galactosidase chemically conjugated to a 36 aa

domain of Tat was successfully delivered to several murine tissues, such as heart, liver and spleen (Fawell *et al.*, 1994). Subsequently, a highly basic 11 aa peptide (TAT) ,YGRKKRRQRRR, was identified to be sufficient for cellular transduction and subcellular localization (Nagahara *et al.*, 1998, Vives *et al.*, 1997). Several studies revealed that the rich basic residues located in the Tat peptide contributes to rapid cellular internalization in a wide variety of mammalian and human cell types, such as peripheral blood lymphocytes, HeLa cells and Jurkat T-cells (Becker-Hapak *et al.*, 2001, Fawell *et al.*, 1994, Nagahara *et al.*, 1998, Vives *et al.*, 1997, Vocero-Akbani *et al.*, 1999; 2000). Therefore, the TAT transduction peptide has been applied for the delivery of macromolecular therapeutics (Gump & Dowdy, 2007).

3.2 Results

3.2.1 Construction of TAT-fused maize RIP and variants by PCR

Maize [Δ1-16, Δ287-300]-Pro-RIP (Pro-RIP-WT) and [Δ1-16, Δ163-164, Δ167-189, Δ287-300]-Pro-RIP (MOD-WT) were gifts from Prof. R.S. Boston. MOD-WT is a one-chain active form whose internal inactivating region (A163-D189) is replaced by a bipeptide linker Leu-Glu. [Δ1-5]-Pro-RIP-WT (Pro-RIP) and [Δ1-5]-MOD-WT (MOD) were generated by polymerase chain reaction mutagenesis (Figure 3.3a) and cloned into pET3a expression vector by

Dr. A.N.S. Mak (Mak *et al.*, 2007). TAT-Pro and TAT-MOD were then constructed by polymerase chain reaction mutagenesis (Figure 3.3b) using TAT-Δ5-Maize-RIP-F and Maize-RIP-R primers and plasmids [Δ1-5]-Pro-RIP-WT (Pro-RIP) and [Δ1-5]-MOD-WT (MOD) as described in Section 2.2.2. TAT-fused maize RIP variants with substitution of HIV-1 PR recognition sites were constructed by polymerase chain reaction mutagenesis using plasmids [Δ1-5]-Pro-RIP-WT (Pro-RIP) and the overlapping primers as described in Section 2.2.2. All desired DNA fragments were cloned into pET3a expression vector at BamHI and NdeI sites. *E. coli* DH5α cells were transformed by the plasmids and clones that contained the interested insert without secondary mutations were screened by PCR and DNA sequencing (Figure 3.3). The HIV-1 protease cleavage sequences TATIM/MQRGN (p2/NC site), VSQNY/PIVQN (MA/CA site) and IRKIL/FLDG (RT/IN site) located in the polyprotein precursor Gag or Gag-Pol of HIV-1 were selected for the study based on their high k_{cat}/K_m values toward HIV-1 protease (Table 3.1). TAT-fused maize RIP variants TAT-Pro-HIV-MA/CA and TAT-Pro-HIV-p2/NC with the substitution of two HIV-1 protease recognition sequences VSQNY/PIVQN (MA/CA site) and TATIM/MQRGN (p2/NC site) respectively, in the 25 aa internal inactivation region were constructed (Figure 3.3c).

TAT-Pro-HIV-p2/NC-RT/IN carried two HIV-1 protease recognition sequences of p2/NC and RT/IN sites, in which the sequences TATIM/MQRGN and IRKIL/FLDG were separated by five residues originated from the internal loop of wild-type maize RIP. TAT-Pro-HIV-MA/CA-3 and TAT-Pro-HIV-MA/CA-2 were generated with shorten protruding aa in the cleaved products by eliminating two or three of the amino acid residues from the MA/CA site, which were adjacent to the N- and C-terminal subunits of maize RIP (Figure 3.3d).

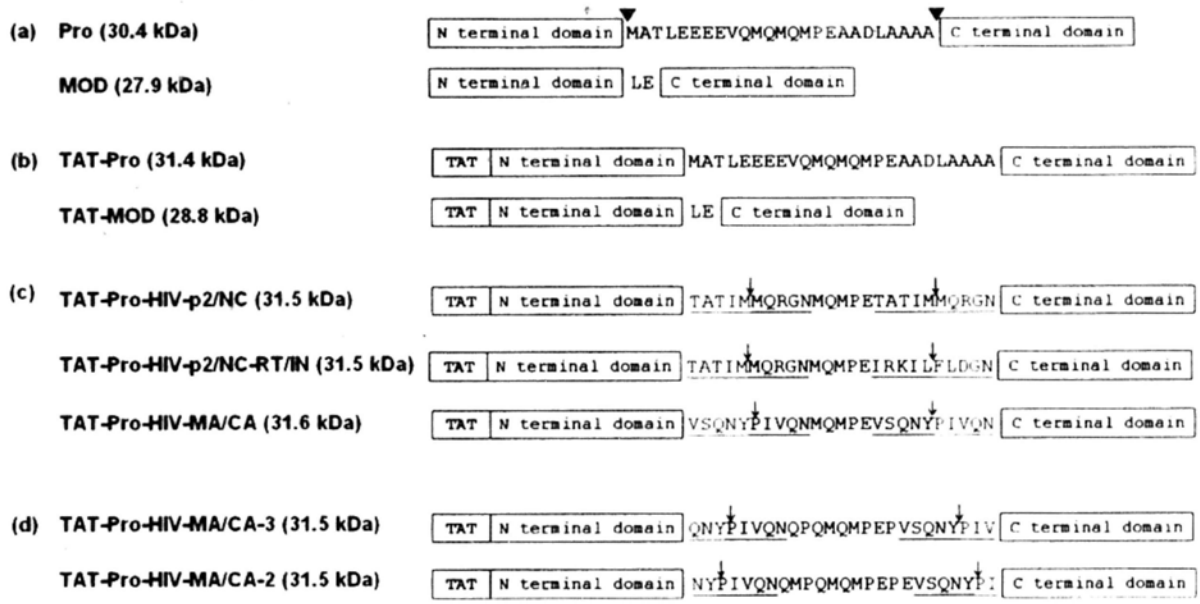

Figure 3.3 Schematic diagrams of TAT fusion maize RIP and its variants. (a) Pro-RIP: artificial maize RIP precursor contains the 25 aa internal inactivation region with deletion of the 16-aa N-terminal and 14-aa C-terminal sequences. Cleavage sites leading to the generation of the active two-chain maize RIP are indicated by arrow heads (▼). MOD: one-chain active form which the two polypeptides fused by a bipeptide of LE. (b) TAT-Pro and TAT-MOD: A Tat sequence was fused to the N-terminus of Pro-RIP and MOD, repectively. (c) TAT-Pro-HIV-p2/NC and TAT-Pro-HIV-MA/CA: TAT-Pro with the first and last 10 amino acid residues replaced by the p2/NC site (TATIM/MQRGN) or the MA/CA site (VSQNY/PIVQN), respectively. TAT-Pro-HIV-p2/NC/RT/IN: TAT-Pro with the first and last 10 amino acid residues replaced by the p2/NC site (TATIM/MQRGN) and RT/IN site (IRKIL/FLDG) (d) TAT-Pro-HIV-MA/CA-2 and TAT-Pro-HIV-MA/CA-3: the N-terminus and the C-terminus of the MA/CA site containing internal inactivating region were shortened to reduce the number of aa left after cleavage to 2 to 3 residues (in red). The underlined sequences are the recognition sites of HIV-1 protease and ↓ indicates HIV-1 protease cleavage site.

3.2.2 Expression and purification of TAT-fused maize RIP and variants

The detail of expression and purification are described in Section 2.2.3. The protein purity was analyzed by 15% SDS-PAGE (Figure. 3.4). All proteins have purities greater than 95%.

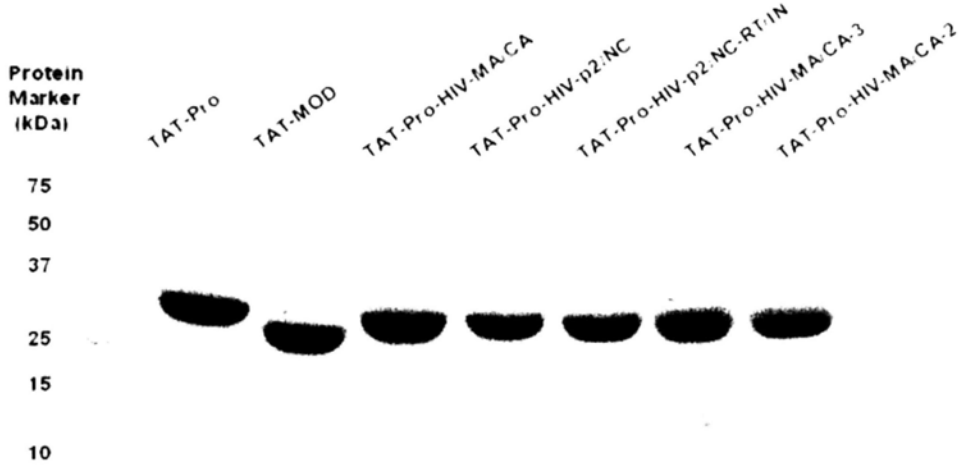

Figure 3.4 SDS-PAGE analysis of purified TAT-fused maize RIP and variants.

3.2.3 *In vitro* cleavage of TAT-fused maize RIP variants

In brief, purified protein samples (100 μM) were incubated with recombinant HIV-1 protease (0.5μg) *in vitro* in 50 mM sodium acetate buffer (pH 5.5) at 37°C. Aliquot (5μl) was collected after 24 hr incubation, 5X loading buffer was then added and the reaction was stopped at 95°C for 5 min before SDS-PAGE analysis (Figure 3.5a). Experimental detail is described in section 2.2.4.11. TAT-Pro-HIV-MA/CA, TAT-Pro-HIV-p2/NC and TAT-Pro-HIV-p2/NC-RT/IN were successfully cleaved *in*

vitro. Two bands of the expected size of the two subunits (around 11 kDa and 17 kDa) were resolved by SDS-PAGE (Figure 3.5a). However, variants TAT-Pro-HIV-MA/CA-3 and TAT-Pro-HIV-MA/CA-2 with shortening flanking sequences of MA/CA site were not cleaved under the same reaction conditions (Figure 3.5b).

3.2.4 Cleavage of TAT-fused maize RIP variants in HIV-infected cells

Variants which were cleaved efficiently by HIV-1 protease *in vitro* were subjected to cleavage assay in HIV-infected cells. HIV-1_{IIIB} acutely infected human T-cell C8166 cell line (1×10^6/ml) was incubated with maize RIP variants (0.2mg/ml) at 37°C for 72h before the isolation of cytoplasmic proteins. The cells were washed thoroughly with 5ml ice-cold PBS twice before trypsinization at 37°C for 10 min. Cell pellets were then washed with 5 ml ice-cold PBS, then were resuspended and lyzed in 200μl modified RIPA buffer with 1mM PMSF. Cytoplasmic proteins were isolated from cell debris by centrifugation at 13000 rpm (12,110 g), 4°C for 15 min. The cellular uptake of proteins and the removal of internal inactivation region in HIV-infected cell were detected by SDS-PAGE and Western blotting using anti-MOD polyclonal antibody specific for maize RIP. Experimental detail is described in section 2.2.4.12. The three variants (TAT-Pro-HIV-MA/CA, TAT-Pro-HIV-p2/NC and

TAT-Pro-HIV-p2/NC-RT/IN) were also cleaved specifically by endogenous HIV-1 protease in HIV-1_{IIIB} acutely infected C8166 cells, resulting in target bands which were detected by anti-MOD antibody in Western blotting (Figure 3.6).

(a)

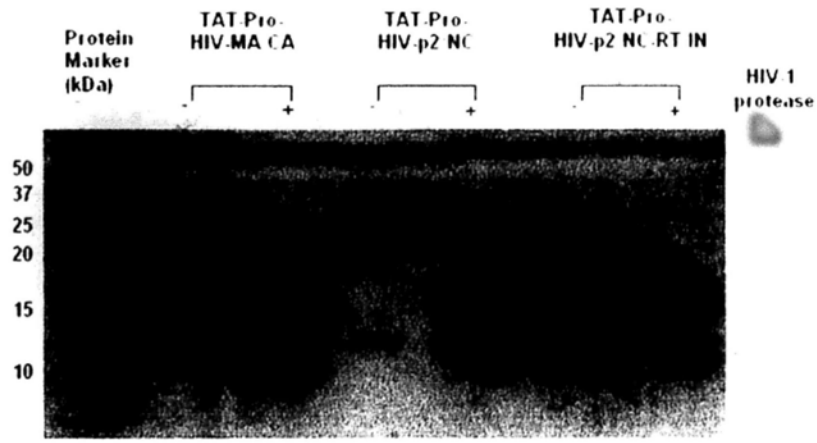

(b)

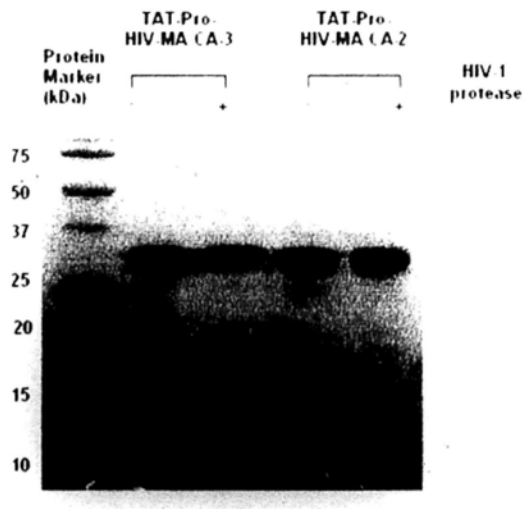

Figure 3.5 Cleavage of TAT-fused maize RIP variants *in vitro*. (a) TAT-Pro-HIV-MA/CA, TAT-Pro-HIV-p2/NC and TAT-Pro-HIV-p2/NC-RT/IN and (b) TAT-Pro-HIV-MA/CA-3 and TAT-Pro-HIV-MA/CA-2 after incubation with purified recombinant HIV-1 protease for 24h were compared with the untreated proteins.

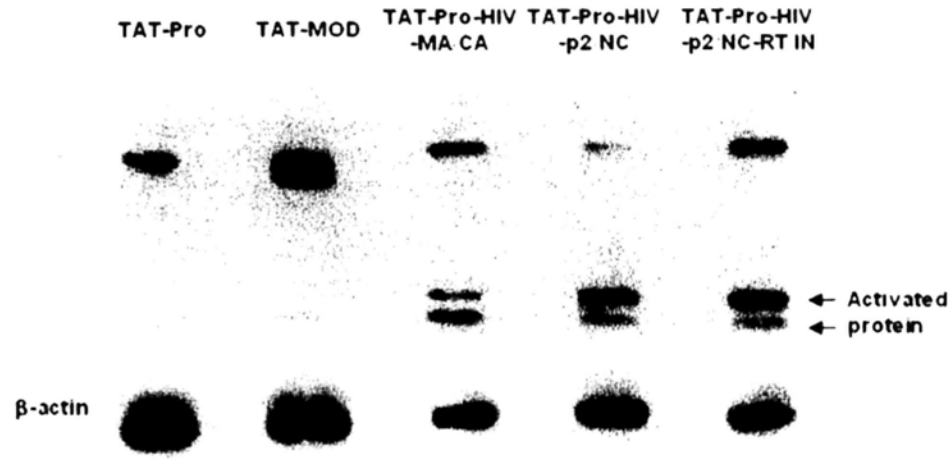

Figure 3.6 Cleavage of TAT fused maize RIP variants in HIV-infected cells. Acutely HIV-1_{IIIB} infected C8166 cells were incubated with protein samples for 72 h and immunoblotted with anti-MOD polyclonal antibody specific for maize RIP and its cleaved form. The engineered internal loop region of TAT-fused maize RIP variants were recognized and cleaved by HIV-1 protease resulted in two subunits of activated form (~11 kDa and 17 kDa).

3.2.5 N-glycosidase activity detection by quantitative real-time PCR assay

To compare the N-glycosidase activity of the maize RIP variants before and after the removal of the internal inactivation region, a quantitative real-time PCR assays was employed to study the N-glycosidase activity in intact cells. HIV-1 protease-cleaved TAT-Pro-HIV-MA/CA, TAT-Pro-HIV-p2/NC and TAT-Pro-HIV-p2/RT-RT/IN were purified by gel filtration chromatography and incubated with mouse macrophages (J774A.1) for 6 h. Total RNA was isolated for

cDNA synthesis. The amount of rRNA depurination was detected quantitatively in site-specific manner using primers that target the altered sequences by quantitative real-time PCR. Experimental details are described in section 2.2.4.7.3. and 2.2.4.7.4.

Two primer sets were used to detect total 28S rRNA of rat and the deadenlyation site of A4324 in rat 28S rRNA caused by maize RIP (Melchior & Tolleson, 2009). The efficiency of primer sets was tested using serial dilutions of cDNA synthesized from RNA of TAT-MOD treated cells corresponding to the control and the altered region. Figure 3.7 shows the linearity of the standard curves throughout the whole range of serial dilutions ($r^2 > 0.99$).

In the present study, I have demonstrated that the different level of depurination of rat 28r RNA by maize RIP and TAT-fused maize RIP in intact cells. Equal amount (5 μM) of maize RIP (Pro and MOD) and TAT-fused maize RIP (TAT-Pro and TAT-MOD) were incubated with mouse macrophage J774A.1. By qRT-PCR, it is found that there are 2.2 and 2.9-fold increases in the relative amount of deadenlyated RNA between Pro and TAT-Pro, and MOD and TAT-MOD respectively, suggesting that the TAT-fused proteins has a higher entry rate (Figure 3.8). The relative N-glycosidase activity of TAT-MOD was about 5.5-fold higher than TAT-Pro in mouse macrophage cells (J774A.1) (Figure 3.8 and 3.9). The cleaved variants (cleaved TAT-Pro-HIV-MA/CA and cleaved TAT-Pro-HIV-p2/NC) also resulted in a

higher level of depurinated rRNA than their uncleaved counterparts *in vivo* (Figure 3.9; Table 3.2), indicating a higher N-glycosidase activity after eliminating the internal inactivation region. However, the amount of depurinated rRNA of variant TAT-Pro-HIV-p2/NC-RT/IN and its cleaved form showed no statistical differences. (Figure 3.9; Table 3.2). It is possible that TAT-Pro-HIV-p2/NC-RT/IN might be somehow cleaved by other endogenous proteases in uninfected cells resulting in enhanced N-glycosidase activity.

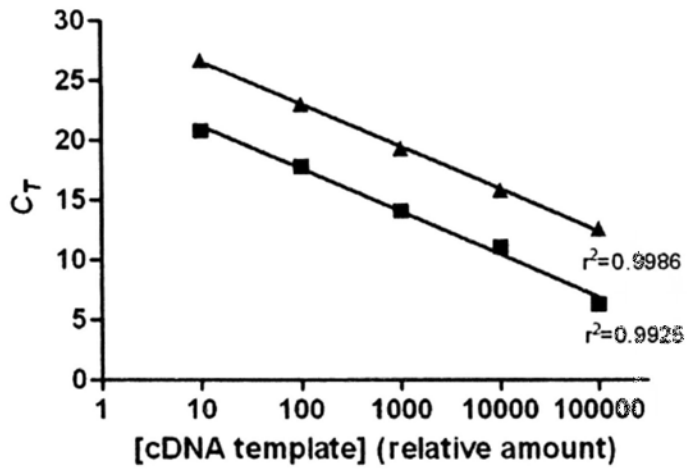

Figure 3.7 Linear range of quantitative real-time PCR of the primer pairs. Signals were obtained from the amplification of serially diluted cDNA synthesized from RNA of TAT-MOD treated cells. ■ indicates total rat 28S rRNA and ▲ indicates depurinated rRNA. The relative amount of cDNA template was plotted against the corresponding threshold cycle number in log scale and fitted with a linear regression model. SEMs are less than 1% of the corresponding C_T values.

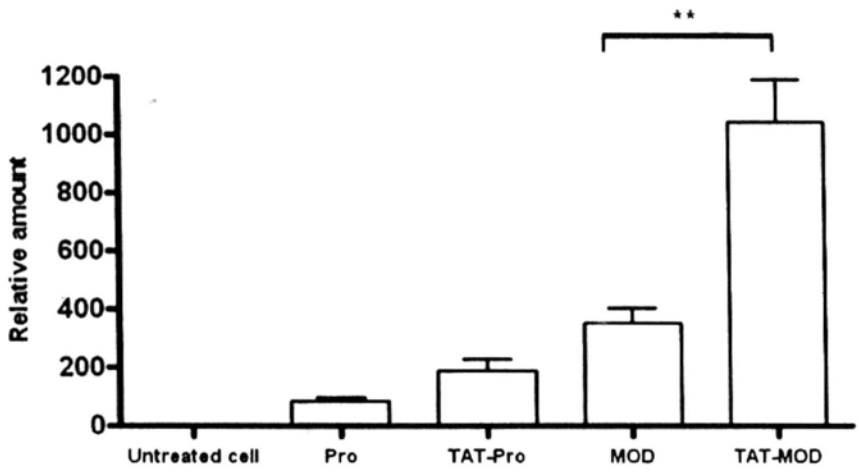

Figure 3.8 Effects of maize RIP and TAT-fused maize RIP on rat 28S rRNA. Untreated cell was used as negative control. Relative amount of depurinated RNA are represented in linear scale with SEMs. (n=6) (**p<0.01)

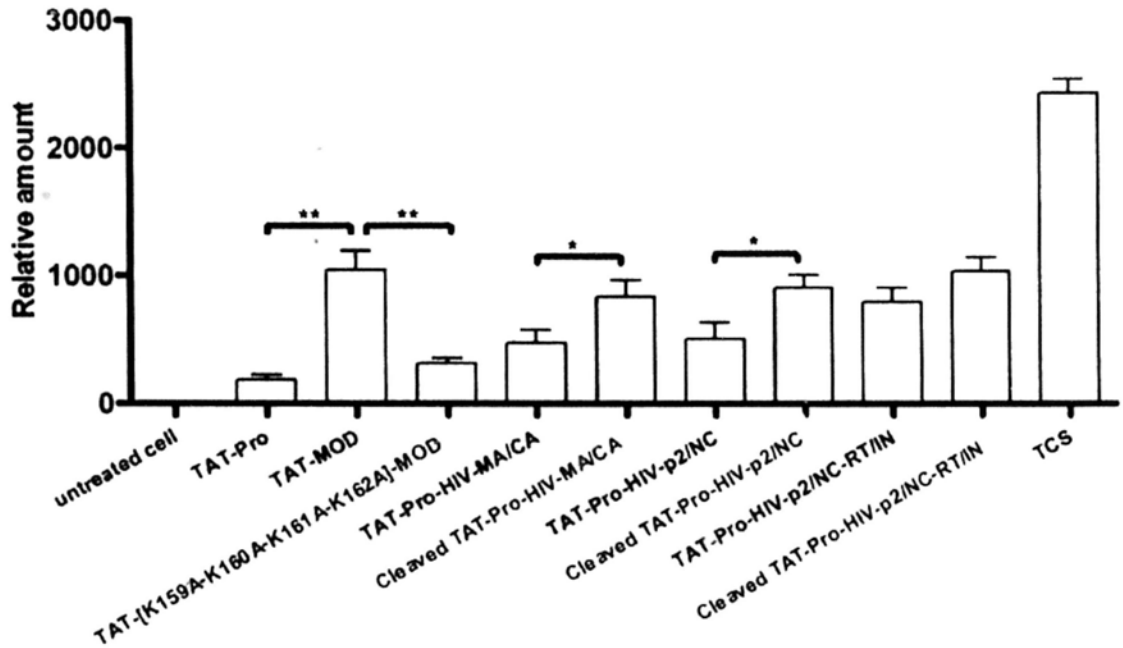

Figure 3.9 Effects of TAT-fused maize RIP, three variants and their cleaved counterparts on rat 28S RNA. Untreated cell and trichosanthin (TCS) were used as negative and positive control respectively. Relative amounts of depurinated RNA are represented in linear scale with SEMs. (n=6) (*p<0.05 and **p<0.01)

Table 3.2 The relative N-glycosidase activity of TAT-fused maize RIP and its variants in mouse macrophage (J774A.1) relative to TAT-Pro.

Protein samples	Relative N-glycosidase activity to TAT-Pro (Fold increase)
TAT-Pro	–
TAT-MOD	5.6
TAT-[K159A-K160A-K161A-K162A]-MOD	1.5
TAT-Pro-HIV-MA/CA	2.0
Cleaved TAT-Pro-HIV-MA/CA	4.4
TAT-Pro-HIV-p2/NC	2.3
Cleaved TAT-Pro-HIV-p2/NC	5.0
TAT-Pro-HIV-p2/NC-RT/IN	4.3
Cleaved TAT-Pro-HIV-p2/NC-RT/IN	5.6

3.3 Discussion

Unlike type II RIP, Maize RIP does not have a domain (lectin B-chain) that facilitates cellular uptake. The cellular uptake of type I RIP, such as saporin and trichosanthin (TCS), is mediated by the low density lipoprotein (LDL) receptor family (Cavallaro *et al.*, 1995, Cavallaro & Soria, 1995, Chan *et al.*, 2000, Roberts & Lord, 2004). It explained the reason of the selective cytotoxicity of trichosanthin in different cell types. TCS is highly cytotoxic to choriocarcinoma cell , such as human choriocarcinoma cell (JAR) which express high level of LDL receptor-related protein (LRP) (Tsao *et al.*, 1986; 1990). By now, there is no study about the mechanism of cellular uptake of maize RIP.

The fusion of the TAT to the N-terminus of maize RIP (Figure 3.3)aimed to

promote cellular transduction to the present cell model C8166 which was then used for HIV-1 infection. This highly basic 11 aa peptide (YGRKKRRQRRR) is derived from a well-characterized HIV-1 Tat, which is capable of mediating the transduction of heterogeneous proteins across cellular membrane in a receptor independent manner (Fawell *et al.*, 1994, Nagahara *et al.*, 1998, Yang *et al.*, 2002). It allows effective and equal transduction of proteins in uninfected and HIV-infected cells in time and dose-dependent manner (Vocero-Akbani *et al.*, 1999). Full-length TAT-fusion proteins have been used in therapeutic purposes for manipulating intracellular processes *in vitro* and *in vivo* (Snyder & Dowdy, 2005, Wadia & Dowdy, 2005) and developed as secretable therapeutic TAT fusion protein in eukaryotic cells (Flinterman *et al.*, 2009). In addition, TAT peptide has been conjugated to molecular imaging probes for optical imaging tumors and pathological conditions (Bullok *et al.*, 2006, Shen *et al.*, 2007). The entry pathway of HIV-1 TAT peptide into the cells has long been controversial. A recent study suggested that the spontaneous translocation of the TAT peptide across the cell membrane involves interactions between the TAT peptide and the phosphate group on the lipid bilayers, the formation of transient pore by the insertion of the charged side chains, and finally the translocation of TAT peptide by diffusion (Herce & Garcia, 2007). Recently, another study suggested that the peptide induces formation of small vesicles and enters the cell by micropinocytosis, instead of spontaneous

formation of transmembrane pores (Yesylevskyy *et al.*, 2009). According to the unpublished data by Dr. Mak, A.N., MOD showed stronger cytotoxic effects in human choriocarcinoma cell (JAR) and mouse macrophage (J774A.1) with IC_{50} 0.37 and 1.2 μM, respectively, while relatively low cytotoxicity (IC_{50} 9.1) towards human T lymphocytes (C8166). The cytotoxicity study together with the protein structure study suggested that cellular uptake mechanism of maize RIP maybe similar to that of type I RIP. In the present study, *in vivo* N-glycosidase study found that the relative N-glycosidase activities of TAT-Pro and TAT-MOD were about 2 to 3-fold higher than that of non-TAT-fused maize RIP (Pro and MOD) in mouse macrophages. This observation suggested that the TAT tag increases the cellular uptake of maize RIPs, hence the N-glycosidase activity (Figure 3.8).

Three HIV-1 protease cleavage sequences VSQNY/PIVQ (MA/CA site), TATIM/MQRG (p2/NC site) and IRKIL/FLDG (RT/IN site) were selected for the construction of HIV-PR activating maize RIP based on their high *kcat/Km* values. In addition, MA/CA cleavage site, which is a typical type 1 retroviral substrate with a small and hydrophobic proline residue (Pro) at P1' position, has been used as a model for studying the substrate specificity of HIV-1 protease (Beck *et al.*, 2000, Billich & Winkler, 1991, Tözsér *et al.*, 1991b). HIV-1 protease, like most aspartic proteases, has a low optimal pH for substrate cleavage (pH 4-5). Changes in pH and salt

concentration affect the *Km* and *kcat* values of HIV-1 protease to substrate peptides (Polgar *et al.*, 1994, Szeltner & Polgar, 1996). It is suggested that data from studies of substrate cleavage of HIV-1 protease at low pH and /or high salt concentration relative to physiological conditions may not reflect the specificity of HIV-1 protease *in vivo* (Billich & Winkler, 1991, Tözsér *et al.*, 1991a,b). In the present study, the 25 aa internal loop region of the wild type maize RIP precursor was substituted by different combinations of HIV-1 protease recognition sequences using overlapping PCR technique (Figure 3.2). In our pilot study, maize RIP variants with shorter internal loop region, such as 20 aa and 16 aa internal loop region, which was substituted by the MA/CA virus cleavage sequences were constructed. However, none of them could be cleaved completely *in vitro* (data not shown). Only the variants with 25 aa internal inactivation region in which the first and the last 10 residues were replaced by the MA/CA site, was completely cleaved by HIV-1 protease *in vitro* under the same reaction conditions. It is suggested that the length of the internal loop is critical for the efficient cleavage. TAT-Pro-HIV-MA/CA, TAT-Pro-HIV-p2/NC and TAT-Pro-HIV-p2/NC-RT/IN with 25 aa internal inactivation loop including two HIV-1 cleavage, were successfully cleaved by HIV-1 protease *in vitro* as in HIV-infected cells (Figure 3.5a and 3.5b) resulting in the formation of two target bands (~11 kDa and 17 kDa). Previous studies suggested that the minimum substrate length is small,

corresponding to positions P4 through P3' flanking the scissile bonds (Pettit *et al.*, 1991; 2002). However, variant TAT-Pro-HIV-MA/CA-3 which had the variant MA/CA sites QNY/PIVQN (P3 to P5') and VSQNY/PIV (P5 to P3') was not cleaved by HIV-1 protease *in vitro* (Figure 3.5b). This suggests that local spatial factors of the maize RIP affect the accessibility of the MA/CA site to HIV-1 protease. Studies of crystal structure of HIV-1 protease-substrate complex have suggested that in spite of the particular amino acid sequences of the cleavage site, the specificity of HIV-1 protease is also determined by the spatial structure of the substrate (Prabu-Jeyabalan *et al.*, 2000). In the past decade, researchers attempted to develop algorithms by bioinformatic methods to analyze and predict HIV-1 protease specificity (Cai *et al.*, 2002, Yang & Chou, 2004, You *et al.*, 2005). The *in silico* studies support that the protease primarily recognizes a conformation rather than a specific amino acid sequence (You *et al.*, 2005). Notable to mention is that the presence of one or two lysine residues near the octameric peptide cleavage site hinder the activity of HIV-1 protease (Bouzide *et al.*, 2005). However, how a symmetrical homodimeric enzyme such as HIV-1 protease to recognize various asymmetric substrates is not well-understood.

Traditionally, the N-glycosidase activity have been detected in cell-free protein synthesis system (Olsnes *et al.*, 1975) or colorimetric detection of released

adenine by HPLC (Heisler *et al.*, 2002). However these methods are less sensitive and specific, and can only measure *in vitro* N-glycosidase activity. In this study, in order to achieve high specificity and sensitivity needed to measure the *in vivo* N-glycosidase activity of the internalized maize RIP variants, quantitative real-time PCR was used. As mentioned in the introduction, RIPs depurinate a single adenine residue in 28S rRNA (Hartley *et al.*, 1996). Reverse transcriptase preferentially inserts an adenine in the cDNA at the location of depurination. During cDNA synthesis, an adenine is incorporated by reverse transcriptase to the site where an adenine in the rRNA template is removed, resulting in an T to A transversion in the sequencing reads (Takeshita *et al.*, 1987). The amount of rRNA depurination was then detected quantitatively in site-specific manner using primers targeting the altered sequences by real-time PCR. The enzymatic activity of several RIPs, such as ricin, Shiga toxin-1, abrin and Pokeweed toxin were examined by this assay (Melchior & Tolleson, 2009). Trichosanthin (TCS), a type 1 RIP, was also included in the present study to validate the effectiveness of detecting *in vivo* N-glycosidase activity. The relative N-glycosidase activity of TCS is about 13.5-fold and 31.5-fold higher than that of TAT-Pro and Pro-RIP, respectively. The observation was consistence with the previous cell-free protein synthesis inhibition studies that maize RIP is less potent than TCS (Hey *et al.*, 1995, Mak *et al.*, 2007, Stirpe & Battelli, 2006). The *in vivo*

N-glycosidase activity of TAT-fused maize RIP variants and their activated counterparts were determined. The *in vitro* HIV-1 protease-cleaved variants, TAT-Pro-HIV-MA/CA and TAT-Pro-HIV-p2/NC had increased N-glycosidase activity in mouse macrophage compared to their un-activated counterparts, which was consistent to the previous observation that the wild-type inactive precursor (Pro-RIP) did not bind to rat ribosomes (Mak *et al.*, 2007). However, variant TAT-Pro-HIV-p2/NC-RT/IN showed high N-glycosidase activity even bearing the internal loop region suggesting the internal inactivation region may be cleaved by endogenous protease in the mouse macrophage.

Previous study of the protein structure of maize RIP by Mak and colleagues showed that [K159A-K160A-K161A-K162A]-MOD, with the four lysine residues located underneath the internal loop region mutated to adenine, has a drastic decrease in protein synthesis using a cell-free ribosome inhibition assay system and reduction of interaction with the ribosome in *in vitro* pull-down assays (Mak *et al.*, 2007). Furthermore, NMR chemical shift perturbation experiments found that the four residues (K143-K146), which form a distinctive positively charged surface, are essential for the binding of MOD to ribosomal protein P2 (Yang *et al.*, 2010). In type I RIP, like TCS, the P2 binding site is in the C-terminal region (Chan *et al.*, 2001, Too *et al.*, 2009). The unique structure of internal inactivation loop may be correlated to

the shift of the P2 binding site to the N-terminus of maize RIP (Yang *et al.*, 2010). In the present study, TAT-[K159A-K160A-K161A-K162A]-MOD showed statistically significant 3.3-fold decrease in the N-glycosidase activity comparing with TAT-MOD (Figure. 3.8). This is the first *in vivo* enzymatic study to illustrate that in spite of the internal inactivation region, the four lysine residues (K143-K146) underneath the internal inactivation region seems to play a crucial role in the N-glycosidase activity of maize RIP.

3.4 Conclusion

I have demonstrated the generation and purification of HIV-1 protease-activated maize RIP variants. By incorporating different combination of HIV-1 protease recognition sites in the 25 aa internal inactivation region, three variants could be successfully cleaved by recombinant HIV-1 protease *in vitro* and in HIV-infected cells. Two of them showed statistically significant increase in N-glycosidase activity in mouse macrophage compared to their uncleaved counterparts. I have also showed that the HIV-protease switching mechanism could generate maize RIP variants with active N-glycosidase activity in intact cells. The next step was to study the anti-HIV activity of maize RIP and its variants in human T lymphocytes (C8166) infected by two T-tropic HIV-1 strains, HIV-1_{IIIB} and HIV-1 RF/V82F/I84V.

Chapter Four

Anti-HIV activity of HIV protease-activated maize RIP

4.1 Introduction

4.1.1 Tropism and syncytium formation of HIV-1

HIV-1 infects cells by targeting CD4 and other co-receptors (CCR5 or CXCR4) on the cell surfaces. Based on viral transmission, HIV-1 is divided into two tropisms namely, M-tropic virus and T-tropic virus (Cheng-Mayer *et al.*, 1988). M-tropic viruses make use of β-chemokine receptor, CCR5 for viral fusion and they are incapable to produce syncytia (Choe *et al.*, 1996, Freed & Martin, 2007, Kozak *et al.*, 1997). T-tropic viruses, which use α-chemokin CXCR4 coreceptors to infect T-cells in a rapid and high cytopathicity, induce syncytium formation (Fenyo *et al.*, 1989, Sullivan *et al.*, 1995). During the symptomatic phase of HIV infection, the emergence of T-tropic variants is the main cause of the accelerated CD4+ T-cell depletion resulting in rapid progression of AIDS (Koot *et al.*, 1993). The level of syncytium formation has been used as a phenotypic indicator of the viral replication in target cells (Schuitemaker *et al.*, 1991, Sylwester *et al.*, 1997, Tersmette *et al.*, 1988). Syncytium is fusion of plasma membrane of HIV infected-cells. Env-expressing cells fuse with Env-negative cells which is mediated by suitable co-receptors, such as

CXCR4 or CCR5, to induce syncytium formation followed by cellular and nuclear fusion, and finally apoptosis (Ferri *et al.*, 2000, Perfettini *et al.*, 2005). It has been claimed that the depletion of CD4-positive cells is correlated to the infection by syncytium-inducing HIV-1 *in vitro* and in human with AIDS (Blaak *et al.*, 2000, Lifson *et al.*, 1986, Sodroski *et al.*, 1986, Sylwester *et al.*, 1997). The extent of syncytium formation is also related to the p24 expression levels. It is suggested that no syncytia are seen until the level of supernatant p24 exceeded 10 ng/ml (Watkins *et al.*, 1997).

4.1.2 Gag protein: Capsid domain

The HIV-1 Gag precursor ($Pr55^{Gag}$) is for the synthesis of proteins for viral assembly and release. The mRNA of $Pr55^{Gag}$ (9.2kb) is spliced by reverse transcriptase for the expression of Gag proteins, matrix (MA), capsid (CA), nucleocapsid (NC) and p6 (Freed & Martin, 2007). CA, also called p24 protein, is essential for promoting virus assembly and core formation, which forms the conical capsid core surrounding the RNA genome in infectious virus. Mutations of CA disrupt HIV-1 replication, including production of defective immature viral particles and formation of impair conical capsid (von Schwedler *et al.*, 2003). Therefore, it plays an active role in the early and late stage in viral replication.

p24 antigen test is first introduced in 1986 as a marker for clinical serum samples by using enzyme-linked immunosorbent assay (ELISA) (Engvall, 2010, Lange *et al.*, 1986). Monoclonal antibodies specific to the p24 proteins and enzyme-linked antibody to the monoclonal antibodies cause color change which can be detected by spectrometer. The assay is quick, simple and reliable for identification and evaluation of HIV progression (Tsoukas & Bernard, 1994). Previous work demonstrated that p24 detection by ELISA detect viral protein as sensitively as polymerase chain reaction which detect viral DNA or RNA (Ledergerber *et al.*, 2000, Schupbach *et al.*, 2000).

4.2 Results

4.2.1 Anti-HIV activity

4.2.1.1 Syncytium formation assay

The syncytium formation assay was performed as described in section 2.2.4.9. Different concentration of proteins were incubated with C8166 cells (3×10^4 which were inoculated with $TCID_{50}$ HIV-1 or HIV-1 RF/V82F/I84V. After 3 days, round and protruding syncytia were formed by fusing 3 to 5 neighboring cells and the number in each well was counted under microscope (Figure 4.1a). Percentage inhibition of syncytial cell formation was calculated from the percentage of syncytium number in treated culture compared with that of the infected control culture (Wang *et al.*, 2008)

(a)

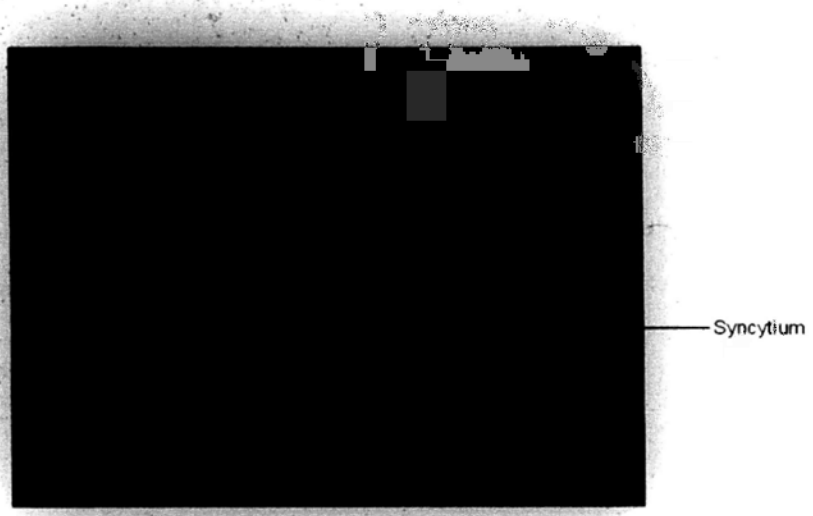

(b)

Figure 4.1 Syncytial reduction assay of HIV-1_{IIIB} acutely infected C8166 after 72 hr infection in (a) positive control, with cells and virus only. The syncytium formed by fusing 3 to 5 neighboring cells and (b) TAT-MOD-treated (200 μg/ml) HIV-infected cells. Cells died without syncytium formation. Photos were taken under light microscope (400X).

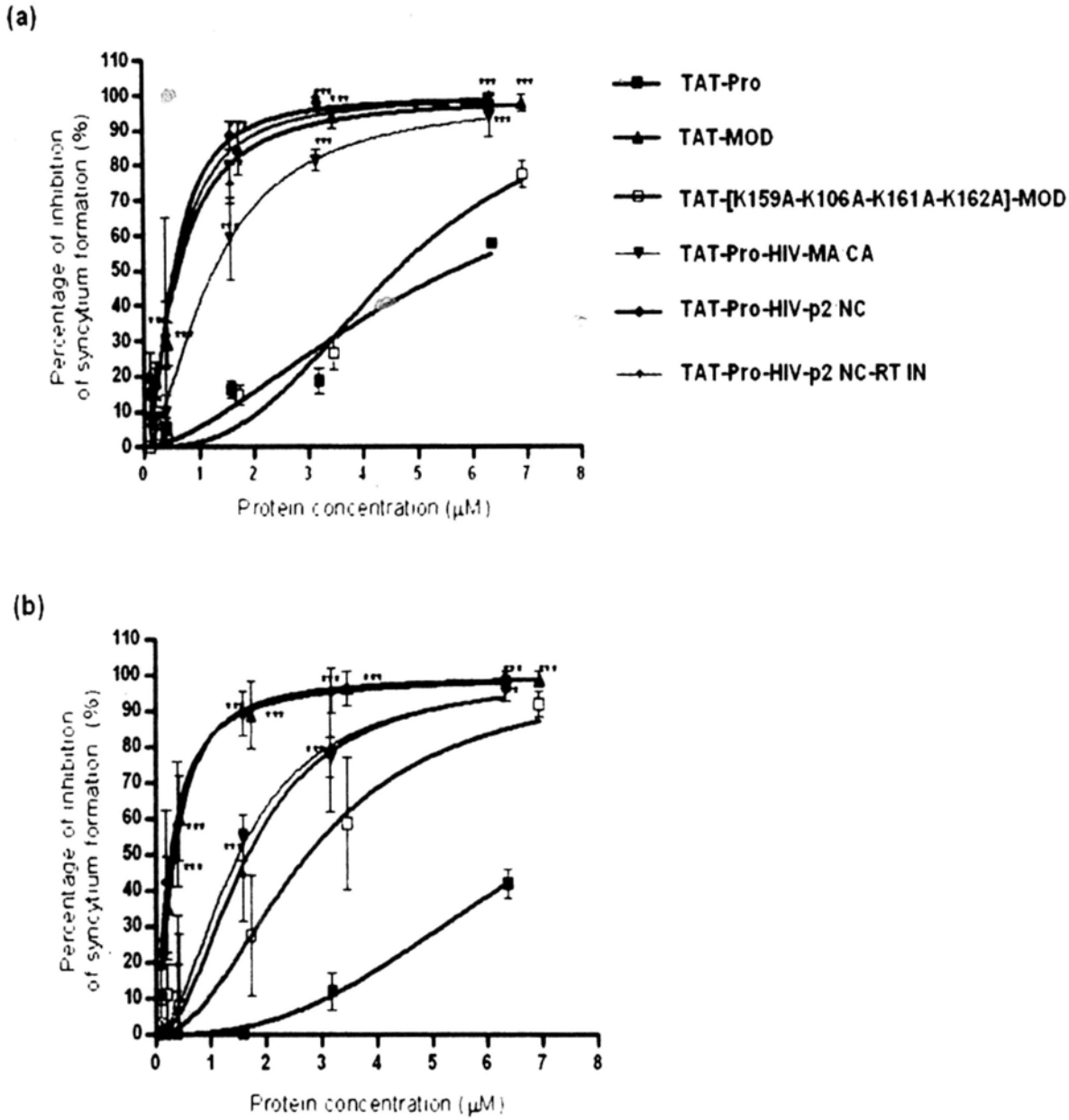

Figure 4.2 Syncytial reduction assay of TAT-fused maize RIP and variants. Acutely infected C8166 cells were inoculated with 100 $TCID_{50}$ HIV-1_{IIIB} in (a) or HIV-1 RF/V82F/I84V in (b). Control assays were performed without the testing compounds in HIV-1-infected and uninfected cultures. Data represent the mean ± SD of three experiments (n=12). ***P<0.001 versus TAT-Pro.

4.2.1.2 p24 antigen reduction assay

HIV-1 p24 antigen in cell-free medium was measured using capture ELISA as described previously in section 2.2.4.10. Briefly, 96-well plates were coated with McAb p5F1 followed by blocking with 5% skim milk, then Triton X-100-treated cell-free culture medium was added, and incubated at 37°C. The plates were then incubated with diluted human polyclonal anti-HIV-1 sera, followed by incubation with HRP (horseradish peroxidase)-labeled goat anti-human IgG.. The plates were read at 490/630 nm and the inhibition percentage of p24 antigen expression and EC_{50} were calculated.

(a)

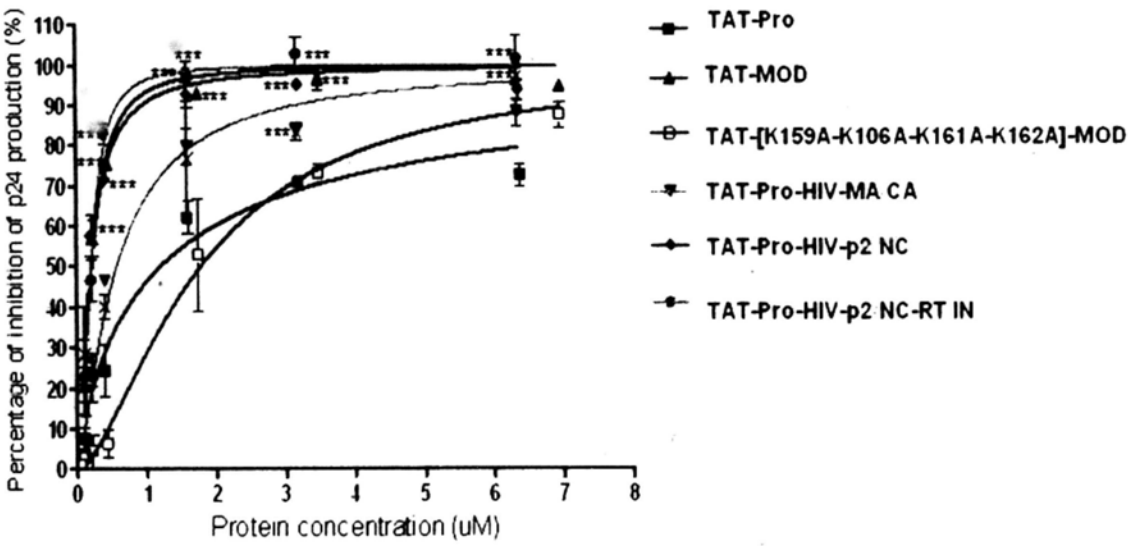

(b)

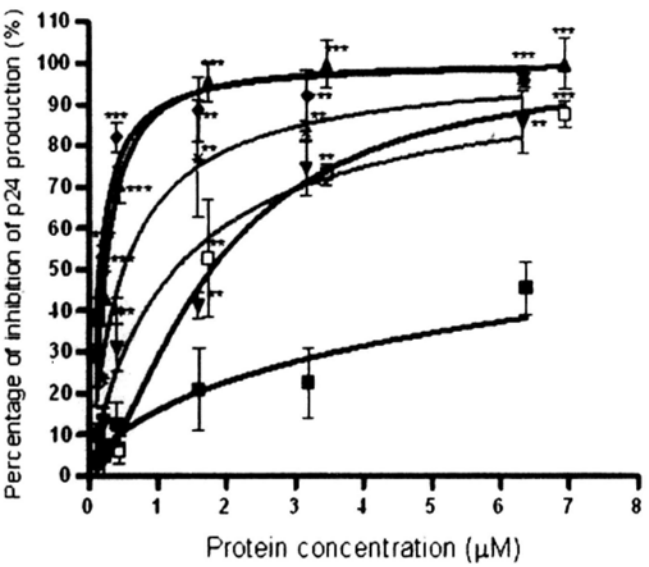

Figure 4.3 Inhibition of p24 antigen production assay of TAT-fused maize RIP and variants. Acutely infected C8166 cells were inoculated with 100 $TCID_{50}$ HIV-1_{IIIB} in (a) or HIV-1 RF/V82F/I84V in (b). The inhibition percentage of p24 antigen expression was calculated in comparison with that of the infected untreated culture. Data represent the mean ± SD of three experiments (n=12). ***P<0.001 versus TAT-Pro.

In HIV-1_{IIIB} acutely infected C8166 cells, TAT-MOD showed concentration-dependent inhibition of HIV replication. The 50% inhibition on syncytium and p24 antigen production were at 0.62 ± 0.08 μM and 0.21 ± 0.02 μM respectively (Figure. 4.1a, 4.2a and Table 4.1). In HIV-1 RF/V82F/I84V acutely infected C8166 cells treated with TAT-MOD, the 50% inhibition on syncytial and p24 antigen production were 0.39 ± 0.05 μM and 0.23 ± 0.03 μM respectively (Figure 4.1b, 4.2b and Table 4.1). TAT-Pro only showed limited inhibitory effects (Table 4.1).

The anti-HIV and cytotoxicity of TAT-Pro-HIV-MA/CA, TAT-Pro-HIV-p2/NC and TAT-Pro-HIV-p2/NC-RT/IN towards HIV-infected cells and uninfected cells were then examined (Figure 4.1, 4.2 and Table 4.1). They were potent in inhibiting syncytium formation and p24 antigen production towards acutely HIV-1_{IIIB} and HIV-1 RF/V82F/I84V infected C8166 cells, whereas TAT-Pro processed limited inhibitory effects. Compared to TAT-MOD, TAT-Pro-HIV-p2/NC and TAT-Pro-HIV-MA/CA were at least 5 folds less cytotoxic towards uninfected C8166 cells (Table 4.1). However, TAT-Pro-HIV-p2/NC-RT/IN showed stronger cytotoxic effects in uninfected cells with IC_{50} 7.72 ± 0.66 μM. TAT-[K159A-K160A-K161A-K162A]-MOD showed low cytoxicity as TAT-Pro in uninfected C8166, as well as limited inhibitory effects on viral replication compared with TAT-MOD and engineered maize RIPs (Table 4.1).

Table 4.1 Anti-HIV activity of TAT-fused maize RIP and variants in HIV-1_{IIIB} and HIV RF/V82F/I84V acutely infected C8166 cells and their cytotoxicity towards uninfected cells

	Uninfected C8166	HIV-1_{IIIB}		HIV-1 protease gene mutants RF/V82F/184V	
	Cytotoxicity IC_{50} (μM)	Syncytium reduction EC_{50} (μM)	p24 antigen reduction EC_{50} (μM)	Syncytium reduction EC_{50} (μM)	p24 antigen reduction EC_{50} (μM)
TAT-Pro	>15.93	5.69 ± 0.96	1.20 ± 0.25	6.02 ± 0.67	10.87 ± 5.13
TAT-MOD	3.27 ± 0.27	0.62 ± 0.08	0.21 ± 0.02	0.39 ± 0.05	0.23 ± 0.03
TAT-[K159A-K160A-K161A-K162A]MOD	>15.93	4.62 ± 0.28	1.60 ± 0.42	2.76 ± 0.47	1.78 ± 0.29
TAT-Pro-HIV-p2/NC	>15.87	0.55 ± 0.05	0.19 ± 0.02	0.33 ± 0.01	0.15 ± 0.03
TAT-Pro-HIV-p2/NC-RT/IN	7.72 ± 0.66	0.60 ± 0.15	0.19 ± 0.02	1.73 ± 0.12	0.50 ± 0.17
TAT –Pro-HIV-MA/CA	>15.78	1.27 ± 0.15	0.57 ± 0.17	1.71 ± 0.13	1.30 ± 0.33

HIV syncytium and p24 production are shown relative to untreated infected control cultures. The values are means ± SD of three experiments (n=12).

4.2.2 N-glycosidase activity in HIV-infected cells

The *in vivo* N-glycosidase activity of TAT-fused maize RIP and selected variants in acutely HIV-1_{IIIB} infected C8166 cells were studied. The experimental details were described in section 2.2.4.7. In brief, the protein samples were incubated with HIV-infected cells for 6 h, then RNA were isolated for reverse transcription. Specific primers which target the depurinated site in 28S rRNA were for quantitative detection of depurinated RNA.

The relative N-glycosidase activity of TAT-MOD in HIV-1_{IIIB} acutely infected C8166 cells was about 4-fold higher than that of the TAT-Pro and the results were consistent with the same assay using mouse macrophage J774A.1 (Figure 3.9 and 4.4). The two selected variants TAT-Pro-HIV-MA/CA and TAT-Pro-HIV-p2/NC, which showed low cytotoxic effects in uninfected cells, were found to show enhanced N-glycosidase activity in acutely HIV-1_{IIIB} infected C8166. The relative N-glycosidase activities of the two variants were comparable to TAT-MOD suggested that the internal inactivation region was effectively removed and the cleaved variants were with catalytic function in HIV-infected cells.

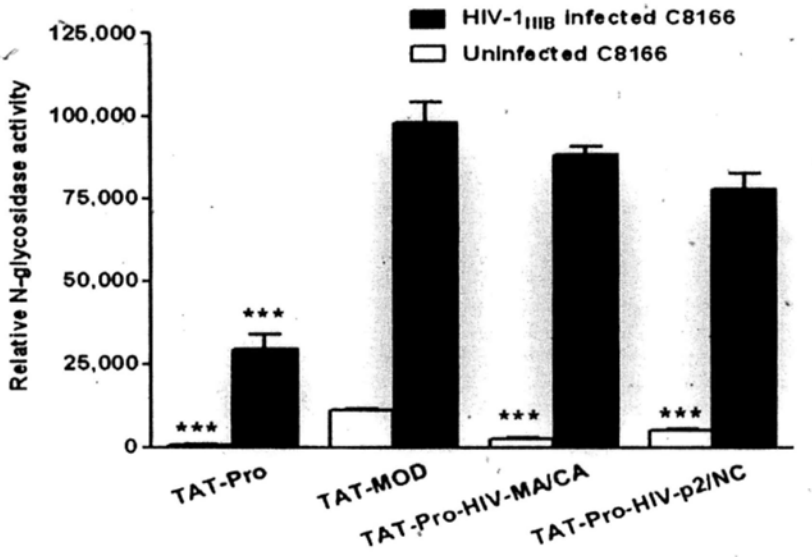

Figure 4.4 N-glycosidase activity of TAT-fused maize RIP and variants in uninfected and HIV-1_{IIIB} acutely infected human T-lymphocyte C8166 cells. Relative N-glycosidase activity was represented in linear scale ± SEM. Grey bars indicate HIV-1_{IIIB} acutely infected C8166 cells while white bars indicate uninfected cells. Student t-test was used for statistical analysis. *** $p<0.001$ versus TAT-MOD (n=6).

4.3 Discussion

TAT-Pro and TAT-MOD were first tested for the inhibition of HIV replication in human C8166 T-cells infected with two different HIV-1 strains, HIV-1_{IIIB} and a HIV-1 protease inhibitor resistant virus strain, (HIV-1 RF/V82F/I84V). The latter strain is among those most commonly observed in patients receiving protease inhibitor-containing regimens (Klei *et al.*, 2007, Shafer, 2002). HIV-1 RF/V82F/I84V consists of single and double gene mutant strains selected *in vitro* in the presence of the protease inhibitors DMP323 (a cyclic urea protease inhibitor) or P9941 (a C-2 symmetrical diol protease inhibitor).

In HIV-1_{IIIB} acutely infected C8166 cells, TAT-MOD showed concentration-dependent inhibition of HIV replication. TAT-Pro only showed limited inhibitory effects (Table 4.1). TAT-Pro-HIV-MA/CA, TAT-Pro-HIV-p2/NC and TAT-Pro-HIV-p2/NC-RT/IN were potent in inhibiting syncytium formation and p24 antigen production towards acutely HIV-1_{IIIB} and HIV-1 RF/V82F/I84V infected C8166 cells (Table 4.1). Compared to TAT-MOD, TAT-Pro-HIV-p2/NC and TAT-Pro-HIV-MA/CA were at least 5 folds less cytotoxic towards uninfected C8166 cells (Table 4.1). The finding supported the hypothesis that maize RIP variants with HIV-1 protease recognition sequences could be only activated in HIV-infected cells and inhibited HIV replication similar to its fully active TAT-MOD, with low

cytotoxity in uninfected cells. However, TAT-Pro-HIV-p2/NC-RT/IN showed stronger cytotoxic effects in uninfected cells. As mentioned in section 3.4, uncleaved TAT-Pro-HIV-p2/NC-RT/IN also showed higher N-glycosidase activity in mouse macrophages compared with other uncleaved variants (TAT-Pro-HIV-MA/CA and TAT-Pro-HIV-p2/NC). It might be due to the non-specific cleavage of the internal region by other endogenous proteases in uninfected cells. Nevertheless, RT/IN cleavage site was determined to be the most efficiently cleaved peptide of the Gag/Pol polyproteins of HIV-1 (Tözsér *et al.*, 1991).

Among the three selected variants, TAT-Pro-HIV-p2/NC possessed the stronger inhibition on the viral replication of HIV-1_{IIIB} and HIV-1 RF/V84F/I84V than variant that carries the MA/CA site (TAT-Pro-HIV-MA/CA). This is probably due to the more efficient cleavage of the p2/NC site in the HIV-1 infected cells. Indeed, the five HIV-1 Gag processing sites are cleaved at rates that vary up to 400-fold in vitro. Initial cleavage occurred at the p2/NC site which release the RNA-binding NC protein followed by an intermediate rate of cleavage at the MA/CA (Pettit *et al.*, 2005a,b, Wiegers *et al.*, 1998). The order of cleavage has been showed to be p2/NC > p1/p6 $\geq$ MA/CA >CA/p2 *in vitro* (Krausslich *et al.*, 1989).

Our observation on the N-glycosidase activity of TAT-MOD and TAT-Pro indicated that the removal of the internal inactivation region increases the cytotoxicity

and anti-HIV activity of maize RIP (Table 4.1). The relative N-glycosidase activity of TAT-MOD in HIV-1_{IIIB} acutely infected C8166 cells was about 4-fold higher than that of the TAT-Pro and the results were consistent with the same assay using mouse macrophage J774A.1 (Figure 3.9 and 4.4). Similarly, by comparing the EC_{50} of inhibition of p24 antigen production in HIV-1_{IIIB} and HIV-1 RF/V82F/I84V infected cells to TAT-Pro, the HIV-1 protease-cleavable variants TAT-Pro-HIV-MA/CA and Pro-TAT-Pro-HIV-p2/NC had 2- to 70-fold increased in the inhibitory power while showing low cytotoxicity towards uninfected C8166 cells.

HIV-1 protease recognition sites have been employed by other groups for the development of anti-HIV agents. Serio and co-workers demonstrated that the introduction of an HIV protease cleavage site into the C-terminus of Vpr inhibited the infectivity of HIV-1 provirus (Serio *et al.*, 1997; 2000). The engineered Vpr with addition of 10 residues of HIV-1 protease cleavage site at the C terminus behaves like the wild-type Vpr proteins. It is proposed that the engineered Vpr can act as a pseudosubstrate for HIV-1 protease in order to reduce protease efficiency, thus lead to incomplete processing of the polyprotein for viral maturation. However, among the nine chimeric Vpr constructs, only the one with MA/CA cleavage site exhibit complete inhibition of single round replication by HIV-1_{NL4-3} (Serio *et al.*, 1997)

Vocero-Akbani and co-workers modified a protease-activated caspase-3 by

placing an HIV-1 protease MA/CA cleavage site (VSQNY/PIVQN) between its p17 and p12 domains, where a 5 aa cleavage sequence (IETD↓S) was originally located between these domains in the wild-type caspase-3 inactive precursor (Vocero-Akbani *et al.*, 1999). This modified caspase-3 induced apoptosis in Jurkat T cells co-transduction with HIV protease (Han *et al.*, 1997). However, it is not known whether the engineered caspase was cleaved efficiently to cause specific killing of the HIV-infected cells.

Recently, Mitrea and co-workers inserted an HIV-1 protease recognition sequence (IFLETS) into a surface loop of a ribonuclease barnase (Bn). The artificial Bn zymogen was proven to be cleaved by HIV-1 protease *in vitro* by SDS-PAGE and confirmed that folding event of cleaved Bn by mass spectrometry, but there has been no study of its catalytic activity in the intact cells (Mitrea *et al.*, 2010). The 6aa HIV-1 protease recognition sequence (IFLETS) which contains sequence of any of the natural substrate of HIV-1 protease was identified by substrate phage display library (Beck *et al.*, 2000). This sequence is found to be cleaved 260 times more efficiently than the natural RT/IN cleavage site at pH 5.6. However, the cleavage efficiency drops dramatically at near physiological condition (pH 6.7) (Beck *et al.*, 2000). IFLETS sequence is shorter than the active site cleft of HIV-1 protease. Studies of the MA/CA site using synthetic peptides suggested that the residues occupying position

P4 through P3' flanking the scissile bonds were critical for specific and efficient cleavage (Bagossi *et al.*, 2005, Pettit *et al.*, 2002). In the present study, variant TAT-Pro-HIV-MA/CA-3 which had the MA/CA sites QNY/PIVQN (P3 to P5') and VSQNY/PIV (P5 to P3') and TAT-Pro-MA/CA-2 with NY/PIVQN (P2 to P5') and VSQNY/PI (P5 to P2') in a 25 aa internal loop length was not cleaved by HIV-1 protease *in vitro*. Therefore the efficiency of cleavage of this engineered Bn in cells is questionable.

TAT-[K159A-K160A-K161A-K162A]-MOD showed low cytoxicity as TAT-Pro in uninfected C8166, as well as limited inhibitory effects on viral replication compared with TAT-MOD and engineered maize RIPs (Table 4.1). The results revealed that besides the internal internal loop region, the four lysines just beneath the loop region is also an important factors determining the anti-HIV activity, as well as N-glycosidase activity (Table 4.1 and Figure 3.9). Nevertheless, it should be further noted that the EC_{50} of TAT-[K159A-K160A-K161A-K162A]-MOD found in the syncytial and p24 antigen production assays are lower than its IC_{50} found in cytotoxity test using uninfected cells (Table 4.1). Additional mechanisms other then inhibiting protein synthesis might contribute to the inhibitory effects in viral replication. Previous studies found that pokeweed antiviral protein isoforms depurinated HIV-1 viral RNA in spite of ribosomal RNA (Rajamohan *et al.*, 1999).

PAP is capable to distinguish capped and uncapped viral mRNA. Subsequently, PAP was found to inhibit the *in vitro* translation viral RNAs of AMV, TBSV and SPMV RNAs without causing detectable depurination of upcapped RNA, suggested that the cap structure is not the only determinant of inhibition of translation by PAP (Vivanco & Tumer, 2003). Trichosanthin depurinated the HIV-1 long-terminal repeats (LTR) in order to inhibit the HIV integration (Zhao *et al.*, 2010). Further investigation of the underlined anti-HIV mechanism of maize RIP is needed to clarify this issue.

4.4 Conclusion

In this chapter, the anti-HIV activities of TAT-fused maize RIP and selected variants were studied. TAT-fused maize RIP and variants possessed potent inhibitory effects on syncytium and p24 antigen production in human T lymphocyte (C8166) infected by two HIV-1 strains. For the TAT-HIV-Pro-MA/C[illegible] and TAT-Pro-HIV-p2/NC, their 50% effective concentrations of p24 antigen production assay were comparable to fully active TAT-MOD. However, they had much lower cytotoxicity towards uninfected cells. Furthermore, the *in vivo* N-glycosidase activity, as well as anti-HIV activity of engineered maize RIP in HIV-infected cells was much enhanced, suggesting removal of the internal activation region by HIV-1 protease increased the amount of depurination of rRNA and the inhibition of HIV replication.

The present study proved the feasibility of the switch-on strategy for regulating the enzymatic activity of maize RIP in target cells which provided an opportunity to enhance its therapeutic applications in the future.

Chapter Five

Conclusion and Future prospective

With the knowledge of the protein structure of maize RIP, the internal inactivation loop was engineered for targeting maize RIP toward HIV-infected cells. A method of construction of HIV-1 protease-activated maize RIP variants by substituting different HIV-1 protease recognition sequences in the inactivation region was demonstrated. In addition, a 11 residues TAT tag was fused to the N-terminal of maize RIP and variants in order to increase the cellular uptake. The TAT-fused maize RIP variants were tested for the effectiveness of cleavage of the modified region by HIV-1 protease. Three variants, each carried a 25 aa internal inactivation region with two 10 aa HIV-1 protease cleavage sites insertion were proved to be successfully cleaved by recombinant HIV-1 protease *in vitro* and in HIV-1 infected human T cells. Moreover, using real-time PCR technique, the level of 28S rRNA depurination was determined. The HIV-1 protease-cleaved variants showed increased N-glycosidase activity compared with their uncleaved counterparts in mouse macrophages.

TAT-fused maize RIP and the three variants possessed potent inhibitory effects on syncytium and p24 antigen production in human T lymphocyte (C8166) infected

by two HIV-1 strains. Among them, two variants TAT-Pro-HIV-MA/CA and TAT-Pro-HIV-p2/NC had 50% effective concentrations of p24 antigen production assay, which was comparable to fully active TAT-MOD and lower cytotoxicity towards uninfected cells. Along with the enhanced inhibition of viral replication, the two variants showed elevated N-glycosidase activity in HIV-infected cells. Nevertheless, my study suggested that inhibiting protein synthesis may not be the only anti-HIV mechanism of maize RIP.

The present study first reported the anti-HIV property of maize RIP and proved the feasibility of the switch-on strategy for regulating the enzymatic activity of maize RIP in HIV-infected cells. By incorporating different pathogen-specific protease recognition sequences into the internal inactivation region, maize RIP in principle can be activated in other pathogenic cells. Moreover, it is theoretically applicable to employ this technique to manipulate the enzymatic function of other RIPs which share similar three-dimensional structures with maize RIP, such as trichosanthin. By real-time PCR technology, it is possible to detect viral DNA and RNA quantitatively at different stages of the reverse transcription process in order to have a clearer picture about the anti-HIV mechanisms of maize RIP.

In the present study, it showed that the therapeutic indexes of the two selected variants, TAT-Pro-HIV-MA/CA and TAT-Pro-HIV-p2/NC, are greater than 72.89 and

83.52 respectively, indicating that they are potential candidates for preclinical study. Simian immunodeficiency virus (SIV)-infected Chinese rhensus macaque can be used to evaluate the anti-HIV and immunogenicity of maize RIP and selected variants in non-human primate AIDS model. Animal study will give us valuable information for exploration of therapeutic applications of maize RIP variants and their prospective in further clinical study.

Appendix

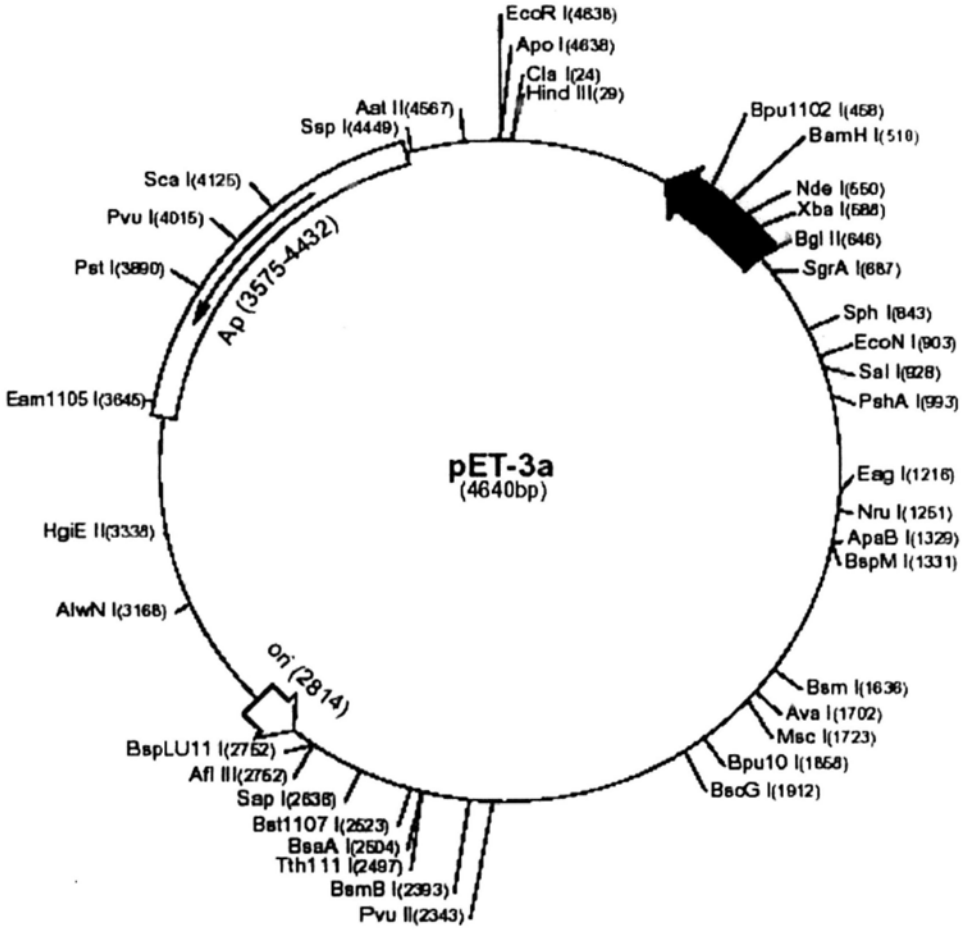

Appendix figure 1. Vector map of pET3a. The map for pET3b is same as pET3a except it is a 4639bp plasmid with 1bp subtraction from each site beyond BamHI at 510. (https://wasatch.biochem.utah.edu/chris/links/pET3a.pdf)

Appendix table 1 Primers for generating TAT-fused maize RIP variants

Variants	1st round PCR (Primers)	2nd round PCR (Primer)
TAT-Pro	TAT-Δ5aa Maize RIP- F Maize-RIP-R	---
TAT-MOD	TAT-Δ5aa Maize RIP- F Maize-RIP-R	---
TAT-Pro-HIV-MA/CA	TAT-Δ5aa Maize RIP- F Pro-RIP-HIV-25-R	TAT-Δ5aa Maize RIP- F Maize-RIP-R
	Pro-RIP-HIV-25-F Maize-RIP-R	
TAT-Pro-HIV-MA/CA-3	TAT-Δ5aa Maize RIP- F 253-3aa-R	TAT-Δ5aa Maize RIP- F Maize-RIP-R
	253-3aa-F Maize-RIP-R	
TAT-Pro-HIV-MA/CA-2	TAT-Δ5aa Maize RIP- F 253-2aa-R	TAT-Δ5aa Maize RIP- F Maize-RIP-R
	253-2aa-F Maize-RIP-R	
TAT-Pro-HIV-p2/NC	TAT-Δ5aa Maize RIP- F HIV-1p2/NC-R	TAT-Δ5aa Maize RIP- F Maize-RIP-R
	HIV-1p2/NC-F Maize-RIP-R	
TAT-Pro-HIV-p2/NC-RT/IN	TAT-Δ5aa Maize RIP- F HIV-1p2/NC-R	TAT-Δ5aa Maize RIP- F Maize-RIP-R
	HIV-1RT/IN-F Maize-RIP-R	

References

Au, T.K., Collins, R.A., Lam, T.L., Ng, T.B., Fong, W.P. and Wan, D.C. (2000) The plant ribosome inactivating proteins luffin and saporin are potent inhibitors of HIV-1 integrase. *FEBS Lett.*, **471,** 169-172.

Bagossi, P., Sperka, T., Feher, A., Kadas, J., Zahuczky, G., Miklossy, G., Boross, P. and Tözsér, J. (2005) Amino acid preferences for a critical substrate binding subsite of retroviral proteases in type 1 cleavage sites. *J. Virol.*, **79,** 4213-4218.

Bailey, A.C. and Fisher, M. (2008) Current use of antiretroviral treatment. *Br. Med. Bull.*, **87,** 175-192.

Barbieri, L., Ferreras, J.M., Barraco, A., Ricci, P. and Stirpe, F. (1992) Some ribosome-inactivating proteins depurinate ribosomal RNA at multiple sites. *Biochem. J.*, **286 (Pt 1),** 1-4.

Barbieri, L., Battelli, M.G. and Stirpe, F. (1993) Ribosome-inactivating proteins from plants. *Biochem. Biophys. Acta*, **1154,** 237-282.

Barbieri, L., Valbonesi, P., Gorini, P., Pession, A. and Stirpe, F. (1996) Polynucleotide: adenosine glycosidase activity of saporin-L1: effect on DNA, RNA and poly(A). *Biochem. J.*, **319 (Pt 2),** 507-513.

Barbieri, L., Valbonesi, P., Bonora, E., Gorini, P., Bolognesi, A. and Stirpe, F. (1997) Polynucleotide:adenosine glycosidase activity of ribosome-inactivating proteins: effect on DNA, RNA and poly(A). *Nucleic Acids Res.*, **25,** 518-522.

8. Barthelemy, I., Martineau, D., Ong, M., Matsunami, R., Ling, N., Benatti, L., Cacallaro, U., Soria, M. and Lappi, D.A. (1993) The expression of saporin, a ribosome-inactivating protein from the plant Saponaria officinalis, in Escherichia coli. *J. Biol. Chem.*, **25,** 6541-6548.

Bass, H.W., Krawetz, J.E., OBrain, G.R., Zinselmeier, C., Habben, J.E. and Boston, R.S. (2004) Maize ribosome-inactivating proteins (RIPs) with distinct expression patterns have similar requirements for proenzyme activation. *J. Exp. Bot.*, **55,** 2219-2233.

Battelli, M.G., Montacuti, V. and Stirpe, F. (1992) High sensitivity of cultured human trophoblast to ribosome-inactivating proteins. *Exp. Cell Res*, **201,** 109-112.

Battelli, M.G., Citores, L., Buonamici, L., Ferreras, J.M., de Benito, F.M., Stirpe, F. and Girbes, T. (1997) Toxicity and cytotoxicity of nigrin b, a two-chain ribosome-inactivating protein from Sambucus nigra: comparison with ricin. *Arch. Toxicol.*, **71,** 360-364.

Beaumelle, B., Alami, M. and Hopkins, C.R. (1993) ATP-dependent translocation of ricin across the membrane of purified endosomes. *J. Biol. Chem.*, **268,** 23661-23669.

Beck, Z.Q., Hervio, L., Dawson, P.E., Elder, J.H. and Madison, E.L. (2000) Identification of efficiently cleaved substrates for HIV-1 protease using a phage display library and use in inhibitor development. *Virology*, **274,** 391-401.

Beck, Z.Q., Morris, G.M. and Elder, J.H. (2002) Defining HIV-1 protease substrate selectivity. *Curr. Drug Targets Infect. Disord.*, **2,** 37-50.

Becker-Hapak, M., McAllister, S.S. and Dowdy, S.F. (2001) TAT-mediated protein transduction into mammalian cells. *Methods*, **24,** 247-256.

Bedimo, R. (2008) Non-AIDS-defining malignancies among HIV-infected patients in the highly active antiretroviral therapy era. *Curr. HIV/AIDS Rep.*, **5,** 140-149.

Billich, A. and Winkler, G. (1991) Analysis of subsite preferences of HIV-1 proteinase using MA/CA junction peptides substituted at the P3-P1' positions. *Arch. Biochem. Biophys.*, **290,** 186-190.

Blaak, H., van't Wout, A.B., Brouwer, M., Hooibrink, B., Hovenkamp, E. and Schuitemaker, H. (2000) In vivo HIV-1 infection of CD45RA(+)CD4(+) T cells is established primarily by syncytium-inducing variants and correlates with the rate of CD4(+) T cell decline. *Proc. Natl. Acad. Sci. U S A*, **97,** 1269-1274.

Bouzide, A., Sauve, G. and Yelle, J. (2005) Lysine derivatives as potent HIV protease inhibitors. Discovery, synthesis and structure-activity relationship studies. *Bioorg. Med. Chem. Let.t*, **15,** 1509-1513.

Bullok, K.E., Gammon, S.T., Violini, S., Prantner, A.M., Villalobos, V.M., Sharma, V.

and Piwnica-Worms, D. (2006) Permeation peptide conjugates for in vivo molecular imaging applications. *Mol. Imaging*, **5,** 1-15.

Cai, Y.D., Liu, X.J., Xu, X.B. and Chou, K.C. (2002) Support Vector Machines for predicting HIV protease cleavage sites in protein. *J. Comput. Chem.*, **23,** 267-274.

Cavallaro, U., Nykjaer, A., Nielsen, M. and Soria, M.R. (1995) Alpha 2-macroglobulin receptor mediates binding and cytotoxicity of plant ribosome-inactivating proteins. *Eur. J. Biochem.*, **232,** 165-171.

Cavallaro, U. and Soria, M.R. (1995) Targeting plant toxins to the urokinase and alpha 2-macroglobulin receptors. *Semin. Cancer Biol.*, **6,** 269-278.

Chan, W.Y., Tam, P.P. and Yeung, H.W. (1984) The termination of early pregnancy in the mouse by beta-momorcharin. *Contraception*, **29,** 91-100.

Chan, W.L., Shaw, P.C., Tam, S.C., Jacobsen, C., Gliemann, J. and Nielsen, M.S. (2000) Trichosanthin interacts with and enters cells via LDL receptor family members. *Biochem. Biophys. Res. Commun.*, **270,** 453-457.

Chan, S.H., Shaw, P.C., Mulot, S.F., Xu, L.H., Chan, W.L., Tam, S.C. and Wong, K.B. (2000) Engineering of a mini-trichosanthin that has lower antigenicity by deleting its c-terminal amino acid residues. *Biochem. Biophy. Res. Comm.*, **270,** 279-285.

Chan, S.H., Hung, F.S., Chan, D.S. and Shaw, P.C. (2001) Trichosanthin interacts with acidic ribosomal proteins P0 and P1 and mitotic checkpoint protein MAD2B. *Eur. J. Biochem..*, **268,** 2107-2112.

Chan, D.S., Chu, L.O., Lee, K.M., Too, P.H., Ma, K.W., Sze, K.H., Shaw, P.C. and Wong, K.B. (2007) Interaction between trichosanthin, a ribosome-inactivating protein, and the ribosome stalk protein P2 by chemical shift perturbation and mutagenesis analyses. *Nucleic Acids Res.*, **35,** 1660-1672.

Chan Tung, C.T., Mansouri, S. and Hudak, K.A. (2008) Expression of pokeweed antiviral protein in mammalian cells activates c-Jun NH2-terminal kinase without causing apoptosis. *Int. J. Biochem. Cell Biol.*, **40,** 2452-2461.

Chaudhry, B., Muller-Uri, F., Cameron-Mills, V., Gough, S., Simpson, D., Skriver, K.

and Mundy, J. (1994) The barley 60 kDa jasminate-induced protein (JIP60) is a novel ribosome-inactivating protein. *Plant J.*, **6,** 815-824.

Cheng-Mayer, C., Seto, D., Tateno, M. and Levy, J.A. (1988) Biological features of HIV-1 that correlate with virulence in the host. *Science*, **240,** 80-82.

Chiou, J.C., Li, X.P., Remacha, M., Ballesta, J.P. and Tumer, N.E. (2008) The ribosomal stalk is required for ribosome binding, depurination of the rRNA and cytotoxicity of ricin A chain in Saccharomyces cerevisiae. *Mol. Microbiol.*, **70,** 1441-1452.

Choe, H., Farzan, M., Sullivan, N., Rollins, B., Ponath, P.D., Wu, L., Mackay, C.R., LaRosa, G., Newman, W., Gerard, N. *et al.* (1996) The beta-chemokine receptors CCR3 and CCR5 facilitate infection by primary HIV-1 isolates. *Cell*, **85,** 1135-1148.

Chomczynski, P. and Mackey, K. (1995) Short technical reports. Modification of the TRI reagent procedure for isolation of RNA from polysaccharide- and proteoglycan-rich sources. *Biotechniques*, **19,** 942-945.

Collins, E.J., Robertus, J.D., LoPresti, M., Stone, K.L., Williams, K.R., Wu, P., Hwang, K. and Piatak, M. (1990) Primary amino acid sequence of alpha-trichosanthin and molecular models for abrin A-chain and alpha-trichosanthin. *J. Biol. Chem*, **265,** 8665-8669.

Costin, J.M. (2007) Cytopathic mechanism of HIV-1. *Virol. J.*, **4,** 100.

Darke, P.L., Nutt, R.F., Brady, S.F., Garsky, V.M., Ciccarone, T.M., Leu, C.T., Lumma, P.K., Freidinger, R.M., Veber, D.F. and Sigal, I.S. (1988) HIV-1 protease specificity of peptide cleavage is sufficient for processing of gag and pol polyproteins. *Biochem. Biophys. Res. Commun.*, **156,** 297-303.

de Silva, T.I., Cotten, M. and Rowland-Jones, S.L. (2008) HIV-2: the forgotten AIDS virus. *Trends Microbiol.*, **16,** 588-595.

Dulbecco, R. (1988) In Dulbecco, R. and and Ginsberg, H. S. (eds.), *Virology*. J.P. Lippincott, Philadelphia, pp. 22-25.

Dunaeva, M., Goebel, C., Wasternack, C., Parthier, B. and Goerschen, E. (1999) The

jasmonate-induced 60 kDa protein of barley exhibits N-glycosidase activity in vivo. *FEBS Lett.*, **452,** 263-266.

Dunaeva, M. and Goerschen, E. (1999) RIP-JIP60 alters conformation of ribosomes in vivo. *Biochem. Biophys. Res. Commun.*, **258,** 572-573.

Dunn, B.M., Goodenow, M.M., Gustchina, A. and Wlodawer, A. (2002) Retroviral proteases. *Genome Biol.*, **3,** REVIEWS3006.

Endo, Y. and Taurugi, K. (1988) The RNA N-glycosidase activity of ricin A-chain. The characteristics of the enzymatic activity of ricin A-chain with ribosomes and with rRNA. *J. Biol. Chem.*, **25,** 8735-8739.

Endo, Y., Gluck, A. and Wool, I.G. (1991) Ribosomal RNA identity elements for ricin A-chain recognition and catalysis. *J. Mol. Biol.*, **221,** 193-207.

Engvall, E. (2010) The ELISA, enzyme-linked immunosorbent assay. *Clin. Chem.*, **56,** 391-320.

Erice, A., Balfour, H.H., Jr., Myers, D.E., Leske, V.L., Sannerud, K.J., Kuebelbeck, V., Irvin, J.D. and Uckun, F.M. (1993) Anti-human immunodeficiency virus type 1 activity of an anti-CD4 immunoconjugate containing pokeweed antiviral protein. *Antimicrob Agents Chemother.*, **37,** 835-838.

Falnes, P. and Sandvig, K. (2000) Penetration of protein toxins into cells. *Curr. Opin. Cell Biol.*, **12,** 407-413.

Fawell, S., Seery, J., Daikh, Y., Moore, C., Chen, L.L., Pepinsky, B. and Barsoum, J. (1994) Tat-mediated delivery of heterologous proteins into cells. *Proc. Natl. Acad. Sci. USA.*, **91,** 664-668.

Fenyo, E.M., Albert, J. and Asjo, B. (1989) Replicative capacity, cytopathic effect and cell tropism of HIV. *AIDS*, **3 Suppl 1,** S5-S12.

Ferri, K.F., Jacotot, E., Blanco, J., Este, J.A., Zamzami, N., Susin, S.A., Xie, Z., Brothers, G., Reed, J.C., Penninger, J.M. *et al.* (2000) Apoptosis control in syncytia induced by the HIV type 1-envelope glycoprotein complex: role of mitochondria and caspases. *J. Exp. Med.*, **192,** 1081-1092.

Flinterman, M., Farzaneh, F., Habib, N., Malik, F., Gaken, J. and Tavassoli, M. (2009) Delivery of therapeutic proteins as secretable TAT fusion products. *Mol. Ther.*, **17,** 334-342.

Florescu, D. and Kotler, D.P. (2007) Insulin resistence, glucose intolerance and diabetes mellitus in HIV-infected patients. *Antivir. Ther.*, **12,** 149-162.

Fouchier, R.A., Brouwer, M., Broersen, S.M. and Schuitemaker, H. (1995) Simple determination of human immunodeficiency virus type 1 syncytium-inducing V3 genotype by PCR. *J. Clin. Microbiol.*, **33,** 906-911.

Frankel, A.D. and Pabo, C.O. (1988) Cellular uptake of the tat protein from human immunodeficiency virus. *Cell*, **55,** 1189-1193.

Frankel, A.D. and Young, J.A. (1998) HIV-1: Fifteen proteins and an RNA. *Annu. Rev. Biochem.*, **67,** 1-25.

Freed, E.O. and Martin, M.A. (2007) In Knipe, D. M. and Howley, P. M. (eds.), *Feilds Virology*. 5th ed. Lippincott, Williams, and Wilkins, Philadelphia, Vol. Chapter 57, pp. 2107-2186.

Girbes, T., Ferreras, J.M., Arias, F.J. and Stirpe, F. (2004) Description, distribution, activity and phylogenetic relationship of ribosome-inactivating proteins in plants, fungi and bacteria. *Mini Rev. Med. Chem.*, **4,** 461-476.

Green, M. and Loewenstein, P.M. (1988) Autonomous functional domains of chemically synthesized human immunodeficiency virus tat trans-activator protein. *Cell*, **55,** 1179-1188.

Gump, J.M. and Dowdy, S.F. (2007) TAT transduction: the molecular mechanism and therapeutic prospects. *Trends Mol. Med.*, **10,** 443-448.

Guo, Q., Zhou, W., Too, H.M., Li, J., Liu, Y., Bartlam, M., Dong, Y., Wong, K.B., Shaw, P.C. and Rao, Z. (2003) Substrate binding and catalysis in trichosanthin occur in different sites as revealed by the complex structures of several E85 mutants. *Protein Eng.*, **16,** 391-396.

Han, Z., Hendrickson, E.A., Bremner, T.A. and Wyche, J.H. (1997) A sequential

two-step mechanism for the production of the mature p17:p12 form of caspase-3 in vitro. *J. Biol. Chem.*, **272,** 13432-13436.

Hartley, M.R., Chaddock, J.A. and Bonness, M.S. (1996) The structure and function of ribosome-inactivating proteins. *Trends Plant Sci.*, **1,** 254-260.

Hartley, M.R. and Lord, J.M. (2004) Cytotoxic ribosome-inactivating lectins from plants. *Biochimica. Biophysica. Acta*, **1701,** 1-14.

Hazebrouck, S., Machtelinckx-Delmas, V., Kupiec, J.J. and Sonigo, P. (2001) Local and spatial factors determining HIV-1 protease substrate recognition. *Biochem. J.*, **358,** 505-510.

He, X.H., Shaw, P.C., Xu, H.L. and Tam, S.C. (1999) Site-directed polyethylene glycol modification of trichosanthin: effects on its biological activities, pharmacokinetics, and antigenicity. *Life Sci.*, **64,** 1163-1175.

Heisler, I., Keller, J., Tauber, R., Sutherland, M. and Fuchs, H. (2002) A colorimetric assay for the quantitation of free adenine applied to determine the enzymatic activity of ribosome-inactivating proteins. *Anal. Biochem.*, **302,** 114-122.

Herce, H.D. and Garcia, A.E. (2007) Molecular dynamics simulations suggest a mechanism for translocation of the HIV-1 TAT peptide across lipid membranes. *Proc. Natl. Acad. Sci. USA*, **104,** 20805-20810.

Hey, T.D., Hartley, M. and Walsh, T.A. (1995) Maize ribosome-inactivating protein (b-32): Homologs in related species, effects on maize ribosomes, and modulation of activity by pro-peptide deletions. *Plant Physol.*, **107,** 1323-1332.

Hudak, K.A., Dinman, J.D. and Tumer, N.E. (1999) Pokeweed antiviral protein accesses ribosomes by binding to L3. *J. Biol. Chem.*, **274,** 3859-3864.

Hudak, K.A., Wang, P. and Tumer, N.E. (2000) A novel mechanism for inhibition of translation by pokeweed antiviral protein: depurination of the capped RNA template. *RNA*, **3,** 369-380.

Hudak, K.A., Bauman, J.D. and Tumer, N.E. (2002) Pokeweek antiviral protein binds to the cap structure of eukaryotic mRNA and depurinates the mRNA downstream of

the cap. *RNA*, **8,** 1148-1159.

Irvin, J.D. and Uckun, F.M. (1992) Pokeweed antiviral protein: ribosome inactivation and therapeutic applications. *Pharmacol. Ther.*, **55,** 279-302.

Jimenez, A. and Vazquez, D. (1985) Plant and fungal protein and glycoprotein toxins inhibiting eukaryote protein synthesis. *Annu. Rev. Microbiol.*, **39,** 649-672.

Jiratchariyakui, W., Wiwat, C., Vongsakui, M., Somanabandhu, A., Leelamanit, W., Fujii, I., Sueannaroj, N. and Ebizuka, Y. (2001) HIV inhibitors from Thai bitter gourd. *Planta Med.*, **67,** 350-353.

Johnson, V.A., Brun-Vezinet, F., Clotet, B., Gunthard, H.F., Kuritzkes, D.R., Pillay, D., Schapiro, J.M. and Richman, D.D. (2008) Update of the drug resistance mutations in HIV-1: 2008. *Top. HIV Med.*, **16,** 138-145.

Kahn, J.O. (1992) Anti-human immunodeficiency virus therapeutics:now and the future. *Semin. Liver Dis.*, **12,** 121-127.

Klei, H.E., Kish, K.K., Lin, P.F.M., Guo, Q., Friborg, J., Rose, R.E., Zhang, Y., Goldfarb, V., Langley, D.R., Wittekind, M. *et al.* (2007) X-ray crystal structure of human immunodeficiency virus type 1 protease mutants complex with Atazanavir. *J. Virol.*, **81,** 9525-9535.

Koot, M., Keet, I.P., Vos, A.H., de Goede, R.E., Roos, M.T., Coutinho, R.A., Miedema, F., Schellekens, P.T. and Tersmette, M. (1993) Prognostic value of HIV-1 syncytim-inducing pheontype for rate of CD4+ cell depletion and progression to AIDS. *Ann. Intern. Med.*, **118,** 681-688.

Kozak, S.L., Platt, E.J., Madani, N., Ferro, F.E.J., Peden, K. and Kabat, D. (1997) CD4, CXCR-4, and CCR-5 dependencies for infections by primary patient and laboratory-adapted isolations of human immunodeficiency virus type 1. *J. Virol.*, **71,** 873-882.

Krausslich, H.G., Ingraham, R.H., Skoog, M.T., Wimmer, E., Pallai, P.V. and Carter, C.A. (1989) Activity of purified biosynthetic proteinase of human immunodeficiency virus on natural substrates and synthetic peptides. *Proc. Natl. Acad. Sci. USA*, **86,** 807-811.

Lange, J.M.A., Pau, D.A., Huisman, H.G., de Wolf, F., van den Berg, H., Coutinho, R.A., Danner, S.A., van der Noordaa, J. and Goudsmit, J. (1986) Persistent HIV antigenaemia and decline of HIV core antibodies associated with transition to AIDS. *Br. Med. J. (Clin. Res. Ed)*, **293,** 1459-1462.

Ledergerber, B., Flepp, M., Boni, J., Tomasik, Z., Cone, R.W., Luthy, R. and Schupbach, J. (2000) Human immunodeficiency virus type 1 p24 concentration measured by boosted ELISA of heat-denatured plasma correlates with decline in CD4 cells, progression to AIDS, and survival: comparison with viral RNA measurement. *J. Infect. Dis.*, **181,** 1280-1288.

Lee-Huang, S.L., Huang, P.L., Kung, H.F., Li, B.Q., Huang, P.L., Huang, P., Huang, H.I. and Chen, H.C. (1991) TAP 29: An anti-human immunodeficiency virus protein from Trichosanthes kirilowii that is nontoxic to intact cells. *Proc. Natl. Acad. Sci USA.*, **88,** 6570-6574.

Lee-Huang, S., Kung, H.F., Huang, P.L., Huang, P.L., Li, B.Q., Huang, P., Huang, H.I. and Chen, H.C. (1991) A new class of anti-HIV agents: GAP31, DAPs 30 and 32. *FEBS Lett.*, **291,** 139-144.

Lee-Huang, S., Kung, H.F., Huang, P.L., Bourinbaiar, A.S., Mprell, L.J., Brown, J.H., Huang, P.L., Tsai, W.P., Vhen, A.Y., Huang, H.I. *et al.* (1994) Human immunodeficiency virus type 1 (HIV-1) inhibition, DNA-binding, RNA-binding, and ribosome inactivating activities in the N-terminal segments of the plant anti-HIV protein GAP31. *Proc. Natl. Acad. Sci.*, **91,** 12208-12212.

Lifson, J.D., Reyes, G.R., McGrath, M.S., Stein, B.S. and Engleman, E.G. (1986) AIDS retrovirus induced cytopathology: giant cell formation and involvement of CD4 antigen. *Science*, **232,** 1123-1127.

Lin, X.L., Lin, Y.Z. and Tang, J. (1994) Relationships of human immunodeficiency virus protease with eukaryotic aspartic proteases. *Methods Enzymol.*, **241,** 195-224.

Liu, R.S., Yang, J.H. and Liu, W.Y. (2002) Isolation and enzymatic characterization of lamjapin, the first ribosome-inactivating protein from cryptogamic algal plant (Laminaria japonica A). *Eur. J. Biochem.*, **269,** 4746-4752.

Lord, J.M., Roberts, L.M. and Robertus, J.D. (1994) Ricin: structure, mode of action,

and some current applications. *FASEB J.*, **8,** 201-208.

Louis, J.M., Wondrak, E.M., Kimmel, A.R., Wingfield, P.T. and Nashed, N.T. (1999) Proteolytic processing of HIV-1 protease precursor, kinetics and mechanism. *J. Biol. Chem.*, **274,** 2343??3442.

Lu, L., Jia, M., Ma, Y., Yang, L., Chen, Z., Ho, D.D., Jiang, Y. and Zhang, L. (2008) The changing face of HIV in China. *Nature*, **455,** 609-611.

Mager, P.P. (2001) The active site of HIV-1 protease. *Med. Res. Rev.*, **21,** 348-353.

Mak, A.N.S., Wong, Y.T., An, Y.J., Cha, S.S., Sze, K.H., Au, S.W., Wong, K.B. and Shaw, P.C. (2007) Structure-function study of maize ribosome- inactivating protein: implications for the internal inactivation region and the sole glutamate in the active site. *Nucleic Acids Res.*, **35,** 6259-6267.

Marchant, A. and Hartley, M.R. (1995) The action of pokeweed antiviral protein and ricin A-chain on mutants in the alpha-sarcin loop of Escherichia coli 23S ribosomal RNA. *J. Mol. Biol.*, **254,** 848-855.

McCutchan, F.E. (2006) Global epidemiology of HIV. *J. Med. Virol.*, **78,** S7-S12.

Melchior, W.B. and Tolleson, W.H. (2009) A functional quantitative polymerase chain reaction assay for ricin, Shiga toxin, and related ribosome-inactivating proteins. *Anal. Biochem*, **396,** 204-211.

Mitrea, D.M., Parsons, L.S. and Loh, S.N. (2010) Engineering an artificial zymogen by alternate frame protein folding. *Proc. Natl. Acad. Sci. USA*, **107,** 2824-2829.

Mlsna, D., Monzingo, A.F., Katzin, B.J., Ernst, S. and Robertus, J.D. (1993) Structure of recombinant ricin A chain at 2.3 A. *Protein Sci.*, **2,** 429-435.

Monzingo, A.F., Collins, E.J., Ernst, S.R., Irvin, J.D. and Robertus, J.D. (1993) The 2.5 A structure of pokeweed antiviral protein. *J. Mol. Biol.*, **233,** 705-715.

Motto, M. and Lupotto, E. (2004) The genetics and properties of cereal ribosome-inactivating proteins. *Mini Rev. Med. Chem.*, **4,** 493-503.

Mundy, J., Leah, R., Boston, R., Endo, Y. and Stirpe, F. (1994) Genes encoding ribosome-inactivating proteins. *Plant Mol. Biol. Rep.*, **12,** s60-62.

Nagahara, H., Vocero-Akbani, A.M., Snyder, E.L., Ho, A., Latham, D.G., Lissy, N.A., Becker-Hapak, M., Ezhevsky, S.A. and Dowdy, S.F. (1998) Transduction of full-length TAT fusion proteins into mammalian cells: TAT-p27Kip1 induces cell migration. *Nat. Med.*, **4,** 1449-1452.

Nakao, H. and Takeda, T. (2000) Escherichia coli Shiga toxin. *J. Nat. Toxins*, **9,** 299-313.

Nielsen, K. and Boston, R.S. (2001) Ribosome-inactivating proteins: a plant perspective. *Annu. Rev. Plant Physiol. Plant Mol. Biol.*, **52,** 785-816.

Nisole, S. and Saib, A. (2004) Early steps of retrovirus replicative cycle. *Retrovirology*, **1,** 9.

O'Keefe, B.R. (2001) Biologically active proteins from natural product extracts. *J. Nat. Prod.*, **64,** 1373-1381.

Olsnes, S. and Pihl, A. (1973) Isolation and properties of abrin: a toxic protein inhibiting protein synthesis. Evidence for different biological functions of its two constituent-peptide chains. *Eur. J. Biochem.*, **35,** 179-185.

Olsnes, S., Fernandez-Puentes, C., Carrasco, L. and Vazquez, D. (1975) Ribosome inactivation by the toxic lectins abrin and ricin. Kinetics of the enzymic activity of the toxin A-chains. *Eur. J. Biochem.*, **60,** 281-288.

Olsnes, S. and Pihl, A. (1981) Chimeric toxins. *Pharmacol. Ther.*, **15,** 355-381.

Olsnes, S. and Kozlvo, J.V. (2001) Ricin. *Toxicon*, **39,** 1723-1728.

Olsnes, S. (2004) The history of ricin, abrin and related toxins. *Toxicon*, **15,** 361-370.

Ouyang, D.Y., Chan, H., Wang, Y.Y., Huang, H., Tam, S.C. and Zheng, Y.T. (2006) An inhibitor of c-Jun N-terminal kinases (CEP-11004) counteracts the anti-HIV-1 action of trichosanthin. *Biochem. Biophys. Res. Commun.*, **339,** 25-29.

Palella, F.J., Delansy, K.M., Moorman, A.C., Loveless, M.O., Fuhrer, J., Satten, G.A., Aschman, D.J. and Holmbery, S.D. (1998) Declining morbidity and mortality among patients with advanced human immunodeficiency virus infection. HIV outpatient study investigators. *N. Engl. J. Med.*, **338,** 853-860.

Pearson, W.R. (1990) Rapid and sensitive sequence comparison with FASTP and FASTA. *Methods Enzymol.*, **183,** 63-98.

Perfettini, J.L., Castedo, M., Roumier, T., Andreau, K., Nardacci, R., Piacentini, M. and Kroemer, G. (2005) Mechanisms of apoptosis induction by the HIV-1 envelope. *Cell Death Differ.*, **12 Suppl 1,** 916-923.

Pettit, S.C., Simsic, J., Loeb, D.D., Everitt, L., Hutchison, C.A.r. and Swanstrom, R. (1991) Analysis of retroviral protease cleavage sites reveals two types of cleavage sites and the structural requirements of the P1 amino acid. *J. Biol. Chem.*, **266,** 14539-14547.

Pettit, S.C., Simsic, J., Loeb, D.D., Everitt, L., Hutchison III, C.A. and Swanstrom, R. (1991) Analysis of retroviral protease cleavage sites reveals two types of cleavage sites and the structural requirements of the P1 amino acid. *J. Biol. Chem.*, **266,** 14539-14547.

Pettit, S.C., Moody, M.D., Wehbie, R.S., Kaplan, A.H., Nantermet, P.V., Klein, C.A. and Swanstrom, R. (1994) The p2 domain of human immunodeficiency virus type 1 Gag regulates sequential proteolytic processing and is required to produce fully infectious virions. *J. Virol.*, **68,** 8017-8027.

Pettit, S.C., Henderson, G.J., Schiffer, C.A. and Swanstrom, R. (2002) Replacement of the P1 amino acid of human immunodeficiency virus type 1 Gag processing sites can inhibit or enhance the rate of cleavage by the viral protease. *J. Virol.*, **76,** 10226-10233.

Pettit, S.C., Clemente, J.C., Jeung, J.A., Dunn, B.M. and Kaplan, A.H. (2005a) Ordered processing of the human immunodeficiency virus type 1 GagPol precursor is influenced by the context of the embedded viral protease. *J. Virol.*, **79,** 10601-10607.

Pettit, S.C., Lindquist, J.N., Kaplan, A.H. and Swanstorm, R. (2005b) Processing sites in the human immunodeficiency virus type 1 (HIV-1) Gag-Pro-Pol precursor are

cleaved by the viral protease at different rates. *Retrovirology*, **2,** 66-71.

Peumans, W.J., Hao, Q. and Van Damme, E.J. (2001) Ribosome-inactivating proteins from plants: more than RNA N-glycosidases? *FASEB J.*, **15,** 1493-1506.

Polgar, L., Szeltner, Z. and Boros, I. (1994) Substrate-dependent mechanisms in the catalysis of human immunodeficiency virus protease. *Biochemistry*, **33,** 9351-9357.

Prabu-Jeyabalan, M., Nalivaika, E. and Schiffer, C. (2000) How does a symmetric dimer recognize an asymmetric substrate? A substrate complex of HIV-1 Protease. *J. Mol. Biol.*, **301,** 1207-1220.

Rajamohan, F., Kurinov, I.V., Venkatachalam, T.K. and Uckun, F.M. (1999a) Deguanylation of human immunodeficiency virus (HIV-1) RNA by recombinant pokeweed antiviral protein. *Biochem. Biophys. Res. Commun.*, **263,** 419-424.

Rajamohan, F., Venkatachalam, T.K., Irvin, J.D. and Uckun, F.M. (1999b) Pokeweed antivirial protein isoforms PAP-I, PAP-II and PAP-III depurinate RNA of human immunodeficiency virus (HIV)-1. *Biochem. Biophys. Res. Commun.*, **260,** 453-458.

Roberts, L.M. and Lord, J.M. (2004) Ribosome-inactivating proteins: entry into mammalian cells and intracellular routing. *Mini Rev. Med. Chem.*, **4,** 505-512.

Robertson, D.L., Sharp, P.M., MaCutchan, F.E. and Hahn, B.H. (1995) Recombination in HIV-1. *Nature*, **374,** 124-126.

Rognvaldsson, T., You, L. and Garwicz, D. (2007) Bioinformatic approaches for modeling the substrate specificity of HIV-1 protease: an overview. *Expert. Rev. Mol. Diagn.*, **7,** 435-451.

Sandvig, K., Olsnes, S. and Pihl, A. (1976) Kinetics of binding of the toxic lectins abrin and ricin to surface receptors of human cells. *J. Biol. Chem.*, **251,** 3977-3984.

Sandvig, K. and van Deurs, B. (1999) Endocytosis and intracellular transport of ricin: recent discoveries. *FEBS Lett.*, **452,** 67-70.

Sandvig, K. and van Deurs, B. (2000) Entry of ricin and Shiga toxin into cells: molecular mechanisms and medical perspectives. *EMBO J*, **19,** 5943-5950.

Sandvig, K. (2001) Shiga toxins. *Toxicon*, **39,** 1629-1635.

Sandvig, K. and Grimmer, S. (2002) Pathways followed by ricin and Shiga toxin into cells. *Histochem. Cell Biol.*, **117,** 131-141.

Schuitemaker, H., Kootstra, N.A., de Goede, R.E.Y., de Wolf, F., Miedema, F. and Tersmette, M. (1991) Monosytotropic human immunodeficiency virus type 1 (HIV-1) variants detectable in all stages of HIV-1 infection lack T-cell line tropism and syncytium-inducing ability in primary T-cell culture. *J. Virol.*, **65,** 356-363.

Schuitemaker, H., Fouchier, R.A., Broersen, S., Groenink, M., Koot, M., van 't Wout, A.B., Huisman, H.G., Tersmette, M. and Miedema, F. (1995) Envelope V2 configuration and HIV-1 phenotype: clarification. *Science*, **268,** 115.

Schupbach, J., Tomasik, Z., Nadal, D., Ledergerber, B., Flepp, M., Opravil, M. and Boni, J. (2000) Use of HIV-1 p24 as a sensitive, precise and inexpensive marker for infection, disease progression and treatment failure. *Int. J. Antimicrob. Agents*, **16,** 441-445.

Serio, D., Rizvi, T.A., Cartas, M., Kalyanaraman, V.S., Weber, I.T., Koprowski, H. and Srinivasan, A. (1997) Development of a novel anti-HIV-1 agent from within: effect of chimeric Vpr-containing protease cleavage site residues on virus replication. *Proc. Natl. Acad. Sci. U S A*, **94,** 3346-3351.

Serio, D., Singh, S.P., Cartas, M.A., Weber, I.T., Harrison, R.W., Louis, J.M. and Srinivasan, A. (2000) Antiviral agent based on the non-structural protein targeting the maturation process of HIV-1: expression and susceptibility of chimeric Vpr as a substrate for cleavage by HIV-1 protease. *Protein Eng.*, **13,** 431-436.

Shafer, R.W. (2002) Genotypic testing for human immunodecifiency virus type 1 drug resistance. *Clin. Microbiol. Rev.*, **15,** 247-277.

Sharp, P.M. and Hahn, B.H. (2008) Prehistory of HIV-1. *Nature*, **455,** 605-606.

Shaw, P.C., Lee, K.M. and Wong, K.B. (2005) Recent advances in trichosanthin, a ribosome-inactivating protein with multiple pharmacological properties. *Toxicon*, **45,** 683-689.

Shen, D., Liang, K., Ye, Y., Tetteh, E. and Achilefu, S. (2007) Modulation of nuclear internalization of Tat peptides by fluorescent dyes and receptor-avid peptides. *FEBS Lett.*, **581,** 1793-1799.

Sierra, S., Kupfer, B. and Kaiser, R. (2005) Basic of the virology of HIV-1 and its replication. *J. Clin. Virol.*, **34,** 233-244.

Sinoussi, F.B. (1996) HIV as the cause of AIDS. *Lancet*, **348,** 31-35.

Snyder, E.L. and Dowdy, S.F. (2005) Recent advances in the use of protein transduction domains for the delivery of peptides, proteins and nucleic acids in vivo. *Expert Opin. Drug Deliv.*, **2,** 43-51.

Sodroski, J., Goh, W.C., Rosen, C., Campbell, K. and Haseltine, W.A. (1986) Role of the HTLV-III/LAV envelope in syncytium formation and cytopathicity. *Nature*, **322,** 470-474.

Stirpe, F., Olsnes, S. and Pihl, A. (1980) Gelonin, a new inhibitor of protein synthesis, nontoxic to intact cells. Isolation, characterization, and preparation of cytotoxic complexes with concanavalin A. *J. Biol. Chem.*, **255,** 6947-6953.

Stirpe, F., Bailey, S., Miller, S.P. and Bodley, J.W. (1988) Modification of ribosomal RNA by ribosome-inactivating proteins from plants. *Nucleic Acids Res.*, **16,** 1347-1357.

Stirpe, F., Barbieri, L., Battelli, M.G., Soria, M. and Lappi, D.A. (1992) Ribosome-inactivating proteins from plants: present status and future prospects. *Biotechnology*, **10,** 305-412.

Stirpe, F. and Battelli, M.G. (2006) Ribosome-inactivating proteins: progress and problems. *Cell. Mol. Life Sci.*, **63,** 1850-1866.

Sullivan, N., Sun, Y., Li, J., Hofmann, W. and Sodroski, J. (1995) Replicative function and neutralization sensitivity of envelope glycoproteins from primary and T-cell line-passaged human immunodeficiency virus type 1 isolates. *J. Virol.*, **69,** 4413-4422.

Svinth, M., Steighardt, J., Hernandez, R., Suh, J.K., Kelly, C., Day, P., Lord, M., Girbes, T. and Robertus, J.D. (1998) Differences in cytotoxicity of native and

engineered RIPs can be used to assess their ability to reach the cytoplasm. *Biochem. Biophys. Res. Commun.*, **249,** 637-642.

Sylwester, A., Murphy, S., Shutt, D. and Soll, D.R. (1997) HIV-induced T cell syncytia are self-perpetuating and the primary cause of T cell death in culture. *J. Immunol.*, **158,** 3996-4007.

Szeltner, Z. and Polgar, L. (1996) Rate-determining steps in HIV-1 protease catalysis. The hydrolysis of the most specific substrate. *J. Biol. Chem.*, **271,** 32180-32184.

Takeshita, M., Chang, C.N., Johnson, F., Will, S. and Grollman, A.P. (1987) Oligodeoxynucleotides containing synthetic abasic sites. Model substrates for DNA polymerases and apurinic/apyrimidinic endonucleases. *J. Biol. Chem.*, **262,** 10171-10179.

Taylor, B.S., Sobieszczyk, M.E., McCutchan, F.E. and and Hammer, S.M. (2008) The challenge of HIV-1 subtype diversity. *N. Engl. Med.*, **358,** 1590-1602.

Tersmette, M., de Goede, R.E., Al, B.J., Winkel, I.N., Gruters, R.A., Cuypers, H.T., Huisman, H.G. and Miedema, F. (1988) Differential syncytium-inducing capacity of human immunodeficiency virus isolates: frequent detection of syncytium-inducing isolates in patients with acquired immunodeficiency syndrome (AIDS) and AIDS-related complex. *J. Virol.*, **62,** 2026-2032.

Too, P.H., Ma, M.K., Mak, A.N., Wong, Y.T., Tung, C.K., Zhu, G., Au, S.W., Wong, K.B. and Shaw, P.C. (2009) The C-terminal fragment of the ribosomal P protein complexed to trichosanthin reveals the interaction between the ribosome-inactivating protein and the ribosome. *Nucleic Acids Res.*, **39,** 602-610.

Tözsér, J., Bláha, I., Copeland, T.D., Wondrak, E.M. and Oroszlan, S. (1991) Comparison of the HIV-1 and HIV-2 proteinases using oligopeptide substrates representing cleavage sites in Gag and Gag-Pol polyproteins. *FEBS Lett.*, **281,** 77-80.

Tözsér, J., Gustchina, A., Weber, I.T., Bláha, I., Wondrak, E.M. and Oroszlan, S. (1991) Studies on the role of the S4 substrate binding site of HIV proteinases. *FEBS Lett.*, **279,** 356-360.

Tözsér, J., Weber, I., Gustchina, A., Bláha, I., Copeland, T.D., Louis, J.M. and

Oroszlan, S. (1992) Kinetic and modelling studies of S3-S3' subsites of HIV proteinases. *Biochemistry*, **31,** 4793-4800.

Tsao, S.W., Yan, K.T. and Yeung, H.W. (1986) Selective killing of choriocarcinoma cells in vitro by trichosanthin, a plant protein purified from root tubers of the Chinese medicinal herb *Trichosanthes kirilowii. Toxicon*, **24,** 831-840.

Tsao, S.W., Ng, T.B. and Yeung, H.W. (1990) Toxicities of trichosanthin and alpha-momorcharin, abortifacient proteins form Chinese medicinal plants, on cultured tumor cell lines. *Toxicon*, **28,** 1183-1192.

Tsoukas, C.M. and Bernard, N.F. (1994) Markers predicting progression of human immunodeficiency virus-related disease. *Clin. Microbiol. Rev.*, **7,** 14-28.

Tumer, N.E., Hwang, D.J. and Bonness, M. (1997) C-terminal deletion mutant of pokeweed antiviral protein inhibits viral infection but does not depurinate host ribosomes. *Proc. Natl. Acad. Sci. USA*, **94,** 3866-3871.

Uckun, F.M., Chelstrom, L.M., Tuel-Ahlgren, L., Dibirdik, I., Irvin, J.D., Langlie, M.C. and Myer, D.E. (1998) TXU (Anti-CD7)-Pokeweed antivirial protein as a potent inhibitor of human immunodeficiency virus. *Antimicrob. Agents Chemother.*, **42,** 383-388.

Uckun, F.M., Bellomy, K., O'Neill, K., Messinger, Y., Johnson, T. and Chen, C.L. (1999) Toxicity, biological activity, and pharmacokinetics of TXU (Anti-CD7)-Pokeweed antiviral protein in chimpanzees and adult patients infected with human immunodeficiency virus. *J. Pharmacol. Exp. Ther.*, **291,** 1301-1307.

Van Damme, E.J.M., Peumans, W.J., Barre, A. and Rouge, P. (1998) Plant lectins: a composite of several distinct families of structurelly and evolutionary related proteins with diverse biological roles. *Crit. Rev. Plant Sci.*, **17,** 575-692.

Vater, C.A., Bartl, L.M., Leszyk, J.D., Lambert, J.M. and Goldmacher, V.S. (1995) Ricin A chain can be chemically cross-linked to the mammalian ribosomal proteins L9 and L10e. *J. Biol. Chem.*, **270,** 12933-12940.

Vivanco, J.M. and Tumer, N.E. (2003) Translation Inhibition of Capped and Uncapped Viral RNAs Mediated by Ribosome-Inactivating Proteins. *Phytopathology*,

93, 588-595.

Vives, E., Brodin, P. and Lebleu, B. (1997) A truncated HIV-1 Tat protein basic domain rapidly translocates through the plasma membrane and accumulates in the cell nucleus. *J. Biol. Chem.*, **272,** 16010-16017.

Vocero-Akbani, A.M., Heyden, N.V., Lissy, N.A., Ratner, L. and Dowdy, S.F. (1999) Killing HIV-infected cells by transduction with an HIV protease-activated caspase-3 protein. *Nat. Med.*, **5,** 29-33.

Vocero-Akbani, A.M., Lissy, N.A. and Dowdy, S.F. (2000) Transduction of full-length Tat fusion proteins directly into mammalian cells: analysis of T cell receptor activation-induced cell death. *Methods Enzymol.*, **322,** 508-521.

von Schwedler, U.K., Stray, K.M., Garrus, J.E. and Sundquist, W.I. (2003) Functional surfaces of the human immunodeficiency virus type 1 capsid protein. *J. Virol.*, **77,** 5439-5450.

Wadia, J.S. and Dowdy, S.F. (2005) Transmembrane delivery of protein and peptide drugs by TAT-mediated transductionin the treatment of cancer. *Adv. Drug Deliv. Rev.*, **57,** 579-596.

Walsh, T.A., Morgan, A.E. and Hey, T.D. (1991) Characterization and molecular cloning of a proenzyme form of a ribosome-inactivating protein from maize. Novel mechanism of proenzyme activation by proteolytic removal of a 2.8-kilodalton internal peptide segment. *J. Biol. Chem.*, **266,** 23422-23427.

Walsh, T.A., Morgan, A.E. and Hey, T.D. (1991) Characterization and molecular cloning of a proenzyme form of a ribosome-inactivating protein from maize. *J. Biol. Chem.*, **266,** 23422-23427.

Wang, P. and Tumer, N.E. (2000) Virus resistance mediated by ribosome inactivating proteins. *Adv. Virus Res.*, **55,** 325-355.

Wang, J.H., Nie, H.L., Tam, S.C., Huang, H. and Zheng, Y.T. (2002) Anti-HIV-1 property of trichosanthin correlates with its ribosome inactivating activity. *FEBS Lett.*, **531,** 295-298.

Wang, J.H., Nie, H.L., Huang, H., Tam, S.C. and Zheng, Y.T. (2003) Independency of anti-HIV-1 activity from ribosome-inactivating activity of trichosanthin. *Biochem. Biophys. Res. Commun.*, **302,** 89-94.

Wang, J.H., Tam, S.C., Huang, H., Ouyang, D.Y., Wang, Y.Y. and Zheng, Y.T. (2004) Site-directed PEGylation of trichosanthin retained its anti-HIV activity with reduced potency in vitro. *Biochem. Biophys. Res. Commun.*, **317,** 965-971.

Wang, M. and Hudak, K.A. (2006) A noval interaction of pokeweed antiviral protein with translation initiation factors 4G and iso4G: a potential indirect mechanism to access viral RNAs. *Nucleic Acids Res.*, **34,** 1174-1181.

Wang, R.R., Gu, Q., Wang, Y.H., Zhang, X.M., Yang, L.M., Zhou, J., Chen, J.J. and and Zheng, Y.T. (2008) Anti HIV-1 activities of compounds isolated from the medicinal plants Rhus chinensis. *J. Ethnopharmacol.*, **117,** 249-256.

Watkins, B.A., Crowley, R., Davis, A.E., Louie, A.T. and Reitz Jr, M.S. (1997) Syncytium formation induced by human immunodeficiency virus type 1 isolates correlates with affinity for CD4. *J. Gen. Virol.*, **78,** 2513-2522.

Weiss, R.A. (2000) Getting to know HIV. *Trop Med Int Health.*, **5,** A10-15.

Wiegers, K., Rutter, G., Kottler, H., Tessmer, U., Hohenberg, H. and Krausslich, H.G. (1998) Sequential steps in human immunodeficiency virus particle maturation revealed by alterations of individual Gag polyprotein cleavage sites. *J. Virol.*, **72,** 2846-2854.

Wlodawer, A. and Gustchina, A. (2000) Structural and biochemical studies of retroviral proteases. *Biochem. Biophys. Acta.*, **1477,** 16-34.

World Health Organization. Rapid advice: Antiretroviral therapy for HIV infection in adults and adolescents. Nov 30, 2009. (http://www.who.int/hiv/pub/arv/rapid_advice_art.pdf)

Xia, X., Hou, F., Li, J. and Nie, H. (2005) Ribosomal protein L10a, a bridge between trichosanthin and the ribosome. *Biochem. Biophys. Res. Commun.*, **336,** 281-286.

Xiong, J.P., Xia, Z.X. and Wang, Y. (1994) Crystal structure of trichosanthin-NADPH

complex at 1.7 A resolution reveals active-site architecture. *Nat. Struct. Biol.*, **1,** 695-700.

Yang, Y., Ma, J., Song, Z. and Wu, M. (2002) HIV-1 TAT-mediated protein transduction and subcellular localization using novel expression vectors. *FEBS Lett.*, **532,** 36-44.

Yang, Z.R. and Chou, K.C. (2004) Bio-support vector machines for computational proteomics. *Bioinformatics*, **20,** 735-741.

Yang, Y., Mak, A.N., Shaw, P.C. and Sze, K.H. (2007) (1)H, (13)C and (15)N backbone and side chain resonance assignments of a 28 kDa active mutant of maize ribosome-inactivating protein (MOD). *Biomol. NMR Assign.*, **1,** 187-189.

Yang, Y., Mak, A.N., Shaw, P.C. and Sze, K.H. (2010) Solution structure of an active mutant of maize ribosome-inactivating protein (MOD) and its interaction with the ribosomal stalk protein P2. *J. Mol. Biol.*, **395,** 897-907.

Yao, Q.Z., Yu, M.M., Ooi, L.S., Ng, T.B., Chang, S.T., Sun, S.S. and Ooi, V.E. (1998) Isolation and Characterization of a Type 1 Ribosome-Inactivating Protein from Fruiting Bodies of the Edible Mushroom (Volvariella volvacea). *J. Agric. Food Chem.*, **46,** 788-792.

Ye, X.Y. and Ng, T.B. (2002) A novel and potent ribonuclease from fruiting bodies of the mushroom Pleurotus pulmonarius. *Biochem. Biophys. Res. Commun.*, **293,** 857-861.

Yesylevskyy, S., Marrink, S.J. and Mark, A.E. (2009) Alternative mechanisms for the interaction of the cell-penetrating peptides penetratin and the TAT peptide with lipid bilayers. *Biophys. J.*, **97,** 40-49.

Yeung, H.W., Li, W.W., Feng, Z., Barbieri, L. and Stirpe, F. (1988) Trichosanthin, alpha-momorcharin and beta-momorcharin:edentity of abortifacient and ribosome-inactivating proteins. *Int. J. Pept. Protein Res.*, **31,** 265-268.

You, L., Garwicz, D. and Rognvaldsson, T. (2005) Comprehensive bioinformatic analysis of the specificity of human immunodeficiency virus type 1 protease. *J. Virol.*, **79,** 12477-12486.

Zarling, J.M., Moran, P.A., Haffar, O., Sias, J., Richman, D.D., Spina, C.A., Myers, D.E., Kuebelbeck, V., Ledbetter, J.A. and Uckun, F.M. (1990) Inhibition of HIV replication by pokeweed antiviral protein targeted to CD4+ cells by monoclonal antibodies. *Nature*, **347,** 92-95.

Zhao, W.L., Feng, D., Wu, J. and Sui, S.F. (2009) Trichosanthin inhibits integration of human immunodeficiency virus type 1 through depurinating the long-terminal repeats. *Mol. Biol. Rep.*, **Epub ahead of print**.

Zheng, G., Bachinsky, D.R., Sramenkovic, I., Strickland, D.K., Brown, D., Andres, G. and McCluskey, R.T. (1994) Organ distribution in rats of two members of the low-density lipoprotein receptor gene family, gp330 and LRP/alpha 2MR, and the receptor-association protein (RAP). *J. Histochem. Cytochem.*, **42,** 531-542.

Zheng, Y.T., Ben, K.L. and Jin, S.W. (2000) Anti-HIV-1 activity of trichosanthin, a novel ribosome-inactivating protein. *Acta Pharmacol. Sin.*, **21,** 179-182.

Zhou, H., Jiao, Z., Pan, J., Hong, J., Tao, J., Li, N., Zhou, Y., Zhang, J. and Chou, K.Y. (2007) Immune suppression via IL-4/IL-10-secreting T cells: a nontoxic property of anti-HIV agent trichosanthin. *Clin. Immunol.*, **122,** 312-322.